TAILORED ARCHITECTURES OF AMMONIUM IONENES

Mana Tamami

Thesis submitted to the faculty of the
Virginia Polytechnic Institute and State University
in partial fulfillment of the requirements for the degree of

Masters of Science in Chemistry

Timothy E. Long (Chair)
Garth L. Wilkes (Member)
S. Richard Turner (Member)
Susan E. Duncan (Member)
Yong Woo Lee (Member)

August 11, 2009
Blacksburg, Virginia

Keywords: biomedical applications, random copolymer ionenes, x-ray scattering, segmented ionenes, salt-triggering, thermomechanical property

TAILORED ARCHITECTURES OF AMMONIUM IONENES

Mana Tamami

ABSTRACT

The synthesis and characterization of a variety of ammonium ionenes from water-soluble coatings to high-performance elastomers are discussed. Water-soluble random copolymer ionenes were synthesized using the Menshutkin reaction from 1,12-dibromododecane, *N*,*N*,*N*′,*N*′-tetramethyl-1,6-hexanediamine, and 1,12-bis(*N*,*N*-dimethylamino)dodecane. The absolute molecular weights were determined for the first time using a multiangle laser light scattering detector in aqueous size exclusion chromatography and the weight-average molecular weights of these ionenes were in the range of 17,000-20,000 g/mol. Charge density increased with increasing molar ratio of *N*,*N*,*N*′,*N*′-tetramethyl-1,6-hexanediamine and the glass transition temperature (T_g) increased from 69 °C to 90 °C as the charge density increased. Small angle x-ray scattering (SAXS) showed isotropic scattering patterns for these ionenes. A limited study on cytotoxicity of these ionenes showed no direct correlation between charge density and cell viability for human brain microvascular endothelial cell line.

A series of low hard segment (HS) content, poly(propylene glycol) (PPG)-based ammonium ionenes were synthesized using a Menshutkin reaction from bromine end-capped PPG oligomers (prepared using acid-chloride reactions) and *N*,*N*,*N*′,*N*′-tetramethyl-1,6-hexanediamine. Matrix assisted laser desorption ionization-time of flight (MALDI-TOF) mass spectrometry, titration analyses, and ^{1}H NMR spectroscopy, confirmed the difunctionality of bromine end-capped PPG oligomers. Thermal analysis revealed T_g's of -60 °C, comparable to pure PPG, using differential scanning calorimetery (DSC), dynamic mechanical analysis (DMA) confirming microphase separation, and an onset of degradation (T_d) at 240 °C.

Synthesis of a series of random block copolymer ammonium ionenes with an aliphatic 1,12-dibromododecane as part of the hard segment (33 wt% HS) enhanced film formation and supported microphase separation property. The T_d and T_g did not change compared to PPG-ionenes with lower HS content. DMA and tensile testing demonstrated the influence of soft segment (SS) molecular weight and hard segment (HS) content on the mechanical properties of segmented ammonium ionenes. DMA showed the onset of flow, ranging from 100-140 ºC for 1K and 2K g/mol PPG-based ionenes respectively. SAXS revealed a Bragg distance scaled with soft segment molecular weight and ranged from 6.6 to 23.4 nm for 1K to 4K g/mol PPG-based ionenes, respectively.

An investigation of the salt-responsive solubility property of random block copolymer PPG-ionenes revealed a dependence on PPG molecular weight. The 1K g/mol PPG-based ionenes with a hydrophilic (HPL)/hydrophobic (HPB) value ranging from one to three showed solubility in both water and one wt% NaCl aqueous solutions. The 2K g/mol PPG-based ionenes containing HPL/HPB value of two to 15 showed cloudy dispersions in water and one wt% NaCl solutions. The 4K g/mol PPG-based ionenes possessed the salt-responsive character; 4K g/mol PPG-based ionenes with HPL/HPB values of one to 12 showed milky dispersions in water, suspended particles in one wt% NaCl solutions and film precipitation at a HPL/HPB molar ratio of 19.

ACKNOWLEDGEMENTS

I would like to thank my advisor, Prof. Timothy Long, for his guidance, encouragement, and support during my three years of graduate school. I am grateful to him for allowing me the opportunity to achieve my scientific goals and providing me with the necessary laboratory resources. I would also like to thank my committee members for their participation and support: Prof. Garth Wilkes, Prof. Richard Turner, Prof. Susan Duncan, and Prof. Yong Woo Lee. Especially I am thankful to Prof. Garth Wilkes for his helpful discussions and advice.

I would like to acknowledge Erika Borgerding for her mentorship during the first year of graduate school. I would specially like to thank Dr. Sharlene Williams for her great mentorship throughout the last two years. She taught me how to work hard, have discipline, and work cleanly. I would also like to thank Rebecca Huyck for helping me with running aqueous SEC and always responding to my questions. I would like to thank all my group members, previous and present, for their advice, encouragement, discussions, time, and support including Gozde, Tomonori, Akshay, Sean, Matt H., Matt G., Mathew, Eva, Funda, Bill, Emily, Andy, Steve, Shijing, Eugene, Tianyu, Nancy, Renlong, Ali, Philippe, Takeo, John, and Mike. I like to thank staff members including Vicki Long, Steve McCartney, Laurie Good, Mary Jane Smith, Millie Ryan, and JaeHee for their assistance.

I would like to thank our collaborators including Dr. Clay Bunyard from Kimberly-Clark, Prof. Robert Moore and Park from Virginia Tech, Prof. Michael Rubinstein from the University of North Carolina, Prof. Karen Winey and David Salas-de la Cruz from University of Pennsylvania. I also acknowledge the funding source from Kimberly-Clark.

Finally, I am forever grateful to my family: Afsaneh, Bahman, and Mehrnaz for their continued love and support in my life endeavors. I am deeply thankful to my father, Prof. Bahman Tamami, he is my role model, a great mentor and a true scientist. Words cannot express my love for him. With all my heart I would like to make him proud and thank him for all his support throughout the years. At the end, I cannot ever forget my parent's sacrifices to provide me encouragement and motivation to pursue my goals. I would be nothing without them on the journey of life.

Table of Contents

List of Figures

List of Tables

List of Schemes

Chapter 1. Introduction to Ammonium Ionenes: From Biomedical Applications to Structure-Property Characterizations

1.1 Abstract

The synthesis and characterization of highly charged polymers or polyelectrolytes has become an important field of study since the 1930s. The charged nature of polyelectrolytes facilitates their use in a variety of novel applications, such as in waste water treatment, cosmetics, pharmaceuticals, and biomedicine, as well as for use as ion selective membranes for fuel cells, as surfactants, conductors, ion exchange resins, and biosensors. One type of polyelectrolyte, known as ionenes, are polycations that contain quaternized nitrogen atoms along their backbone. Ionenes offer significant potential for use in biomedical applications because of the ability to tailor their molecular weight, charge density, solution concentration, chemical composition, and counterions. This chapter discusses polyelectrolytes in general and ammonium ionenes in particular, especially with respect to their potential for use in biomedical applications and structure-property characterization.

Key words: ionenes, biomedical applications, polyelectrolyte complexes (PECs), gene delivery, antimicrobials

1.2 Introduction to polyelectrolytes

Charged polymers, known as polyelectrolytes, are polymers that contain ionizable groups in a high concentration (> 15 mole%) of repeating units.[1] Electrostatic interactions between charges on polyelectrolytes greatly influence their behavior, especially in comparison to uncharged polymers. Linear polyelectrolytes have an extended or rod-like conformation in pure water due to the repulsion between ionic sites. This behavior is called the polyelectrolyte effect. When salt is added to the polyelectrolyte, the charges are screened and the chain conformation changes from rod-like to coil-like conformation. The chain conformation of polyelectrolytes has four stages in multivalent salt solutions.[2] In stage one the polyelectrolyte shows an extended rod-like conformation in pure water. In stage two, ion-bridging occurs between divalent counterions and two ionic sites on the polymer backbone and thus polyelectrolyte remains soluble. In stage three, due to the high volume of charge screening, the polyelectrolyte precipitates out. In stage four, when the salt concentration is increased even higher, the polyelectrolyte will redissolve in the solution due to even higher charge screening. The behavior of polyelectrolytes is also dependent on solution pH, ionic strength, molecular weight, temperature, and concentration.[2] Eisenberg[3] divided polyelectrolytes into two groups, those that are water soluble and those that are water swellable due to either covalent crosslinking or strong ionic association.

According to Eisenberg, water-soluble systems include polycations and polyanions. Polycations are divided into three categories, based on the charged atom: 1) polymers containing ammonium groups (Figure 1.1), 2) polymers containing sulfonium groups (Figure 1.2), and 3) polymers containing phosphonium groups (Figure 1.3). Poly(carboxylic acid) salts, poly(sulfonic acid) salts, and poly(phosphonic acid) salts are examples of water-soluble polyanions. Water-swellable

systems include polyelectrolyte-based networks which can either be homopolymers or copolymers and are used as ion-exchange resins. Other water-swellable systems are polysalt complexes that are formed when polyanionic homopolymers bind to polycationic homopolymers.

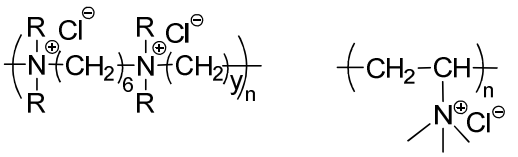

(a) (b)

Figure 1.1. x,y-ionene (a), Poly(vinyl trimethyl ammonium chloride) (b)

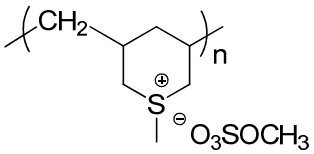

Figure 1.2. Poly(methyldiallyl sulfonium methyl sulfate)

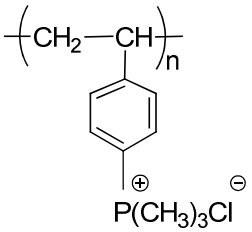

Figure 1.3. Poly(vinyl benzyl trimethyl phosphonium chloride)

1.3 Polyelectrolytes for use in biomedical applications

Polyelectrolytes include polycations or polyanions that are either naturally occurring polymers or are synthesized via different polymerization techniques. Proteins, DNA and RNA, the building blocks of life, are natural polyelectrolytes. Researchers studied the novel applications of polyelectrolytes.[4, 5] Cationic polyelectrolytes have potential in many biomedical applications ranging from antimicrobials, gene delivery, co-delivery of drugs and genes, to bioseparation of DNA from RNA and protection of RNA from degradation. Cakmak et al.[6] synthesized various molecular weights of ionenes to use as antimicrobial agents using a reaction of epichlorohydrin and benzyl amine. They showed that high molecular weight polycations have enhanced antimicrobial properties even at low concentrations.

Due to the positive nature of polycations, they readily complex with negatively charged DNA or RNA for use in non-viral gene delivery. Long et al.[7] reviewed the important parameters for polycations used as non-viral gene delivery vectors versus viral vectors. They reported that the synthesis of polycations for gene and drug delivery, using controlled free radical polymerization methods, enables a novel architectural design, controlled molecular weight, and low molecular weight distribution of the polymer.

Co-delivery of drugs and DNA enhances gene expression. It can contribute to the combined effect of drug and gene therapies.[8-11] Wang et al.[12] reported the synthesis of cationic biodegradable polyelectrolyte and its ability to co-deliver drugs and genes to the same cell. Due to the amphiphilic behavior of polyelectrolyte, it can self-assemble to core-shell nanoparticles in an aqueous solution (Figure 1.4). Core-shell nanoparticles utilize cholesterol side chains to bind with drugs, and use charged main chains to bind with DNA. The nanoparticle/DNA complex show low cytotoxicity and are suitable for delivering anticancer drugs.

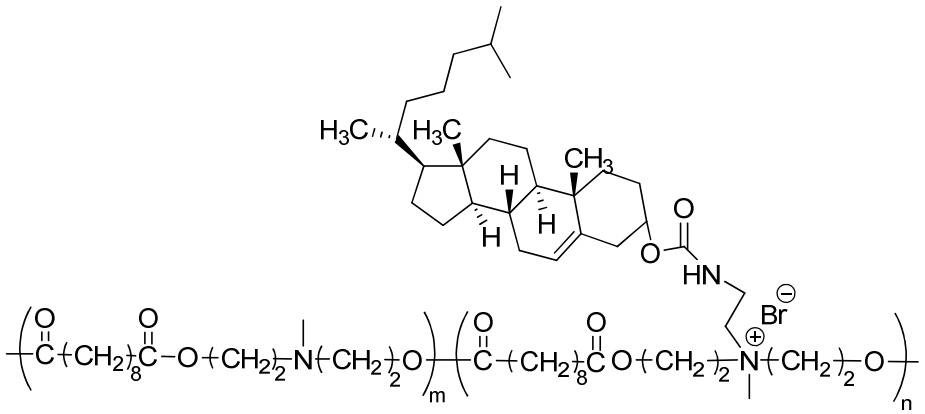

Figure 1.4. Chemical structure of a cationic amphiphilic polymer[12]

When oppositely charged polyions with high charge densities interact with one another they form polyelectrolyte complexes (PECs). One significant application of polyelectrolytes and their corresponding PECs is their use in bioseparation techniques. In these techniques an insoluble PECs are desirable. It is hypothesized that a number of modifying factors such as temperature, pH, and ionic strength can influence the phase separation behavior of PECs.[4, 5, 13] Wahlund et al.[14] studied the phase separation of PECs formed by either RNA or DNA in water-salt solutions having different ionic strengths. In a water-salt solution, DNA molecules maintain the double-stranded conformation and the corresponding PECs precipitate at certain charge ratios. Conversely, a non-precipitated fraction of flexible RNA strands does not precipitate at any charge ratio due to the higher insolubility of a fraction of RNA with increasing salt content. Therefore using water-salt solutions with different salt concentrations showed promise in developing new bioseparation techniques.

Recent studies[15] have explored the role of RNA in gene expression and crucial metabolic processes. However, in order to make RNA sufficiently stable, methodologies have developed to prevent its degradation. Polyelectrolytes bind with RNA to protect it from degradation. Khan et al.[16] developed a novel method to protect RNA against enzymatic degradation. They used

hyperbranched cationic polymer to make a complex with RNA, forming water-soluble nanoparticles to prevent RNA from cleavage. RNA nanoparticles of different shapes and sizes self-assemble and resist environmental stress. One method is to use nanoparticles to deliver multiple therapeutic agents to the same cell at the same time.

1.4 Introduction to ammonium-based ionenes

Ammonium polyionenes, or ionenes, are ion-containing polymers that have quaternary nitrogen atoms in their macromolecular backbone. Gibbs et al.[17] first synthesized low molecular weight ionenes through a polycondensation reaction of dimethylamino-N-alkyl halides in order to investigate the effect of alkyl substituents on ring closure. However, ionenes are usually synthesized from a reaction of a ditertiary amine and a dihalide called Menshutkin reaction (Figure 1.5).

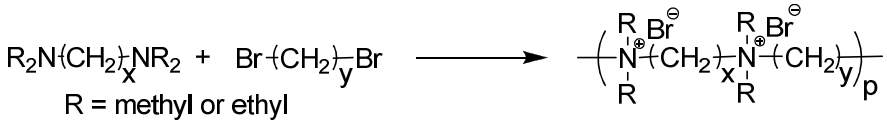

Figure 1.5. General synthetic scheme for ammonium ionene

The ionene is named from the number of methylene spacers, which correspond to the diamine and dihalide monomers, respectively (i.e. x,y-ionene). Rembaum et al.[18-20] synthesized the first aliphatic ionenes using this reaction and explored their solution properties. The number of methylene spacers in each repeating unit is used in ionene nomenclature. There are different parameters such as chemical composition, molecular weight, charge density, counterion, solution concentration, and end groups that influence the properties and applications of ionenes.[21] In particular, the ability to tune charge density through monomer selection, makes ionenes ideal

models for investigating structure-property relationships of well-defined cationic polymers. The properties of any polymer relates to its chemical composition. The chemical composition of a polymer is based on the chemical compositions of its repeating units. In synthesizing ionenes with desired properties, one must use or design monomers having certain chemical structures or exchange the counterion. So far, two general types of ionenes were synthesized; segmented[22-26] and non-segmented[17, 19, 27-30] which are either linear, crosslinked or branched. Segmented ionenes have low T_g oligomeric spacers between their ionic sites and can have elastomeric properties. Non-segmented ionenes have shorter distances between their ionic sites which lead to higher charge density.

Both small molecules and macromolecules containing quaternized nitrogens in the backbone repeating unit have potential applications in the biomedical field. Ionenes are good polyelectrolyte models in gene therapy.[12] In addition, several applications of ionenes as components of cosmetics, flocculants for water treatments, antimicrobial agents and components for photovoltaic cells were discussed in the literature.[31] Several biomedical applications of ammonium ionene are discussed below.

1.5 Ionenes as antimicrobial agents

Infectious microorganisms such as bacteria, fungi, viruses, and protozoa grow on both living and non-living surfaces, including teeth, skin, medical implants, vascular tissue, mucosa and medical devices. As it is well known, microbial infections of living organisms, which can affect other organs in the body, are treated with antimicrobial agents.[38] Many microorganisms resist various antimicrobial agents. Therefore, effective antimicrobial agents play an important role in wound and skin infection treatments.

Ionenes were used to treat microbial infections and also prevent the clustering of microorganisms on a surface. Rembaum et al.[32] described the antimicrobial properties of ammonium-based ionenes. Narita et al.[33] showed that ionenes with longer hydrophobic segments are more destructive to cells. They have proposed that the reason might be due to the local solubilization of the lipid membrane via hydrophobic interaction. On the other hand, ionenes having shorter hydrophobic segments have higher charge density and bind to cells more efficiently, but do not disrupt the cell membrane.[34]

Several US patents have detailed methods for coating biomedical devices such as stents, catheters, and contact lenses with cationic antimicrobial layers.[35-37] Moreover, Fitzpatrick et al.[38] invented novel antimicrobial ionenes having quaternized nitrogen or phosphorous to treat microbial infections in a mammal, manage wound infections, and treat skin, oral mucosa and gastrointestinal tracts. The ionenes described herein, have several advantages over conventional treatments including the absence of irritation, low toxicity, and high sustainability to warm blooded animals. These ionenes do not degrade in the digestive tract, allowing for oral and topical treatment.

1.6 Ionenes in gene therapy

The basic concept of gene therapy is that disease is treated with transferring genetic material into targeted cells to supplement the defective genes responsible for disease development.[39] Gene therapy strategies were originally designed using viral vectors for DNA delivery. Although viruses provide high transfection efficiencies, viral immunogenicity has raised safety concerns, limiting their effectiveness.[40] As mentioned earlier, synthetic polycations are viable candidates for non-viral gene delivery vectors. The advantages of non-viral vectors over viral vectors are

that they do not integrate into chromosomes, they introduce DNA into non-dividing cells, they do not possess infective risk, and are significantly less expensive and easier to handle.[41] The major disadvantage of non-viral systems is their low transfection efficiency.[42] In other words, the non-viral delivery vectors should overcome intracellular barriers, such as endosomes and nuclear membranes.

Ionenes are one type of polycation that bind to DNA, cause charge inversion and form polyplexes.[43] Such mechanisms allow DNA to cross the cell membrane and become incorporated into the cell. Even though the transfection efficiency of polyplexes is lower than that of viral vectors, polymers condense larger amounts of DNA which can compensate for losses in transfection efficiency.[44] The degree of polymerization (DP) and charge density of polycations directly impact transfection efficiency.[45]

Godbey et al.[46] studied the transfection efficiency of DNA complexed with polyethylenimine (PEI) and found that gene expression increases with increasing PEI molecular weight. In addition to molecular weight, the charge density of polyelectrolytes affects their ability to bind to DNA. Trukhanova et al.[47] investigated the selective binding of ionenes with DNA in the presence of polyanions. Negatively charged species affected higher charge density ionenes significantly compared to lower charge density ionenes. Thus, altering the charge density of ionenes will modify their ability to successfully separate from DNA and efficiently transfer the gene. Wolfert et al. [48] showed similar results based on methacrylate-derived polycations. They reported the choice of starting materials impacts the charge density of ionenes. They synthesized ionenes with the same degree of polymerization but different charge densities.

Another important factor in gene delivery is the degradation or dissociation of PECs inside the cell. The most common method for disrupting ionic association in PECs is to increase the

ionic strength of the solution. Zelikin et al.[49] studied the influence of DP and charge density on the dissociation of (2,4- and 2,8-) ammonium ionenes with poly(methacrylic acid) in different salt solutions. Another factor influencing the degradation of PECs is molecular weight. Schaffer et al.[50] described how higher molecular weight polymers bind to DNA more efficiently, but restrict the ability of DNA to get released. Thus, studying the factors that influence PECs dissociation is crucial to the field of gene delivery.

To date, gene therapy research has typically focused on polycation-DNA complexes; however new studies of polycation-RNA complexes are under investigation. As mentioned earlier, Wahlund et al.[14] studied the formation of insoluble PECs from RNA and 2,5-ionene in order to separate RNA from plasmid DNA using different concentrations of water-salt solutions. The 2,5-ionene was synthesized from N,N,N',N'-tetramethylethylenediamine and 1,5-dibromopentane via the Menshutkin reaction. The strong binding of bromide counterions (Br^-) and the relatively low molar mass of the chains led to insoluble PECs. Therefore, the stability of the PECs depended strongly on the composition of the added salt, the degree of polymerization and the charge density of the chains.

1.7 Synthetic strategies for segmented ammonium-based ionene synthesis

Ionene properties are highly dependent on monomer selection. Kohjiya et al.[23] and Ikeda et al.[51] designed ionenes that have poly(tetramethylene oxide) (PTMO) segments within their backbone. Figure 1.6 and Figure 1.7 illustrate both synthetic strategies. Ikeda used one pot synthesis to prepare PTMO-based ionenes, this was the advantage over the Kohjiya synthetic path way. Leir et al.[52] designed the reaction of α,ω-bis(dimethylamino) poly(tetramethylene oxide) with various dihalides to synthesize a series of elastomeric ionenes (Figure 1.8). Various

diamine compounds were used with a similar synthetic strategy. Mechanical properties of the corresponding elastomeric ionenes were subsequently studied.[53-55]

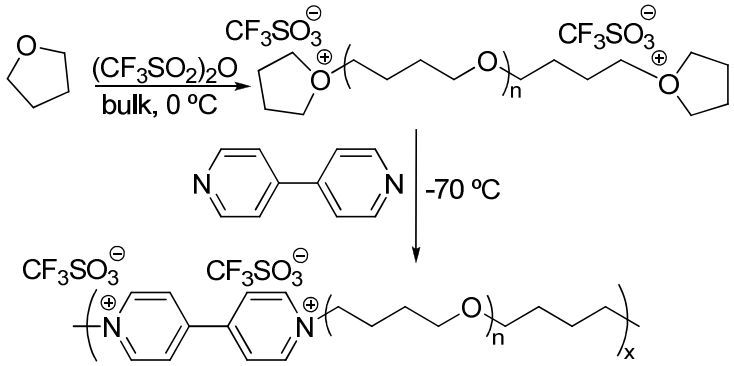

Figure 1.6. Synthetic strategy for PTMO-based ionenes[23]

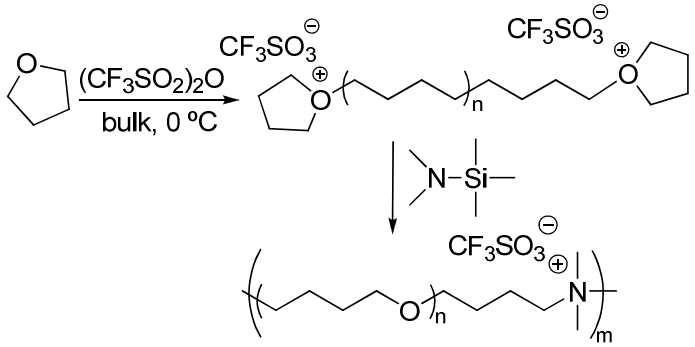

Figure 1.7. One-pot synthesis of high molecular weight PTMO-based ionene[51]

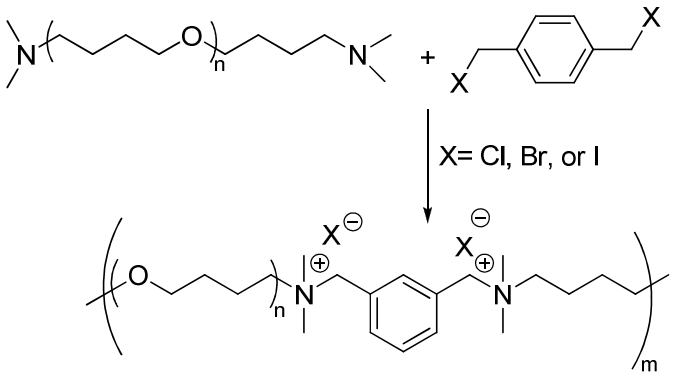

Figure 1.8. Synthesis of PTMO-based ionene[52]

Poly(ethylene glycol) (PEG) is used in many biomedical applications. Jeon et al.[56] discovered that PEG inhibits the adsorption of proteins. This behavior is used especially when PEG is attached to the hydrophobic surface of a substrate in water. PEG has a smaller refractive index compared to other water-soluble synthetic polymers and has low van der waals interactions with proteins. The chain length and surface density of PEG determines the resistancy of PEG towards proteins. When protein reaches the PEG surface, steric effects compete with van der waals interactions and become dominant. PEGs with longer chains and higher surface density result in higher protein resistancy.

In addition, PEG shows low cytotoxicity levels.[59, 60] Hassook et al. have synthesized ionenes with PEG-based monomers (Figure 1.9).[57]

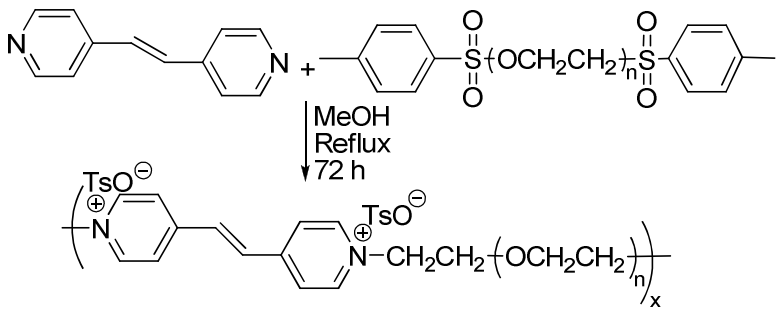

Figure 1.9. Synthesis of PEG-based ionene[57]

Burmistr et al.[58] synthesized PEG-based ionenes having different PEG lengths (Figure 1.10). They reported that ionenes having various PEG segment lengths, show temperature-dependant conductivities.

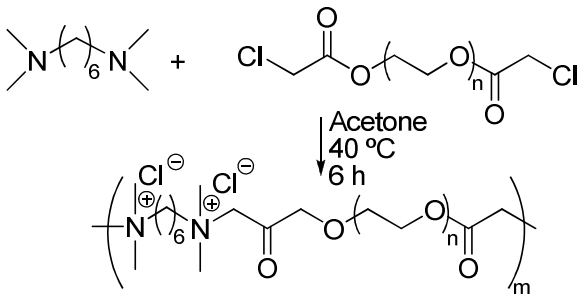

Figure 1.10. Synthesis of PEG-based ionene[58]

1.8 Structure-property relationships of ammonium-based ionenes

Ionenes have received increased attention in the literature. Therefore the synthesis of novel ionenes with new functionalities will reveal meaningful structure-property relationships. Klun et al.[59] studied the structure-property relationships of several ionenes having poly(tetramethylene oxide) (PTMO) segments as part of their backbone. Molecular weight measurements were performed on high resolution columns using 0.1 molar LiBr in DMF as the eluent. The data showed that the degree of polymerization of their ionenes was quite low. Ionenes that had geminal diethyl groups showed steric congestion and had the lowest degree of polymerization. Low angle light scattering showed lower absolute molecular weights for these ionenes compared to their polystyrene equivalent molecular weights.

Differential scanning calorimetry (DSC) and differential thermal analysis (DTA) were used to obtain thermal data for these ionenes. Two parameters were used to define the thermal characteristics in these novel ionenes: PTMO segments and ionene segments. Ionene segments are the portions of the polymer that are between PTMO segments. Thermal data described in Table 1.1 showed that ionene (label 2) in Figure 1.11 which had no PTMO segments, had only a single T_g. Ionenes (labels: 10, 11, and 12) with PTMO segments in Figure 1.11 showed a T_g and

a T_m. Ionene (label 15) has T_g's of -70 ºC and 27 ºC corresponding to PTMO and ionene segments respectively. The fact that there are two T_g's for these types of ionenes confirms the presence of a two phase morphology in which the PTMO and ionene segments are located in different domains.

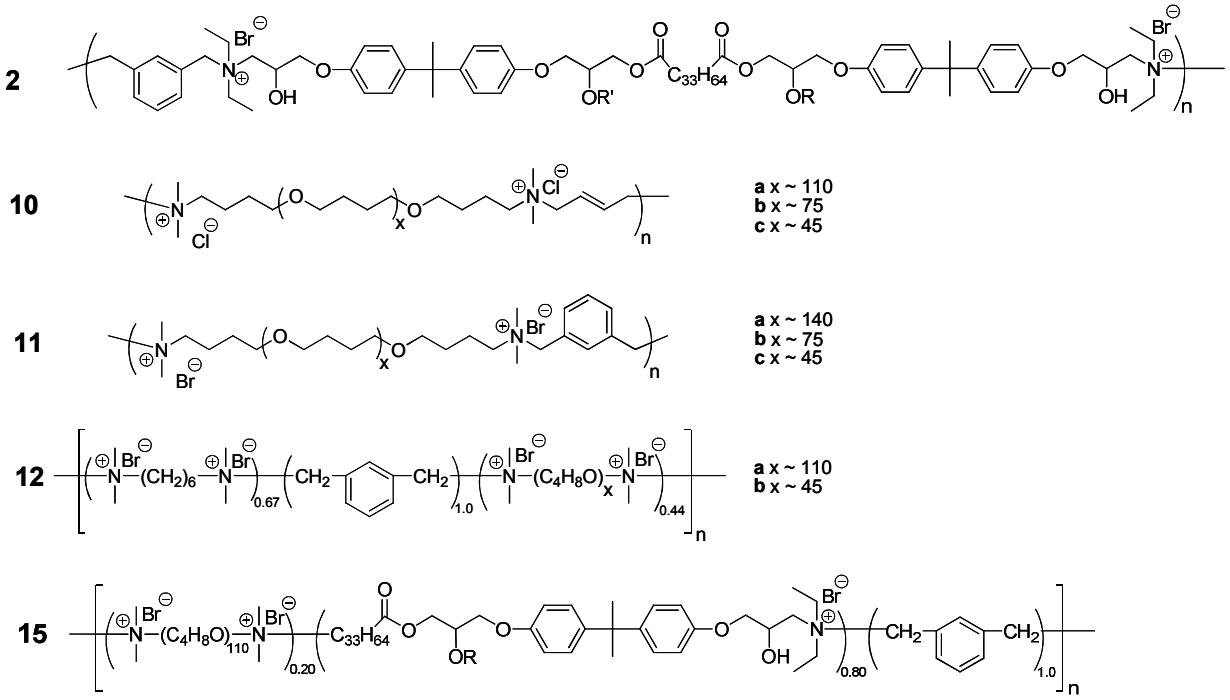

Figure 1.11. Synthesis of PTMO-based ionenes[59]

Table 1.1. DSC results of PTMO-based ionenes[59]

Polymer	Weight % Ionene[a]	Ionene Segment T_g	PTMO Segment T_g	Ionene Segment T_{HT}	PTMO Segment T_{melt}	PTMO Segment $T_{cryst.}$	PTMO % Crystallinity at 20°C[b]
2	100	24	—	211	—	—	—
10a	3	—	−75	220	17, 49	—	32
10c	4	—	−66	210	13	—	0
10c (2nd heat)	4	—	−69	> 240	33	—	53
11a	3	—	−80	200	15, 41	—	28
11a (2nd heat)	3	—	−80	200	29	—	45
11c	7.5	—	−76	196	10	−26	0
11c (2nd heat)	7.5	—	−71	> 230	28	—	47
12a	13	—	−77	230	24, 47	—	39
12b	26	—	−76	201	16	−22	0
12b (2nd heat)	26	—	—	> 230	32	—	60
15	54	27	−70	210	—	—	0
28	16	—	−73	225	54	—	50

[a](100 − weight % PTMO segment).
[b]Calculated on the basis of the PTMO melting endotherm peak area using a value of 41 cal/g.[21]

The ambient temperature, stress-strain behavior of these ionenes is directly related to their microphase-seperated morphology. Ionene (label 2) in Figure 1.11 does not have PTMO segments. It has a high modulus and tensile strength due to its ionic domains. Ionic domains in ionenes with PTMO segments having no crystallinity (labeled as 11c, 12b, and 15) act as physical crosslinks between the flexible PTMO segments. This behavior will impart elastomeric property to the ionene. Ionenes with crystalline PTMO segments (labeled as 10a and 11a) show higher modulus and greater toughness compared to ionenes having amorphous PTMO segments. All the PTMO-containing ionenes show high ultimate elongation. The onset of stress induced crystallization is seen at ca. 300% elongation for amorphous PTMO containing ionenes.

The effect of the ionic spacing on the stress-strain behavior was studied. Ionenes (labeled 11a and 11c) were compared to ionenes (labeled 12a and 12b). In 11a and 11b, ionic sites are widely apart by PTMO segments, whereas in 12a and 12b two thirds of the ionic sites are only six carbons apart. When ionic sites are far apart, ionic associations are satisfied intermolecularly. This will lead to active physical crosslinking which causes higher tensile strength in ionenes

labeled as 11 series. When ionic sites are closer to one another in the backbone, intramolecular ionic associations become dominant. Intramolecular associations compared to intermolecular associations do not induce active physical crosslinking, therefore ionenes labeled as 12 series have lower tensile strength and greater elongation. It should be mentioned that generally ionenes are hygroscopic due to their charged nature. Therefore water absorption can highly impact their mechanical behavior. The presence of water will interfere and weaken ionic interactions. This will lead to a decrease in tensile strength and will impact the structural integrity of ionenes.

Static electricity or high electrical charge on the surface of plastics can often cause problems.[59] This causes handling issues during storage and transport, as well as dust contamination that impact the performance of the end-product. In addition, there are risks of electrical shock and electrical discharge. Thus, antistatic agents, or antistats, help to reduce the surface resistivity and disperse the high electrical charge on the surface of plastics. Ionenes are good antistats because of their ability to attract water to their surface, and prevent and dissipate the static buildup. A worthwhile goal is to obtain an antistat that would function at both low and high relative humidities. PEG-based ionenes are good candidates for antistatic agents, due to the hydrophilicity of PEG segment. Another measure of the physical properties of ionenes is moisture-vapor transmission and oxygen permeability. Klun et al.[59] measured moisture-vapor transmission of the synthesized ionenes shown in Figure 1.11. Two different techniques were used, a gel and a bottle method. In the gel method, the polymer contacts an aqueous gel that has 99% water. This method is utilized to simulate contact of the polymer to a moist surface-like skin. The gel membrane properties are able to dissolve and transport the desired solute. They indicated that their PEG-based ionenes have acceptable moisture-vapor transmission values, but

interestingly, poor oxygen permeability. Thus, it seems that the inherent moisture sensitivity of these ionenes prevent their use as membrane components.

Ikeda et al.[60] studied the effect of counterions on the morphology of PTMO-based ionenes shown in Figure 1.12. PTMO-based ionenes possess elastic properties at low elongations and show plastic deformations at high elongations. Counterions determine the size of ionic domains and distance between the domains. While ionenes with bromide counterions have smaller and shorter ionic domains, those with chloride counterions have larger and longer ionic domains. Therefore, different mechanical and thermal properties are seen in these types of ionenes containing different counterions.

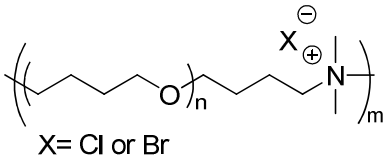

Figure 1.12. PTMO-based ionenes[60]

PTMO-based ionenes with chloride counterions were abbreviated as IP-Cl and those with bromide counterions were abbreviated as IP-Br. The IP-Br and IP-Cl samples had same molecular weights between their ionic sites and showed similar intrinsic viscosities. The counterions affect the mechanical properties of IP-Br and IP-Cl ionenes.

Both IP-Cl and IP-Br samples showed low stresses at low elongations. However, at higher elongations, PTMO crystallized and therefore the tensile stress increased to 30 MPa at 800% elongation. Ionenes have physical crosslinking behavior. IP-Br samples had more tensile strength compared to IP-Cl samples because strain-induced crystallization of PTMO segment was more significant in IP-Br than IP-Cl.

The plot of G' versus temperature for IP-Br and IP-Cl samples (Figure 1.13) shows three main drops in temperature: (1) T_g of the amorphous PTMO phase at ca. -80 ºC; (2) the melting of

the PTMO crystalline phase at ca. 20 ºC; (3) dissociation of ionic aggregates at ca. 200 ºC. Ionenes are classified as physically crosslinked elastomers. The higher G' curve of IP-Br compared to IP-Cl is due to the effect of counterions and larger crosslinking density for IP-Br than IP-Cl.

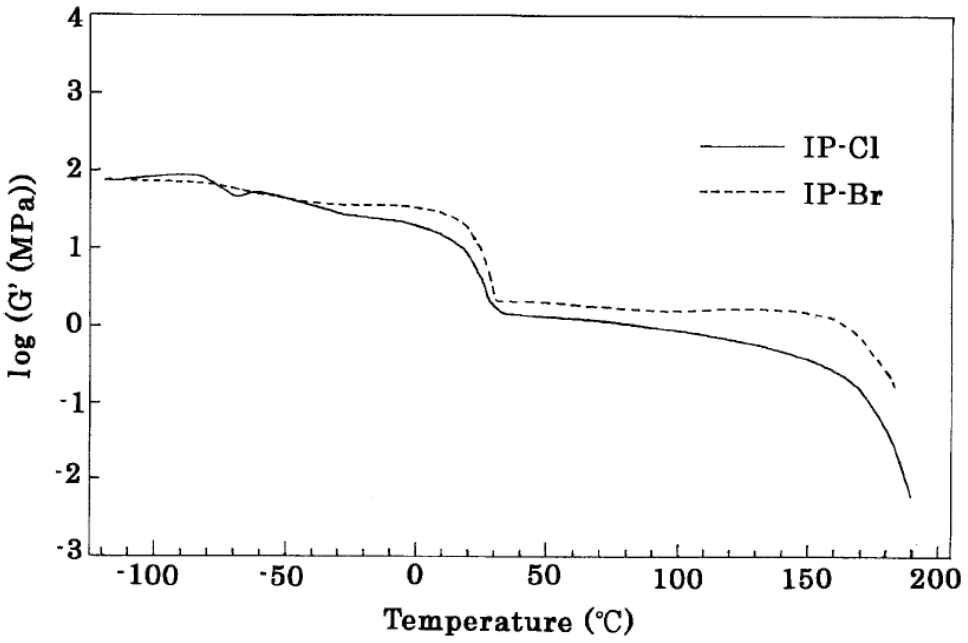

Figure 1.13. Dynamic mechanical behavior of the bromide (IP-Br) versus the chloride (IP-Cl) PTMO ionene[60]

Ionic segments were suggested to be tighter and more stable in IP-Br than IP-Cl ionenes. The DSC curves showed that IP-Br has a broader and higher ionic dissociation temperature (IP-Cl at ca. 200 ºC and IP-Br at ca. 226.6 ºC) (Figure 1.14). PTMO crystallization did not occur in IP-Br. IP-Br had mostly an amorphous phase rather than the crystalline phase at room temperature.

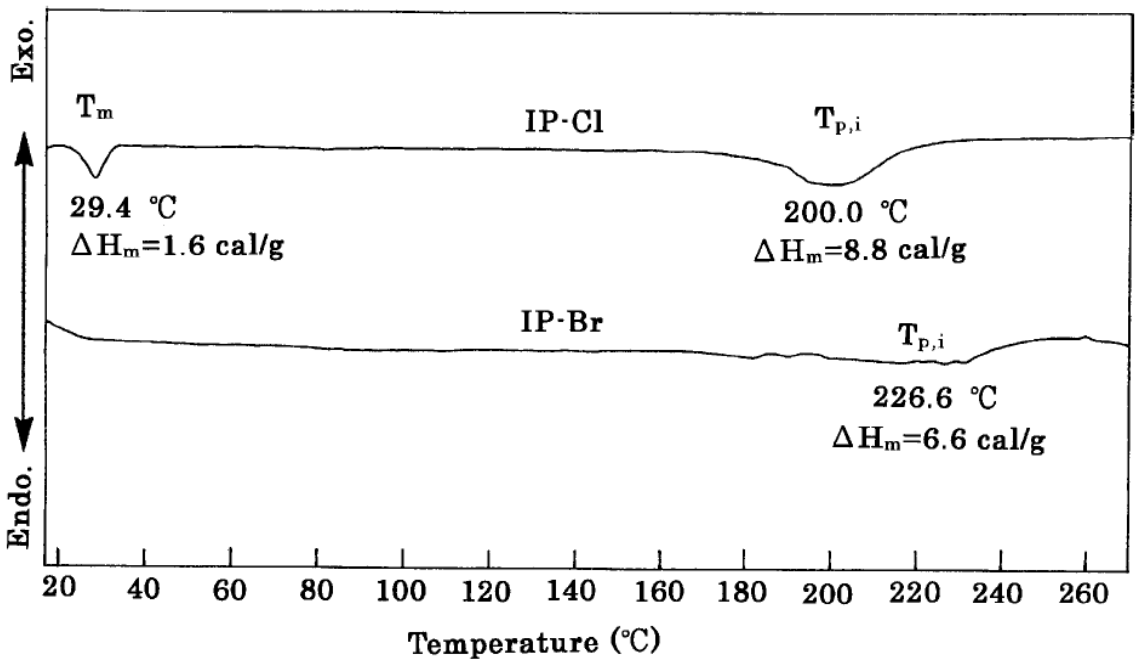

Figure 1.14. DSC curves of IP-Br and IP-Cl measured from r.t. to 270 ºC[60]

The results of DSC, DMA, and tensile measurements provided indirect information regarding the morphology. The morphology of IP-Br and IP-Cl samples were determined by small angle x-ray scattering (SAXS) and wide angle x-ray diffraction (WAXD). SAXS showed a single broad scattering peak for both samples. This means that there is no well ordered morphology that can be recognized from the respective peak position. Ikeda et al. used SAXS and DSC data to propose schematics of the morphology of each sample. As shown in Figure 1.15, this scheme proposes that the structure of IP-Cl is composed of three phases including a matrix of amorphous PTMO segment, a crystalline PTMO segment and ionic domains. However, IP-Br showed two phases including the matrix of PTMO segments and ionic segments without a crystalline phase.

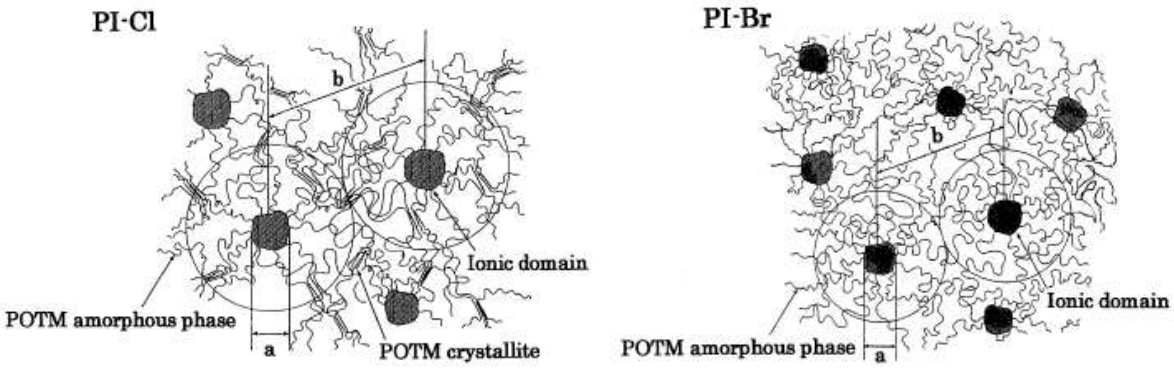

Figure 1.15. Schematic of IP-Cl and IP-Br ionenes[60]

The WAXD measurements confirmed the crystalline phases in IP-Cl, and showed a diffraction ring and amorphous hallow for IP-Cl at room temperature. However, only an amorphous hallow was observed for IP-Br. These results showed that IP-Br did not posses a crystalline phase, which was consistent with the DSC and SAXS measurements. These observations led to larger physical crosslinking density for IP-Br than IP-Cl. Thus, ionenes are physically crosslinked elastomers, in which their counterion can play an important role on mechanical and morphological properties.

Yamashita et al.[61] compared the swelling and mechanical properties of specific polybutadiene ionene (PBI) with a segmented polybutadiene urethane (PBU) (Figure 1.16).

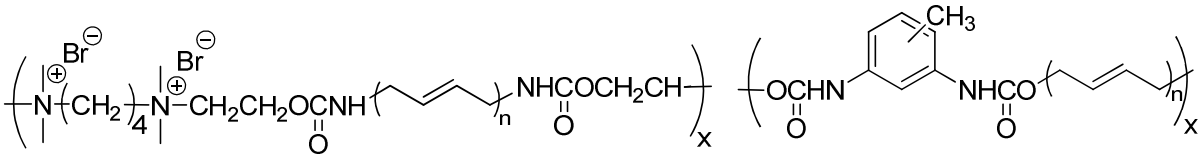

Figure 1.16. Chemical structure of polybutadiene on the left and polybutadiene urethane on the right[61]

The solubility, tensile strength, and thermoplastic behavior of PBI compared to PBU were determined. They studied the effect of ionic segments on the solubility of PBI. The solubility of polybutadiene did not change significantly. The low ionic content of the ionene did not alter the solubility property of polybutadiene.

The mechanical properties of PBI and PBU were compared using tensile strength at break (T_B) and the elongation at break (E_B). PBI showed significantly larger T_B and E_B than PBU at room temperature. These results suggested that PBI contained non-covalent crosslinking. As mentioned earlier, ionic groups in ionenes can aggregate and produce ionic clusters, which lead to physical crosslinking.

Burmistr et al.[62] showed the use of ammonium-based ionenes as surface modifiers in clay-based nanocomposites (Figure 1.17). The surface modifier reduces the surface energy of clay and improves its wettability. The role of ionene cations in the organosilicate is to decrease the surface energy of clay and enhance its wetting characteristics with the polymer. Ammonium-based ionenes have higher thermal stability in comparison with low molecular weight quaternary ammonium salts and aliphatic amines. Also ionenes are effective inhibitors of oxidizing degradation. These make ionenes good candidates as surface modifiers.

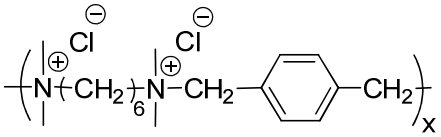

Figure 1.17. Chemical structure of ammonium-based ionene as surface modifier[62]

Ionene showed in Figure 1.17 was mixed with bentonite clay. Ionene bentonite-clay were characterized and compared with bentonite-clay using wide-angle x-ray scattering (WAXS) and TGA. The x-ray scattering showed that the bentonite-clay modified with ionene has more

ordered structure. TGA showed that the ionene bentonite-clay degraded faster compared to the bentonite-clay at around 280 ºC.

The ionene bentonite-clay was mixed with polyamide (PA), polystyrene (PS), and polypropylene (PP) to prepare nanocomposites. The tensile strength increased for PA and PS composites containing ionene up to 2 wt%. Increasing ionene-bentonite clay content beyond 2 wt% showed reduced adsorption due to the aggregation of the ionene-clay nanolayers.

The thermal properties of polymer-clay composites were examined using TGA. Similar to the mechanical properties, PA and PS composites have higher thermal stabilities and higher thermal decomposition temperatures than their pure polymers, while PP composites did not show any thermal property changes. The three composites showed distinct thermodegradation properties due to the barrier effect of the layer structure of organo-bentonites. Although PP composites did not show changes, PA and PS composites had different thermodegradation properties.

Feng et al.[63] investigated the structure-property behavior of elastomeric PTMO-based ionenes. These ionenes were synthesized from α,ω-bis(dimethylamino) poly(teramethylene oxide) as the soft segment and dibenzyl halide with various spacers as the hard segment (Figure 1.18).

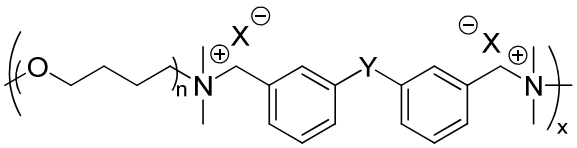

Figure 1.18. Chemical structure of PTMO-based ammonium ionene[63]

These ionenes were similar to segmented urethane ionomers. In particular, their distinct domain formation observed in SAXS analysis was comparable in dimensional scale to urethane ionomers. Thermal and mechanical properties of these ionenes were studied based on four

objectives: 1) molecular weight of the PTMO soft segment 2) counterions (Br^- vs Cl^-) 3) different hard segments 4) charge density.

Ambient temperature stress-strain behavior of ionenes having different molecular weights of PTMO soft segments was measured. PTMO ionenes showed a tensile strength of 40 MPa at 1000% elongation which is significant for elastomeric materials.

As mentioned earlier Ikeda et al.[60] proposed that PTMO-based ammonium ionenes with bromine counterions have shorter and smaller ionic domains compared to PTMO-based ammonium ionenes with chlorine counterions. On the other hand, Feng et al.[63] indicated that for a given level of elongation attained, systems having chlorine counterions consistently show higher stress values compared to systems having bromine counterions. This is due to the fact that chlorine is more electronegative than bromine, therefore promotes better packing and stronger association within ionene species. The difference between the two proposed results by Ikeda et al. and Feng et al.[63] is highly dependant on the chemistry of the ionene samples. Figure 1.12 and Figure 1.18 show the differences in chemical structures.

Table 1.2 shows the effect of spacer group on Young's modulus for ionene samples with either bromine or chlorine counterions. The table represents two sets of Young's modulus measurements: (1) "Fresh" refers to values after heating the sample at 60 ºC for 1-2 hours and quenching to ambient temperature to remove any PTMO crystallinity; (2) "Aged" refers to values obtained after the sample was aged for at least one month at ambient temperature. Regardless of the nature of the halides, ionenes without spacers had higher modulus than ionenes with spacers. Effect of charge on promoting the phase separation is basically related on how far the ionic sites are from one another. If the spacer length between ionic sites is high, therefore the charge density becomes low, which leads to poorer association and weaker phase separation.

Table 1.2. Young's moduli of ionene samples[63]

Sample	Young's modulus (MPa)	
	Fresh[a]	Aged[b]
IB-NS-34	4.1	4.3
IB-NS-35	2.7	35.2
IB-NS-38	3.5	3.3
IB-NS-100	3.1	62.7
IB-S-34	3.5	8.6
IB-S-65	2.6	27.0
IB-S-66	2.3	56.8
IB-S-100	3.1	50.1
IC-NS-38	3.9	3.3
IC-NS-66	3.3	12.2
IC-NS-100	3.6	49.2
IC-S-65	2.7	50.4
IC-S-66	1.8	32.0
IC-S-100	2.6	48.6

1.9 Conclusions

This chapter briefly described the biomedical applications of ammonium ionenes and their structure-property relationships. Due to the positively charged nature of these materials, they have the ability to complex with negatively charged DNA and RNA. This complexation with DNA, also known as polyplex formation, can lead to the efficient introduction of DNA into cells, which is a new avenue in non-viral gene delivery. Moreover, the complexation of ionenes with RNA results in the separation of plasmid DNA from RNA, which has potential for the development of novel bioseparation techniques. In addition, ionenes show antimicrobial properties due to their hydrophobic-hydrophobic interactions with the cell lipid bilayer. These applications are highly dependent on charge density, molecular weight, solution concentration, as well as the hydrophobicity of the ionene, which determines whether the ionene is suitable for gene delivery or antimicrobial applications.

1.10 References

[1] Dobrynin, A. V.; Rubinstein, M. *Prog. Polym. Sci.* **2005,** 30, (11), 1049-1118.

[2] Solis, F. J.; Olvera de la Cruz, M. *J. Chem. Phys.* **2000,** 112, (4), 2030-2035.

[3] Eisenberg, A. a. K., M, *Ion containing polymers: Physical properties and structure*. 1977; Vol. 2.

[4] Kabanov, V. A., *Macromolecular complexes in chemistry and biology*. Springer, Berlin: New York, 1994.

[5] Izumrudov, V. A., *Smart polymers for bioseparation and bioprocessing*. Taylor and Francis: London, 2002.

[6] Cakmak, I.; Ulukanli, Z.; Tuzcu, M.; Karabuga, S.; Genctav, K. *Eur. Polym. J.* **2004,** 40, (10), 2373-2379.

[7] Heath, W. H.; Senyurt, A. F.; Layman, J.; Long, T. E. *Macromol. Chem. Phys.* **2007,** 208, (12), 1243-1249.

[8] Zhang, X.; Collins, L.; Sawyer, G. J.; Dong, X.; Qiu, Y.; Fabre, J. W. *Hum. Gene Ther.* **2001,** 12, (18), 2179-2190.

[9] Malone, R. W.; Hickman, M. A.; Lehmann-Bruinsma, K.; Sih, T. R.; Walzem, R.; Carlson, D. M.; Powell, J. S. *J. Biol. Chem.* **1994,** 269, (47), 29903-7.

[10] Kishida, T.; Asada, H.; Itokawa, Y.; Yasutomi, K.; Shin-Ya, M.; Gojo, S.; Cui, F.-D.; Ueda, Y.; Yamagishi, H.; Imanishi, J.; Mazda, O. *Mol. Ther.* **2003,** 8, (5), 738-745.

[11] Janat-Amsbury, M. M.; Yockman, J. W.; Lee, M.; Kern, S.; Furgeson, D. Y.; Bikram, M.; Kim, S. W. *Mol. Ther.* **2004,** 9, (6), 829-836.

[12] Wang, Y.; Gao, S. J.; Ye, W. H.; Yoon, H. S.; Yang, Y. Y. *Nature Materials* **2006,** 5, (10), 791-796.

[13] Margolin, A. L.; Sherstyuk, S. F.; Izumrudov, V. A.; Zezin, A. B.; Kabanov, V. A. *Eur. J. Biochem.* **1985,** 146, (3), 625-32.

[14] Wahlund, P.-O.; Izumrudov, V. A.; Gustavsson, P.-E.; Larsson, P.-O.; Galaev, I. Y. *Macromol. Biosci.* **2003,** 3, (8), 404-411.

[15] Hentze, M. W.; Izaurralde, E.; Seraphin, B. *EMBO Reports* **2000,** 1, (5), 394-398.

[16] Khan, J. A.; Kainthan, R. K.; Ganguli, M.; Kizhakkedathu, J. N.; Singh, Y.; Maiti, S. *Biomacromolecules* **2006,** 7, (5), 1386-1388.

[17] Gibbs, C. F.; Marvel, C. S. *J. Am. Chem. Soc.* **1934,** 56, 725-7.

[18] Noguchi, H.; Rembaum, A. *Macromolecules* **1972,** 5, (3), 253-60.

[19] Rembaum, A.; Baumgartner, W.; Eisenberg, A. *J. Polym. Sci., Part C: Polym. Lett.* **1968,** 6, (3), 159-71.

[20] Rembaum, A.; Noguchi, H. *Macromolecules* **1972,** 5, (3), 261-9.

[21] Williams, S. R.; Long, T. E. *Prog. Polym. Sci.* **2009**.

[22] Kohjiya, S.; Ohtsuki, T.; Yamashita, S. *Makromol. Chem., Rapid Commun.* **1981,** 2, (6-7), 417-20.

[23] Kohjiya, S.; Yamashita, S. *Kautsch. Gummi Kunstst.* **1991,** 44, (12), 1128-32.

[24] Dimitrov, I. V.; Berlinova, I. V. *Macromol. Rapid Commun.* **2003,** 24, (9), 551-555.

[25] Burmistr, M. V.; Sukhyy, K. M.; Shilov, V. V.; Pissis, P.; Polizos, G.; Spanoudaki, A.; Gomza, Y. P. *Solid State Ionics* **2005,** 176, (19-22), 1787-1792.

[26] Somoano, R.; Yen, S. P. S.; Rembaum, A. *J. Polym. Sci., Part C: Polym. Lett.* **1970,** 8, (7), 467-79.

[27] Lehman, M. R.; Thompson, C. D.; Marvel, C. S. *J. Am. Chem. Soc.* **1933,** 55, 1977-81.

[28] Casson, D.; Rembaum, A. *Macromolecules* **1972,** 5, (1), 75-81.
[29] Tsutsui, T.; Tanaka, R.; Tanaka, T. *J. Polym. Sci., Part B: Polym. Phys.* **1976,** 14, (12), 2259-71.
[30] Meyer, W. H.; Rietz, R. R.; Schaefer, D.; Kremer, F. *Electrochim. Acta* **1992,** 37, (9), 1491-4.
[31] Klun, T. P.; Wendling, L. A.; Van Bogart, J. W. C.; Robbins, A. F. *J. Polym. Sci., Part A: Polym. Chem.* **1987,** 25, (1), 87-109.
[32] Rembaum, A. *Applied Polymer Symposia* **1973,** No. 22, 299-317.
[33] Narita, T.; Ohtakeyama, R.; Nishino, M.; Gong, J. P.; Osada, Y. *Colloid. Polym. Sci.* **2000,** 278, (9), 884-887.
[34] Tashiro, T. *Macromol. Mater. Eng.* **2001,** 286, (2), 63-87.
[35] Jen, J. S.; Jones, R. E.; Homesley, P. M.; Petisce, J. Methods for providing biomedical devices with hydrophilic antimicrobial coatings. 2005-68008 2006193894, 20050228., 2006.
[36] Lan, J.; Vanderlaan, D.; Willcox, M.; Aliwarga, Y. Biomedical devices with antimicrobial cationic peptide and protein coatings. 2001-US4524 2002064183, 20010209., 2002.
[37] Lydon, M.; Gravett, D. M.; Whitbourne, R. J. Antimicrobial needle coating for extended infusion. 2005-US40512 2006053007, 20051109., 2006.
[38] Fitzpatrick; Richard J. (Marblehead, M., Shackett; Keith K. (Athol, MA), Klinger; Jeffrey D. (Sudbury, MA) Ionene polymers and their use as antimicrobial agents 6,955,806, January 17, 2002.
[39] Anderson, W. F. *Science* **1992,** 256, (5058), 808-13.
[40] Nazir, S. A.; Metcalf, J. P. *J. Investig. Med.* **2005,** 53, (6), 292-304.
[41] Ledley, F. D. *Hum. Gene Ther.* **1995,** 6, (9), 1129-44.
[42] Ferrari, S.; Geddes, D. M.; Alton, E. W. F. W. *Adv. Drug Del. Rev.* **2002,** 54, (11), 1373-1393.
[43] Nguyen, T. T.; Grosberg, A. Y.; Shklovskii, B. I. *J. Chem. Phys.* **2000,** 113, (3), 1110-1125.
[44] Storrie, H.; Mooney, D. J. *Adv. Drug Del. Rev.* **2006,** 58, (4), 500-514.
[45] Zelikin, A. N.; Putnam, D.; Shastri, P.; Langer, R.; Izumrudov, V. A. *Bioconjugate Chem.* **2002,** 13, (3), 548-553.
[46] Godbey, W. T.; Wu, K. K.; Mikos, A. G. *J. Biomed. Mater. Res.* **1999,** 45, (3), 268-275.
[47] Trukhanova, E. S.; Izumrudov, V. A.; Litmanovich, A. A.; Zelikin, A. N. *Biomacromolecules* **2005,** 6, (6), 3198-3201.
[48] Wolfert, M. A.; Dash, P. R.; Nazarova, O.; Oupicky, D.; Seymour, L. W.; Smart, S.; Strohalm, J.; Ulbrich, K. *Bioconjugate Chem.* **1999,** 10, (6), 993-1004.
[49] Zelikin, A. N.; Akritskaya, N. I.; Izumrudov, V. A. *Macromol. Chem. Phys.* **2001,** 202, (15), 3018-3026.
[50] Schaffer, D. V.; Fidelman, N. A.; Dan, N.; Lauffenburger, D. A. *Biotechnol. Bioeng.* **2000,** 67, (5), 598-606.
[51] Ikeda, Y.; Murakami, T.; Urakawa, H.; Kohjiya, S.; Grottenmuller, R.; Schmidt, M. *Polymer* **2002,** 43, (12), 3483-3488.
[52] Leir, C. M.; Stark, J. E. *J. Appl. Polym. Sci.* **1989,** 38, (8), 1535-47.
[53] Feng, D.; Wilkes, G. L.; Lee, B.; McGrath, J. E. *Polymer* **1992,** 33, (3), 526-535.

[54] Feng, D.; Venkateshwaran, L. N.; Wilkes, G. L.; Leir, C. M.; Stark, J. E. *J. Appl. Polym. Sci.* **1989,** 37, 1549-1565.
[55] Ikeda, Y.; Murakami, T.; Yuguchi, Y.; Kajiwara, K. *Macromolecules* **1998,** 31, (4), 1246-1253.
[56] Jeon, S. I.; Lee, J. H.; Andrade, J. D.; De Gennes, P. G. *J. Colloid Interface Sci.* **1991,** 142, (1), 149-58.
[57] Han, H.; Vantine, P. R.; Nedeltchev, A. K.; Bhowmik, P. K. *J. Polym. Sci, Part A : Polymer Chemistry* **2006,** 44, 1541-1554.
[58] Burmistr, M. V.; Sukhyy, K. M.; Shilov, V. V.; Pissis, P.; Polizos, G.; Spanoudaki, A.; Gomza, Y. P. *Solid State Ionics* **2005,** 176, 1787-1792.
[59] Klun, T. P.; Wendling, L. A.; Van Bogart, J. W. C.; Robbins, A. F. *Journal of Polymer Science, Part A: Polymer Chemistry* **1987,** 25, (1), 87-109.
[60] Ikeda, Y.; Yamato, J.; Murakami, T.; Kajiwara, K. *Polymer* **2004,** 45, (25), 8367-8375.
[61] Yamashita, S.; Itoi, M.; Kohjiya, S.; Kidera, A. *J. Appl. Polym. Sci.* **1988,** 35, (7), 1927-35.
[62] Burmistr, M. V.; Sukhyy, K. M.; Shilov, V. V.; Pissis, P.; Spanoudaki, A.; Sukha, I. V.; Tomilo, V. I.; Gomza, Y. P. *Polymer* **2005,** 46, (26), 12226-12232.
[63] Feng, D.; Venkateshwaran, L. N.; Wilkes, G. L.; Leir, C. M.; Stark, J. E. *J. Appl. Polym. Sci.* **1989,** 38, (8), 1549-65.

Chapter 2. Structure-Property Relationships of Water-Soluble, 12,6/12-Random Copolymer Ammonium Ionenes

2.1 Abstract

Water-soluble random copolymer ammonium ionenes with different charge densities were synthesized using the Menshutkin reaction from 1,12-dibromododecane, *N*,*N*,*N*′,*N*′-tetramethyl-1,6-hexanediamine, and 1,12-bis(*N*,*N*-dimethylamino)dodecane. The macromolecular structures were confirmed by ^{1}H NMR spectroscopy. *In situ* FTIR spectroscopy revealed that the reaction completes upon 20 h. The absolute weight-average molecular weights in the range of 17000 g/mol to 20000 g/mol were determined using multiangle laser light scattering (MALLS) detector in aqueous size exclusion chromatography (SEC). All ionenes showed a single glass transition temperature (T_g) using differential scanning calorimetry (DSC). Thermogravimetric analysis (TGA) showed a one step degradation. The degradation temperature was observed around 248 ºC. The ionene films were too brittle and were not suitable for mechanical property measurements. The morphology was examined using small angle x-ray scattering. Cell viability of human brain microvascular endothelial cells (HBMEC) were studied in the presence of ionene solutions. There was not a direct correlation between ionene charge density and cell viability.

Keywords

Ammonium ionene copolymers, thermal properties, small angle x-ray scattering, cytotoxicity

2.2 Introduction

Ionenes are ion-containing polymers that have quaternary nitrogen atoms in their macromolecular backbone. Ionenes are usually synthesized from the reaction of a ditertiary amine and the dihalide called Menchutkin reaction.[1] The ionene is named from the number of methylene spacers, which correspond to the diamine and dihalide monomers, respectively (i.e. x,y-ionene). Gibbs et al.[2] were first to synthesize this type of polycations from dimethylamino-N-alkyl halides. Kern et al.[3] were first to report that ionenes were synthesized through the Menchutkin reaction. Rembaum et al.[4-6] synthesized ionenes and explored the polymerization rates in different solvents. Two general types of ionenes are synthesized; segmented [7-11] and non-segmented [2, 4, 12-15]. Segmented ionenes have elastomeric low T_g oligomeric spacers (e.g. PTMO, PPG) between their ionic sites. They show elastomeric properties and resemble urethane ionomers. Non-segmented ionenes (e.g. 12,12-ionene) have shorter spacers (e.g. methylene units) between their charged sites and thus have higher charge densities. Factors that affect the polymerization of non-segmented ionenes include solvent, reaction temperature, time, and monomer concentration.

The critical and challenging factor in charged polymers is their molecular weight determination. The difficulty is due to ionic aggregation[16], non-size exclusion events[17], and electrostatic interactions with negatively charged stationary phase[18]. Previously, SEC analyses on ionenes were limited to relative molecular weight calculations which corresponded to standard equivalent molecular weights. Kopecka et al.[19] obtained relative molecular weights for 5,2 and 10,2-ionenes using polyacrylamide standards. Reisinger et al.[20] determined relative molecular weights of ionenes using poly(vinylpyridinium) standards. Recently from our laboratories, Layman et al.[21] accomplished absolute weight-average molecular weights for

12,12- and 6,12-ionenes using multiangle laser light scattering (MALLS) detector with aqueous size exclusion chromatography (SEC). Williams et al.[22] used absolute weight-average molecular weights for structure-property characterization of 12,12-ionenes.

One of the specifications of ionenes is their high thermal stability. The presence of quaternized nitrogens throughout the main chain, makes ionenes thermally stable to ~225-250 ^{o}C.[14, 22] The ionic association in ion-containing polymers is termed physical crosslinking as well. Physical crosslinking in ion-containing polymers raises the glass transition temperature compared to their nonionic counterparts.[23] The distance between charge sites in ionenes can be long-chain elastomeric, low T_g oligomeric segments (segmented) or short-chain rigid segments (non-segmented). The long chain elastomeric segment has higher chain mobility which corresponds to low T_g ionenes. The short-chain segments decrease the mobility of the main chain and increase the T_g. The glass transition temperature of ionenes is also dependent on the chemical structure and the size of counterion. Meyer et al.[15] showed that larger counterions (tetraphenylborate or ethylorangesulfonate) led to less packing and lower T_g's, on the other hand smaller counterion such as BF_4^- induced better packing and raised the T_g. The T_g of a polymer is highly dependant on its molecular weight.[24] Williams et al.[22] varied the stoichiometric balance of monomers, controlled the molecular weight of 12,12-ionenes and showed an increase in T_g with increase in the molecular weight.

In ionenes the ionic sites are systematically situated throughout the backbone and provide us an ease to investigate the effect of charge density or ion concentration on mechanical properties as well as thermal properties. Tanaka et al.[14] synthesized x,y-ionenes, x = 6,12 and y = 3~10, and performed dynamic mechanical analysis to study the effect of ion concentration on mechanical relaxations. Three mechanical relaxations were seen, T_α, T_β, and T_γ. T_α or T_g was

dependant on the ion concentration of the polymers. T_α was inversely proportional to the average spacing ((x+y)/2) between ionic sites. The ion concentration decreases as the spacing between ionic sites increase, this lowers the electrostatic repulsion which leads to more chain mobility and lower T_α or T_g values. Williams et al.[22] studied the relationships between the molecular weight and mechanical behavior of 12,12-ionene series using dynamic mechanical analysis (DMA) and tensile measurements. Two transitions were observed for 12,12-ionenes, T_g and ionic dissociation temperature. Despite T_g, ionic dissociation temperature was independent of molecular weight and was around 85-88 ºC. This was due to ionic content remaining constant as the molecular weight was increased.

Water-soluble ionenes offer many potential biomedical applications. Earlier research in non-viral gene delivery showed that cationic ionenes can complex DNA and allow the introduction of DNA into cells.[25-29] This is particularly important since viral vectors have several disadvantages including activation of the host immune response, limited DNA carrying capacity, and high cost. One potential limitation of ionenes is the presence of permanent positive charge on quaternized nitrogens throughout the backbone. The endosomal polyplex release is pH sensitive and for high transfection efficiency, the polymer needs to buffer the endosome.[30, 31] Ionenes with permanent charge lack the pH control and corresponding endosomal release. However, ionenes are good polyelectrolyte models in gene therapy.

Ionenes show pronounced antimicrobial properties compared to low molecular weight ammonium salts due to the cooperative effect of high charge density throughout the backbone.[32] Narita et al.[33] showed that ionenes with longer hydrophobic segments and therefore lower charge density are more destructive to cells than ionenes with higher charge density. Ionenes with higher charge density can bind to cells more efficiently, but do not disrupt the cell

membrane.[34] In addition, other applications of ionenes are components of cosmetics[35], photovoltaic cells[36], and flocculants for water treatments.

In this chapter the synthesis and structure-property characterization of a new random copolymer ammonium ionenes will be discussed.

2.3 Experimental

2.3.1 Materials

1,12-dibromododecane (98%) was purchased from Sigma-Aldrich and recrystallized from ethanol and dried in *vacuo* (0.1 mmHg) for 24 h before the polymerization reaction. *N*,*N*,*N*′,*N*′-tetramethyl-1,6-hexanediamine (99%) was purchased from Acros Organics and was distilled from calcium hydride. Methanol (MeOH, Fisher, HPLC grade) was distilled from calcium hydride. Dimethylamine solution (60% in water) was purchased from Aldrich. Tetrahydrofuran (THF, EMD Science, HPLC grade), diethyl ether (Fisher, 99.9%, anhydrous) and sodium hydroxide (Mallinckrodt Chemicals, 99%) were used as received.

2.3.2 Synthesis of 1,12-bis(*N*,*N*-dimethylamino)dodecane

The synthesis of this monomer was based on a modified literature procedure.[37] 1,12-dibromododecane (10.10 g, 0.0308 mol) was introduced into a round-bottomed flask containing THF (125 mL). The solution was cooled to -78 ºC for 30 minutes. Dimethylamine (478 mL, 60% in water) was added to the flask slowly. The flask was warmed to 23 ºC and stirred for 24 h. Upon reaction completion, the solvent was removed with rotary evaporator. Subsequent white residue was redissolved in diethyl ether and 2.0 M NaOH(aq). The mixture was stirred for 2 h. The ether layer was separated with separatory funnel and dried over magnesium sulfate. Ether

was evaporated and a yellow crude product was obtained. The product was further purified via vacuum distillation (100 ºC and 150 mTorr). A transparent liquid was obtained in 47% yield. ^{1}H NMR (400 MHz, CD_3OD): δ = 2.26 (t, 4H), 2.19 (s, 12H), 1.45 (dd, 4H), 1.26 (s, 16H). ^{13}C NMR (100 MHz, CD_3OD): δ = 123.8, 59.7, 44.3, 29.6, 29.5, 27.5, 27.2. FAB-MS (m/z calculated = 256.48, found = 257.29).

2.3.3 Synthesis of 12,6/12-ammonium ionenes

A series of 12,6/12-ammonium ionenes having various molar ratios of monomers (Table 2.1) were synthesized through step-growth polymerization. A flame-dried, 50 mL, two-neck, round-bottomed flask equipped with a condenser, stirrer and purging N_2 was charged with 1:1 equivalent ratio of diamines to dibromide. The diamines used were *N*,*N*,*N*′,*N*′-tetramethyl-1,6-hexanediamine and 1,12-bis(*N*,*N*-dimethylamino)dodecane and the dibromide was 1,12-dibromododecane. Distilled methanol was added to the reaction flask via syringe (20 wt% solids). Polymerization was performed for 24 h under reflux condition.

Table 2.1. Monomer molar ratios

Sample	1,12-Dibromo dodecane	*N*,*N*,*N*′,*N*′-Tetramethyl-1,6-hexanediamine	1,12-Bis(*N*,*N*-dimethylamino)dodecane
1	1.0	0	1
2	1.0	0.1	0.9
3	1.0	0.2	0.8
4	1.0	0.4	0.6
5	1.0	0.5	0.5
6	1.0	0.6	0.4
7	1.0	0.8	0.2
8	1.0	0.9	0.1
9	1.0	1.0	0

2.3.4 Preparation of ionene films

Upon reaction completion, the polymer solution was poured into a Teflon mold (30 mm x 25 mm). Slow removal of methanol was critical in order to avoid bubbles. The films were dried at

room temperature for 2-3 days. Subsequently, the polymer films were heated up to 70 ºC for 2 days, and eventually dried in *vacuo* (0.1 mmHg) for 24 h to ensure complete removal of methanol. Ionene films were stored in petri dishes containing dririte and placed in desiccator until their thermal and morphological properties were measured.

2.3.5 Cell culture

Human Brain Microvascular Endothelial cells (HBMEC) were isolated and harvested as previously described.[38] These cells were positive for factor VIII-Rag, carbonic anhydrase IV, Ulex Europeus Agglutinin I, and took up fluorescently labeled low-density lipoprotein and expressed γ glutamyl transpeptidase, demonstrating their brain endothelial cell characteristics. Contamination of nonendothelial cells such as pericytes and glial cells was less than 1%. HBMEC were cultured in RPMI 1640-based medium enriched with 10% fetal bovine serum (Mediatech), 10% NuSerum (Becton Dickinson), 30 μg/mL of endothelial cell growth supplement (ECGS; Becton Dickinson), 15 U/mL of heparin (Sigma), 2 mM L-glutamine, 2 mM sodium pyruvate, nonessential amino acids, vitamins, 100 U/mL of penicillin, and 100 μg/mL of streptomycin (all reagents from Mediatech). Cultures were incubated at 37 °C in a humid atmosphere of 5% CO2.

2.3.6 Cell viability assay

Cell viability was determined with CellTiter 96® non-radioactive cell proliferation assay. The HBMEC were harvested. A 100 µL cell suspension was introduced to a 96 well plate (5x103 cells/well) and incubated for 24h at 37 ºC, 5% CO_2. Ionene solutions were prepared at 1 mg/mL in PBS and 100 µL of this solution was added to each well. The plate was incubated for 24h at

37 ºC, 5% CO_2. 100 µL of MTT solution was added to each well and was incubated for 4h at 37 ºC, 5% CO_2. Solubilization DMSO solution (100 µL) was added to each well and mixed (rocking) for 30 min. Absorbance at 570 nm was measured for each well.

2.4 Characterization

^{1}H NMR was utilized to confirm the monomer and polymer compositions in $CDCl_3$ and CD_3OD at 23 ºC with a 400 MHz Varian Inova spectrometer. *In situ* FTIR analysis was performed on a Metler Toledo React IR 4000 instrument with a stainless steel ATR probe. An average absorbance was plotted every 5 minutes from 256 infrared scans for 24 h. FAB-MS was obtained on a JEOL HX110 dual focusing mass spectrometer. Thermogravimetric analysis (TGA) was conducted on a TA Instruments Hi-Res TGA 2950 with a heating rate of 10 ºC/min under a nitrogen atmosphere. Differential scanning calorimetery (DSC) was conducted on a TA Instruments Q100, under nitrogen at 10 ºC/min. Size exclusion chromatography (SEC) was performed on Waters size exclusion chromatograph using a mobile phase that was recently developed in our research group.[21] The SEC was equipped with a Waters 1515 isocratic HPLC pump, a Waters 717plus autosampler, a Wyatt miniDAWN multiangle laser light scattering (MALLS) detector operating a He-Ne laser at 690 nm, a Waters 2414 differential refractive index detector operating at a wavelength of 880 nm and 35 ºC, and a Viscotek 270 viscosity detector. Samples were run at 0.8 mL/min through 2x Waters Ultrahydrogel linear columns and 1x Waters Ultrahydrogel 250 column, with all columns measuring at 7.8 x 300 mm and equilibrated to 30 ºC. The mobile phase was a ternary mixture comprised of 54/23/23 (v/v/v) water/methanol/glacial acetic acid, 0.54 M NaOAc, pH = 4. The mobile phase was vacuum filtered through NALGENE® MF75^{TM} Series Media-Plus Filter Units with a minimum pore size of 0.200 µm. The specific refractive index increment (dn/dc) was measured using a Wyatt

OptiRex refractive index detector operating at 690 nm and 30 ºC. The dn/dc values were determined using Wyatt Astra V software. Small angle x-ray scattering was performed on solvent-cast dried films. The multiangle x-ray scattering system (MAXS) generated Cu x-ray from a Nonius FR 591 rotating-anode generator operated at 40 kV and 85 mA. The beam was focused by doubly focusing mirror-monochromator optics in an integral vacuum system. The scattering data were collected over an interval of 1 h using a Bruker Hi-Star multiwire detector with a sample-to-detector distance of 11 and 54 cm.

2.5 Results and Discussion

2.5.1 Effect of charge density on thermal properties and morphology

The goal was to synthesize a series of 12,6/12-ammonium ionenes having various charge densities in order to investigate the effect of charge on thermal, mechanical, biological, and morphological behavior. Therefore, a series of random copolymer ammonium ionenes were synthesized using the Menshutkin reaction (Scheme 2.1). The nomenclature of these ionenes is based on the number of methylene units from diamine monomers (12,6) followed with the number of methylene units from the dibromide monomer (12).

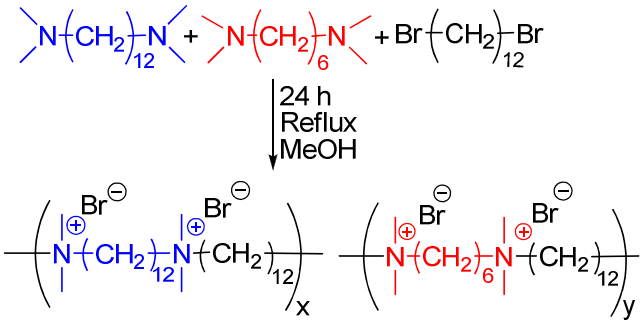

Scheme 2.1. Synthesis of 12,6/12-ammonium ionenes

One of the important parameters in the synthesis of step-growth polymers is to have highly pure monomers. Following the synthesis of 1,12-bis(*N*,*N*-dimethylamino)dodecane, the crude monomer was vacuum distilled and its color was changed from yellow into a clear liquid. *N*,*N*,*N*′,*N*′-tetramethyl-1,6-hexanediamine was distilled from calcium hydride. 1,12-dibromododecane was recrystallized from ethanol. The polymerization reaction took place for 24 h under refluxing methanol. The reaction completion was determined via *in situ* FTIR spectroscopy. Our group has shown that *in situ* FTIR is a great technique to follow reaction progress and explore reaction rates.[39] The reaction of 12,6/12-ionenes was followed with *in situ* FTIR growth to monitor the absorbance of C-N^+ stretch at ~905 cm^{-1} (Figure 2.1). No further growth of C-N^+ stretch was seen after 22 h (Figure 2.2).

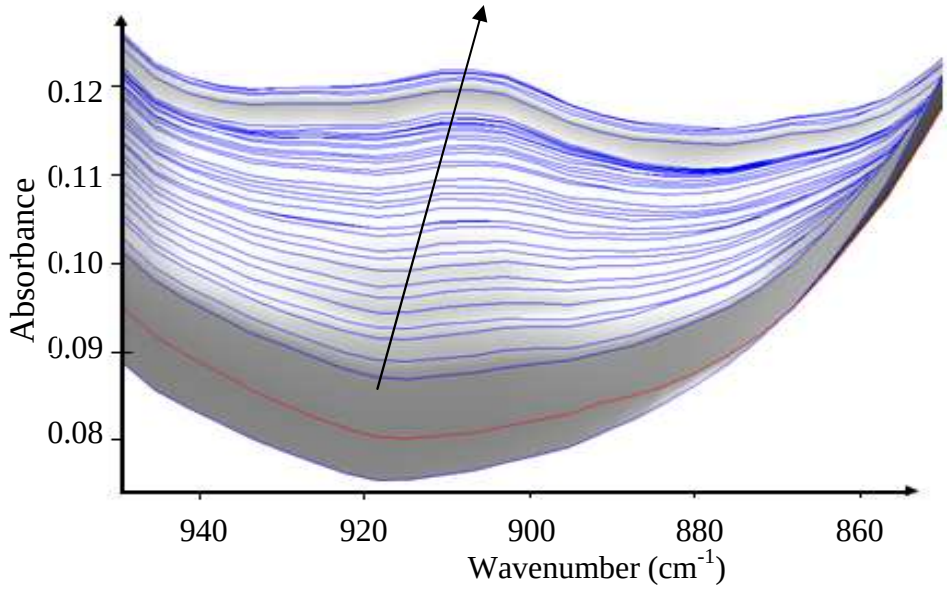

Figure 2.1. *In situ* FTIR spectroscopy of 12,6/12-ammonium ionene indicating a growth at 905 cm^{-1}

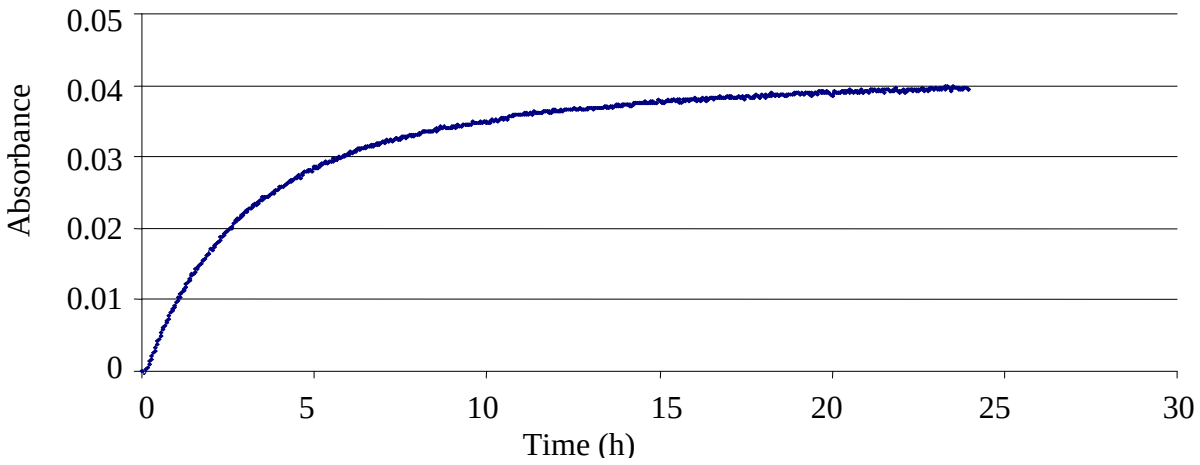

Figure 2.2. Reaction profile for 12,6/12-ammonium ionene at 905 cm^{-1}

The chemical structure of the ionenes was confirmed by ^{1}H NMR spectroscopy (Figure 2.3). The peak at 2.2 ppm, which represents the methyl protons of diamine monomers shifted to ~3.1 ppm in the polymer. This peak is due to the methyl protons connected to the quaternized nitrogens. A 1:1 stoichiometery of diamine to dihalide monomers was used to obtain high molecular weight polymers. The absolute molecular weights of these ionenes were determined using an online multiangle laser light scattering (MALLS) detector in aqueous size exclusion chromatography (SEC). Weight-average molecular weight of these ionene series were in the range of 17000-20000 g/mol.

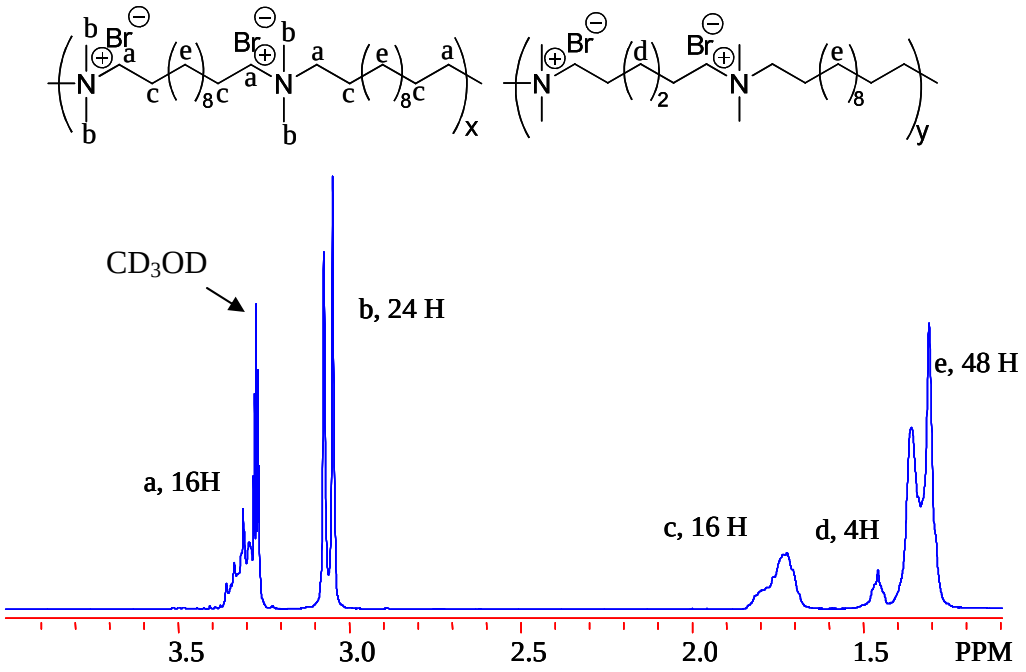

Figure 2.3. ^{1}H NMR (CD_3OD) of 12,6/12-ammonium ionene with 0.5,0.5/1.0 ratios

Thermal properties of ionene series were analyzed using DSC and TGA. The DSC revealed a single T_g for all ionenes. According to Table 2.1, the molar ratio of *N*,*N*,*N*′,*N*′-tetramethyl-1,6-hexanediamine is increasing from top to bottom. Increasing the shorter segment bearing the quaternized nitrogens, will lead to a higher charge density within the polymer backbone. In general, the increase in charge density leads to an increase in T_g.[14] Table 2.2 shows that as the charge density increases, the glass transition temperature increases. Herein, we need to consider that as the ratio of 1,6-diamine is increasing and the ratio of 1,12-diamine is decreasing accordingly, the chain lengths and hence the molecular weight of these ionenes would decrease. Thus, this fact can slightly affect the T_g values.

Table 2.2. Effect of charge density on glass transition temperature T_g

	1,12-diamine : 1,6-diamine: 1,12-dibromododecane	T_g (°C)
Charge density increase ↓	1:0:1	69
	0.9:0.1:1	70
	0.8:0.2:1	72
	0.6:0.4:1	73
	0.5:0.5:1	75
	0.4:0.6:1	79
	0.2:0.8:1	82
	0.1:0.9:1	87
	0:1:1	90

Thermal degradation temperature for all ionenes was determined via TGA. The onset degradation temperature for 12,6/12-ammonium ionene series was at ca. 248 ºC. As previously described, Williams et al.[22] showed that the degradation of 12,12-ammonium ionenes occurred in a single step via the dequaternization of nitrogens through a Hoffman elimination (Figure 2.4).

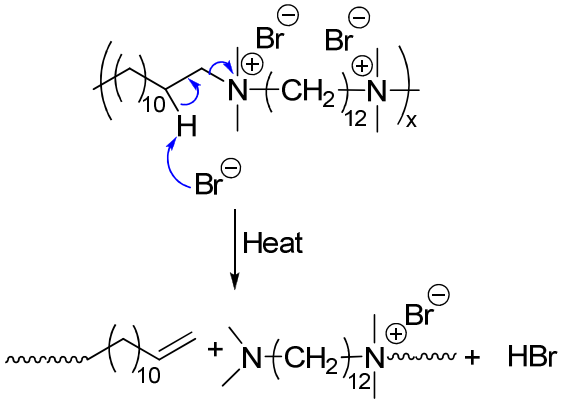

Figure 2.4. Proposed mechanism of Hoffman degradation of 12,12-ammonium ionene[22]

Williams et al.[22] reported a multiangle x-ray scattering profile of 12,12-ionene having 20000 g/mol. Both stretched and unstreched samples were isotropic and showed two peaks at 14 nm^{-1} and 4 nm^{-1} corresponding to amorphous and ionic scattering respectively. The x-ray scattering was performed on the 12,6/12-ionene series as well. In Figure 2.5, ionenes having 0 to 40% of 1,12-bis(*N*,*N*-dimethylamino)dodecane showed two peaks. The peak having the Bragg distance

$d_1 \sim$ 0.4 nm is proposed to be an amorphous peak and the one having $d_2 \sim$ 1.6 nm is considered to be a scattering of ionic aggregates. The Bragg distance, d_2 decreases slightly as the mole percentage of 1,12-bis(*N*,*N*-dimethylamino)dodecane increases. If all methylene units have a trans conformation, d_2 correlates with the real space distance of 12 methylene units. The Bragg distance, d_3 peak around 7 nm was observed for ionenes having 50 to 90% 1,12-bis(*N*,*N*-dimethylamino)dodecane. In the ionene sample having 50% of 1,12-bis(*N*,*N*-dimethylamino)dodecane, the d_3 peak is very significant. Increasing the 1,12-bis(*N*,*N*-dimethylamino)dodecane monomer ratio causes this peak to broaden. In the 12,12-ionene the complete disappearance of this peak is observed. It is hypothesized that d_3 corresponds to the scattering of nanophase aggregates that are in sheet-like or lamellar configuration. The next step to obtain a better understanding of this peak was to stretch the sample and investigate a change in orientation. Figure 2.6 shows that ionene having 50% 1,12-bis(*N*,*N*-dimethylamino)dodecane monomer showed anisotropy upon stretching. Nanophase aggregates seem to orient along the stretched direction. Table 2.3 lists the thermal properties and Bragg distances of random copolymer ammonium ionene series.

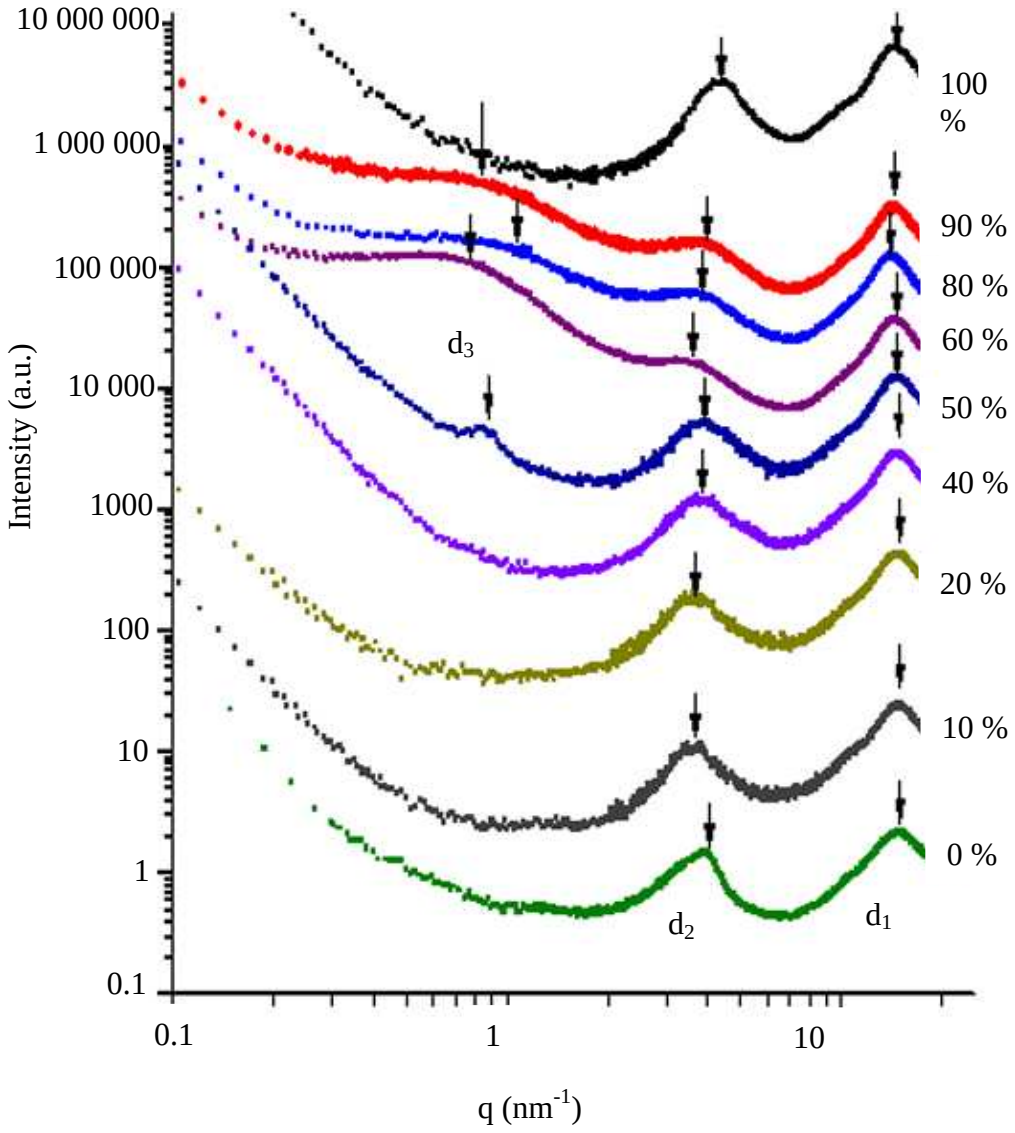

Figure 2.5. Small angle x-ray scattering of 12,6/12-ammonium ionene series

Un-stretched

Stretched

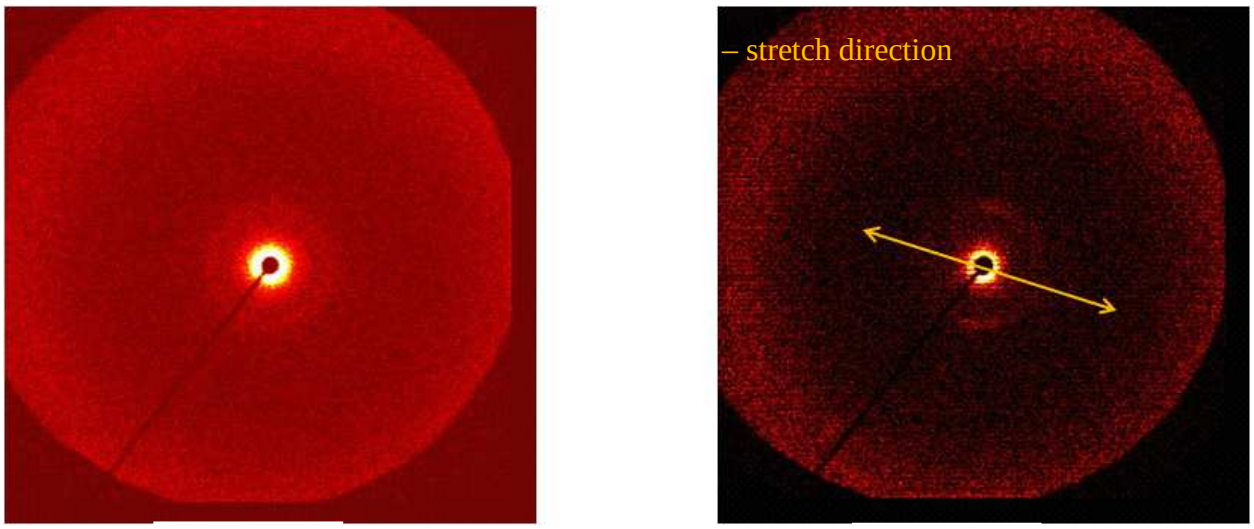

Isotropic

Anisotropic

Figure 2.6. 2-D x-ray scattering of stretched and un-stretched 12,6/12-ammonium ionene with 0.5,0.5/1.0 ratios

Table 2.3. Bragg spacings of 12,6/12-ammonium ionene series

Monomer molar ratios	**Bragg Spacings (nm)**		
1,12-diamine : 1,6-diamine: 1,12-dibromododecane	**d_1**	**d_2**	**d_3**
1:0:1	0.432	1.420	-
0.9:0.1:1	0.440	1.55	6.75
0.8:0.2:1	0.440	1.51	6.16
0.6:0.4:1	0.420	1.67	7.85
0.5:0.5:1	0.424	1.62	7.30
0.4:0.6:1	0.424	1.64	-
0.2:0.8:1	0.417	1.71	-
0.1:0.9:1	0.416	1.74	-
0:1:1	0.412	1.58	-

2.5.2 Effect of charge density on cytotoxicity of 12,6/12-ammonium ionenes

In order to investigate the cytotoxicity of random copolymer ionene series, 3-(4,5-dimethylthiazol-2-yl)-2,5-diphenyltetrazolium bromide called MTT assay was performed on three 12,6/12-ionene samples within the series. The 12,6/12-ammonium ionene series having different molar ratios of monomers and therefore different charge densities gave an opportunity

to investigate the effect of charge density on cytotoxicity of a number of these ionenes. The MTT assay was performed on three different ionenes with various molar ratios. On cellular level using an MTT assay, mitochondria of living cells reduces yellow MTT (tetrazolium salt) to purple formazon. The absorbance of purple formazon is measured at 570 nm and relates to number of cells that are alive. Three ionenes used are listed in Table 2.4. The ionene concentrations used for the MTT assay ranged from 1-100 µg/mL. One control well without polymer was used for all the experiments. Figure 2.7 illustrates the viability of HBMEC as a function of 12,6/12-ammonium ionene concentrations. We were interested in looking at the effect of charge density on cell viability. Interestingly, there was not a direct correlation between ionene charge density and cell viability. The ionenes were highly toxic. A considerable cell death was observed for concentration of 10 µg/mL and higher for the three ionene samples having different molar ratios.

Table 2.4. Monomer molar ratios of ionenes used for MTT assay

1,12-diamine:1,6-diamine:Br-1,12-Br
1:0:1
0.2:0.8:1
0.1:0.9:1

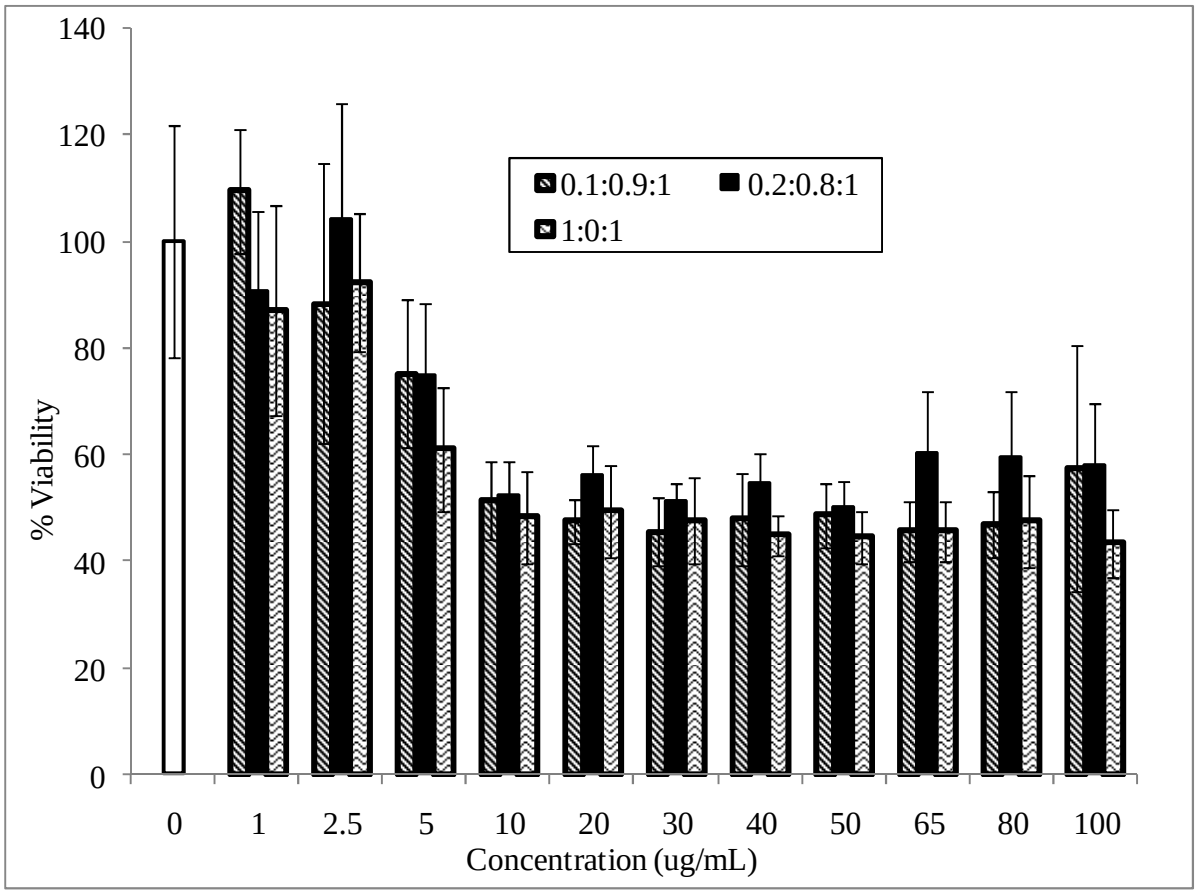

Figure 2.7. MTT assay for HBMEC having various concentrations of 12,6/12-ammonium ionenes

2.6 Conclusions

A series of water-soluble random copolymer ionenes were synthesized from 1,12-dibromododecane, *N*,*N*,*N*′,*N*′-tetramethyl-1,6-hexanediamine, and 1,12-bis(*N*,*N*-dimethylamino)dodecane via the Menshutkin reaction. ^{1}H NMR spectroscopy confirmed the ionene structures. *In situ* FTIR spectroscopy revealed that the reaction completes upon 20 h. Ionenes showed a single glass transition temperature. Their glass transition temperature increased from 69 ºC to 90 ºC as the charge density of ionenes increased. The ionenes thermally degraded in one step. The onset degradation temperature was observed at around 248 ºC. These ionenes were too brittle and not suitable for mechanical property measurements. The x-ray

scattering indicated the formation of ionic domains. The MAXS profile indicated an amorphous peak at 14 nm^{-1}, and second scattering peak around 4 nm^{-1}. Ionenes having 0.5-0.9 molar ratios of 1,12-bis(*N*,*N*-dimethylamino)dodecane monomer showed a scattering peak at $\sim$ 1 nm^{-1}. In addition the effect of charge density on cell viability was investigated. Interestingly there was no correlation between charge density and cell viability. A considerable HBMEC death was seen from 10 µg/mL and higher.

2.7 Acknowledgements

We would like to acknowledge Mr. David Salas-de la Cruz and Karen Winey in the Department of Chemical and Biomolecular Engineering, and the Department of Material Science Engineering, at the University of Pennsylvania, Philadelphia, PA for performing the SAXS analysis. This work is based upon work supported by the Kimberly-Clark Corporation.

2.8 References

[1] Abboud, J. L. M.; Notario, R.; Bertran, J.; Sola, M. *Progress in Physical Organic Chemistry* **1993,** 19, 1-182.
[2] Gibbs, C. F.; Marvel, C. S. *J. Am. Chem. Soc.* **1934,** 56, 725-7.
[3] Kern, W.; Brenneisen, E. *Journal fuer Praktische Chemie (Leipzig)* **1941,** 159, 219-40.
[4] Rembaum, A.; Baumgartner, W.; Eisenberg, A. *J. Polym. Sci., Part C: Polym. Lett.* **1968,** 6, (3), 159-71.
[5] Noguchi, H.; Rembaum, A. *Macromolecules* **1972,** 5, (3), 253-60.
[6] Hadek, V., Noguchi, H., Rembaum, A. *Polymer Preprints* **1971,** 12, (90).
[7] Kohjiya, S.; Ohtsuki, T.; Yamashita, S. *Makromol. Chem., Rapid Commun.* **1981,** 2, (6-7), 417-20.
[8] Kohjiya, S.; Yamashita, S. *Kautsch. Gummi Kunstst.* **1991,** 44, (12), 1128-32.
[9] Dimitrov, I. V.; Berlinova, I. V. *Macromol. Rapid Commun.* **2003,** 24, (9), 551-555.
[10] Burmistr, M. V.; Sukhyy, K. M.; Shilov, V. V.; Pissis, P.; Polizos, G.; Spanoudaki, A.; Gomza, Y. P. *Solid State Ionics* **2005,** 176, (19-22), 1787-1792.
[11] Somoano, R.; Yen, S. P. S.; Rembaum, A. *J. Polym. Sci., Part C: Polym. Lett.* **1970,** 8, (7), 467-79.
[12] Lehman, M. R.; Thompson, C. D.; Marvel, C. S. *J. Am. Chem. Soc.* **1933,** 55, 1977-81.
[13] Casson, D.; Rembaum, A. *Macromolecules* **1972,** 5, (1), 75-81.
[14] Tsutsui, T.; Tanaka, R.; Tanaka, T. *J. Polym. Sci., Part B: Polym. Phys.* **1976,** 14, (12), 2259-71.

[15] Meyer, W. H.; Rietz, R. R.; Schaefer, D.; Kremer, F. *Electrochim. Acta* **1992,** 37, (9), 1491-4.
[16] Wittgren, B.; Welinder, A.; Porsch, B. *J. Chromatogr. A* **2003,** 1002, (1-2), 101-109.
[17] Wu, C., *Handbook of size exclusion chromatography*. Marcel Dekker: New York: 1995.
[18] Jiang, X.; Horst, A.; Steenbergen, M. J.; Akeroyd, N.; Nostrum, C. F.; Schoenmakers, P. J.; Hennink, W. E. *Pharm. Res.* **2006,** 23, (3), 595-603.
[19] Kopecka, K.; Tesarova, E.; Pirogov, A.; Gas, B. *J. Sep. Sci.* **2002,** 25, (15-17), 1027-1034.
[20] Reisinger, T.; Meyer, W. H.; Wegner, G.; Haase, T.; Schultes, K.; Wolf, B. A. *Acta Polym.* **1998,** 49, (12), 710-714.
[21] Layman, J. M.; Borgerding, E. M.; Williams, S. R.; Heath, W. H.; Long, T. E. *Macromolecules* **2008,** 41, (13), 4635-4641.
[22] Williams, S. R.; Borgerding, E. M.; Layman, J. M.; Wang, W.; Winey, K. I.; Long, T. E. *Macromolecules* **2008,** 41, (14), 5216-5222.
[23] Eisenberg, A. a. K., M, *Ion containing polymers: Physical properties and structure*. 1977; Vol. 2.
[24] Odian, G., *Principles of polymerization*. Fourth ed.; John Wiley & Sons, Inc., Hoboken: New Jersey, 2004.
[25] Li, S. D.; Huang, L. *Gene Ther.* **2006,** 13, (18), 1313-1319.
[26] Storrie, H.; Mooney, D. J. *Adv. Drug Del. Rev.* **2006,** 58, (4), 500-514.
[27] Elouahabi, A.; Ruysschaert, J. M. *Mol. Ther.* **2005,** 11, (3), 336-347.
[28] Trukhanova, E. S.; Izumrudov, V. A.; Litmanovich, A. A.; Zelikin, A. N. *Biomacromolecules* **2005,** 6, (6), 3198-3201.
[29] Nguyen, T. T.; Grosberg, A. Y.; Shklovskii, B. I. *J. Chem. Phys.* **2000,** 113, (3), 1110-1125.
[30] Putnam, D.; Gentry, C. A.; Pack, D. W.; Langer, R. *Proc. Natl. Acad. Sci. U. S. A.* **2001,** 98, (3), 1200-1205.
[31] Zhao, X.; Pan, F.; Zhang, Z.; Grant, C.; Ma, Y.; Armes, S. P.; Tang, Y.; Lewis, A. L.; Waigh, T.; Lu, J. R. *Biomacromolecules* **2007,** 8, (11), 3493-3502.
[32] Rembaum, A. *Applied Polymer Symposia* **1973,** No. 22, 299-317.
[33] Narita, T.; Ohtakeyama, R.; Nishino, M.; Gong, J. P.; Osada, Y. *Colloid. Polym. Sci.* **2000,** 278, (9), 884-887.
[34] Tashiro, T. *Macromol. Mater. Eng.* **2001,** 286, (2), 63-87.
[35] Jacquet, B.; Lang, G. Quaternized polymer for use as a cosmetic agent in cosmetic compositions for the hair and skin. 77-849657
4217914, 19771108., 1980.
[36] Factor, A.; Heinsohn, G. E. *J. Polym. Sci., Part C: Polym. Lett.* **1971,** 9, (4), 289-95.
[37] Spencer, T. A.; Onofrey, T. J.; Cann, R. O.; Russel, J. S.; Lee, L. E.; Blanchard, D. E.; Castro, A.; Gu, P.; Jiang, G.; Shechter, I. *J. Org. Chem.* **1999,** 64, (3), 807-818.
[38] Lee, Y. W.; Lee, W. H. *Journal of Nutritional Biochemistry* **2008,** 19, (12), 819-825.
[39] Lizotte, J. R.; Long, T. E. *Macromol. Chem. Phys.* **2004,** 205, (5), 692-698.

Chapter 3. Synthesis and Characterization of Segmented Poly(propylene glycol)-Based Ammonium Ionenes

3.1 Abstract

Bromine end-capped poly(propylene glycol) (PPG) oligomers were successfully synthesized using the reaction of 6-bromohexanoyl chloride with 1000, 2000, and 4000 g/mol PPGs. ^{1}H NMR spectroscopy, titration studies, and MALDI-TOF mass spectrometry revealed the difunctionality of the oligomers. Titration analysis after bromine end-capping also confirmed the absence of hydroxyl functionality. Segmented PPG-based ammonium ionenes were synthesized with the Menshutkin reaction from bromine end-capped PPG oligomers and *N*,*N*,*N*′,*N*′-tetramethyl-1,6-hexanediamine. A 1:1 stoichiometric ratio of diamine to dihalide monomers ensured high molecular weight ionenes. Dynamic mechanical analysis (DMA) and tensile testing established the influence of soft segment (SS) molecular weight and hard segment (HS) content on mechanical properties of segmented ammonium ionenes. In addition, PPG-based ammonium ionenes containing 1,12-dibromododecane, to increase the aliphatic HS content were synthesized to enhance the mechanical properties. Tensile analysis of segmented ionenes with 33 wt% HS at ambient temperature demonstrated an average tensile strength at break ranging from 0.2-2.4 MPa and elongations at break ranging from 20-80%. DMA showed the onset of flow of ionenes containing low HS content ranged from 20-80 ºC, while onset of flow of ionenes containing higher HS content occured in the range of 100-140 ºC. All segmented ionenes showed a single glass transition temperature of approximately -66 ºC. Small angle x-ray scattering (SAXS) profiles showed a single peak at ca. 0.27-0.95 nm^{-1} for the segmented ionenes, which confirmed microphase separation.

Keywords: poly(propylene glycol), segmented ionenes, block copolymer, structure-property relationships

3.2 Introduction

Ammonium polyionenes, or simply ionenes, are ion-containing polymers that have quaternary nitrogen atoms in their macromolecular backbone. Gibbs et al.[1] first synthesized low molecular weight ionenes through a polycondensation reaction of dimethylamino-N-alkyl halides. However, ionenes are usually synthesized from a reaction of a ditertiary amine and a dihalide called the Menshutkin reaction. Rembaum et al.[2-4] synthesized the first aliphatic ionenes using this reaction and explored their solution properties. The ionene is named from the number of methylene spacers, which correspond to the diamine and dihalide monomers, respectively (i.e. x,y-ionene). There are different parameters such as chemical composition, molecular weight, charge density, counterion, solution concentration, and end groups that influence the properties and applications of ionenes.[5] In particular, the ability to tune charge density through monomer selection makes ionenes ideal models for investigating structure-property relationships of well-defined cationic polymers. Two general types of ionenes were synthesized; segmented[6-11] and non-segmented,[1, 4, 11-14] which are either linear, cross-linked, or branched. Segmented ionenes show elastomeric properties and resemble urethane ionomers. Non-segmented ionenes have shorter distances between ionic sites, which lead to higher charge density, water solubility, but poor mechanical properties.

Previously, Leir et al.[12] synthesized poly(tetramethylene oxide) (PTMO) ionenes based on the reaction of α,ω-bis(dimethylamino) PTMO oligomers with 1,4-dibromo-*p*-xylene. Wilkes et al.[13, 14] investigated the structure-property relationships of ionenes possessing poly(tetramethylene oxide) (PTMO) soft segments as a function of molecular weight. The

ionenes were elastomeric and had enhanced tensile strengthes due to strain-induced crystallization of the PTMO segment. SAXS analysis showed multiple scattering peaks which confirmed the microphase separation between the dihalide component compared to the PTMO segment. The ionene having a lower molecular weight PTMO segments showed enhanced mechanical properties compared to the higher molecular weight PTMO segments due to more ionic associations and stronger physical crosslinks. Ikeda et al. [15] studied the effect of counterion on the morphology of PTMO-containing ionenes. Counterions determine the size of the ionic domains and distance between the domains. Ionenes with bromide counterions had smaller and shorter ionic domains compared to ionenes with chloride counterions.

Many polymer properties are dependant on the molecular weight of the polymer. Therefore, molecular weight determination is a critical factor for polymers. Typically, obtaining accurate absolute molecular weights of charged polymers is more difficult due to intermolecular associations. However, different techniques employing salt solutions are used to reduce or eliminate electrostatic interactions. Historically, molecular weight measurements of ionenes were based on intrinsic viscosity measurements. Rembaum et al.[16] investigated the absolute molecular weights of 3,4- and 6,6-ionenes using intrinsic viscosity measurements and light scattering. In order to eliminate tiresome calculations and time-consuming viscosity measurements, recently our research group.[17] successfully achieved molecular weight characterization of 12,12- and 6,12-ammonium ionenes using multiangle laser light scattering (MALLS) with aqueous size exclusion chromatography (SEC). We have also evaluated the thermal and mechanical properties of 12,12-ammonium ionenes as a function of ionene molecular weight.[18]

Water-soluble ionenes also enable many potential biomedical applications. Earlier research in non-viral gene delivery showed that cationic ionenes complex DNA and allow the transfection of DNA.[19-23] This is particularly important since viral vectors have several disadvantages including activation of the host immune response, limited DNA carrying capacity, and high cost. One potential limitation of ionenes is the presence of permanent positive charge on the quaternized nitrogens throughout the backbone. The endosomal polyplex release is pH-sensitive and for high transfection efficiency, the polymer needs to buffer the endosome.[24, 25] Ionenes with permanent charge lack the pH control and corresponding endosomal release and thus have low gene transfection efficiency. Gene transfection efficiency for polycations is defined as binding of polycation to DNA, delivery of DNA into cells, and releasing the DNA inside the cell. It is dependant on the degree of polymerization (DP) and charge density of the polycation.[26] The ability to tune charge density and molecular weight in ionenes through monomer selection makes them good polyelectrolyte models for gene therapy.[22, 27] In addition, several applications of ionenes as components of cosmetics,[28] flocculants for water treatments,[29] antimicrobial agents,[30] and components for photovoltaic cells are discussed in the literature.[31] Following the antimicrobial behavior of ionenes, Narita et al.[32] showed that ionenes with longer hydrophobic segments and therefore lower charge density were more destructive to cells than ionenes with higher charge density. Ionenes with higher charge density bind to cells more efficiently, but did not disrupt the cell membrane.[33]

Segmented ionenes offer improved mechanical properties compared to non-segmented ionenes and resemble polyurethanes in terms of mechanical properties. Their advantage over polyurethanes is the one-step reaction synthesis and safer reaction components. Researchers have studied the structure-property relationships of well-defined segmented ionenes based on various

soft segments[5], including PTMO, PPG, poly(ethylene glycol) (PEG), or polydienes, including polybutadiene and polyisoprene. In this manuscript, the synthesis and structure-property characterization of PPG-based ammonium ionenes is discussed. In earlier work on PPG-based ionenes, Rembaum et al.[10] addressed electronionic conductivities of PPG-based ionene solutions. This chapter emphasizes thermal, mechanical, and morphological behavior of two PPG-based ionenes. The significance of PPG segmented ionenes compared to PTMO ionenes is the absence of soft segment (SS) crystallization. The disadvantage of PTMO ionenes is that crystallization occurs at ambient conditions and influences modulus and ultimate mechanical behavior. On the other hand, atactic PPG is amorphous even at high molecular weights. Therefore, ultimate ionene strength is due only to the ionic associations in the absence of crystallinity in the SS.

3.3 Experimental

3.3.1 Materials

PPG 2200 and 4200 (Acclaim) and 1000 (Arcol) were kindly provided by Bayer Material Science. 6-bromohexanoyl chloride (97%) was purchased from Alfa Aesar. Triethyl amine was purchased from Aldrich and distilled from calcium hydride. 1,12-dibromododecane (98%) was purchased from Sigma-Aldrich and recrystallized from ethanol. Pyridine (HPLC grade), acetic anhydride, n-butanol, and potassium hydroxide (0.5 *N*), were purchased from Sigma-Aldrich and used as received. Phenolphthalein and *N*,*N*,*N*′,*N*′-tetramethyl-1,6-hexanediamine (99%) were purchased from Acros Organics and used as received. Methanol (MeOH, HPLC grade) and chloroform (Optima) were purchased from Fisher and used as received. Tetrahydrofuran (THF, HPLC grade) was passed through an alumina column and a molecular sieves column before use.

3.3.2 Synthesis of bromine end-capped PPG (Br-PPG-Br)

Dichloromethane (DCM) (100 mL) and PPG (10.00 g, 1 eq) were added into a two-neck, round-bottomed flask equipped with a magnetic stir bar, addition funnel, and nitrogen inlet. Distilled triethylamine (2.2 eq) was added to the flask with a syringe. The flask was cooled to 0 ºC. 6-bromohexanoyl chloride (2.2 eq) was added to the addition funnel containing DCM (50 mL) with a syringe and subsequently added to the reaction flask in a dropwise fashion. The reaction was allowed to proceed for 24 h. Triethylamine salt was filtered through a fritted funnel. The product in DCM was introduced into a separatory funnel and washed twice with saturated $NaHCO_3$(aq) and twice with distilled water. The DCM layer was separated and dried over magnesium sulfate, filtered and evaporated to yield the product. The product was further dried under vacuum (97% yield). ^{1}H NMR (400 MHz, $CDCl_3$) for bromine end-capped 1K PPG is as follows:

δ = 1.1 (m, 58H, per chain, $[BrCH_2CH_2CH_2CH_2CH_2CO]_2$-O-$[CH(\mathbf{C}\boldsymbol{H_3})CH_2O)]_x$-),

1.45 (m, 4H, per chain, $[BrCH_2CH_2\mathbf{C}\boldsymbol{H_2}CH_2CH_2CO]_2$-O-$[CH(CH_3)CH_2O)]_x$-),

1.6 (m, 4H, per chain, $[BrCH_2CH_2CH_2\mathbf{C}\boldsymbol{H_2}CH_2CO]_2$-O-$[CH(CH_3)CH_2O)]_x$-),

1.85 (m, 4H, per chain, $[BrCH_2\mathbf{C}\boldsymbol{H_2}CH_2CH_2CH_2CO]_2$-O-$[CH(CH_3)CH_2O)]_x$-),

2.3 (m, 4H, per chain, $[BrCH_2CH_2CH_2CH_2\mathbf{C}\boldsymbol{H_2}CO]_2$-O-$[CH(CH_3)CH_2O)]_x$-),

3.4-3.7 (m, 63H, per chain, $[Br\mathbf{C}\boldsymbol{H_2}CH_2CH_2CH_2CH_2CO]_2$-O-$[\mathbf{C}\boldsymbol{H}(CH_3)\mathbf{C}\boldsymbol{H_2}O)]_x$-).

3.3.3 Synthesis of PPG-based ammonium ionenes

Bromine end-capped PPG (2g, 1eq) and *N*,*N*,*N*′,*N*′-tetramethyl-1,6-hexanediamine (1eq) were added to a two-neck, round-bottomed flask equipped with an overhead mechanical stirrer and nitrogen inlet. The reaction was allowed to proceed for 24 h at 80 ºC in bulk. The PPG-based ionene was dissolved in MeOH to the correct viscosity for pouring and cast into films. The slow

removal of methanol was required to avoid film defects. Methanol was then allowed to evaporate at room temperature for 3 d. Subsequently, the films were heated in Teflon™ molds at approximately 50-60 ºC for 2 d. Finally, the polymer films were dried in *vacuo* (0.1 mm Hg) at 30 ºC for 24 h. Ionene films were stored in petri dishes containing dessicant and placed in desiccator until their thermal, mechanical and morphological properties were measured. ^{1}H NMR spectroscopy confirmed the structures (Figure 3.1).

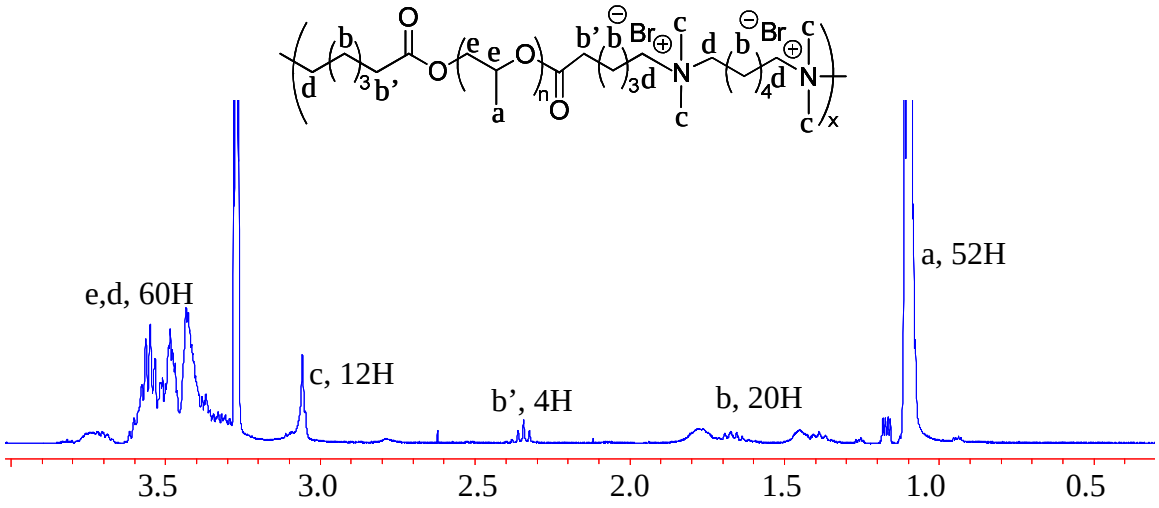

Figure 3.1. ^{1}H NMR (CD_3OD) of 1K PPG-ionene

3.3.4 Synthesis of PPG-based ammonium ionenes having 33 wt% hard segment (HS)

A flame-dried, 50 mL, two-neck, round-bottomed flask was charged with bromine end-capped 1000 g/mol PPG (2.0 g, 0.5 eq) and 1,12-dibromododecane (0.48 g, 1.47 mmol, 0.5 eq). The flask was purged with nitrogen. *N*,*N*,*N*′,*N*′-tetramethyl-1,6-hexanediamine (0.64 mL, 2.90 mmol, 1 eq) was added to the flask. The polymerization was performed in the absence of solvent for 24 h at 80 ºC. 2000 and 4000 g/mol PPG-ionenes containing 33 wt% HS were also synthesized under the same procedure. The HS wt% corresponds to the overall weight of 1,6-

hexane diamine and 1,12-dibromododecane. Figure 3.2 shows the ^{1}H NMR of 1000 g/mol PPG-ionene having 33 wt% HS. The molecular structures of the 2000 and 4000 g/mol PPG-ionenes were confirmed as well.

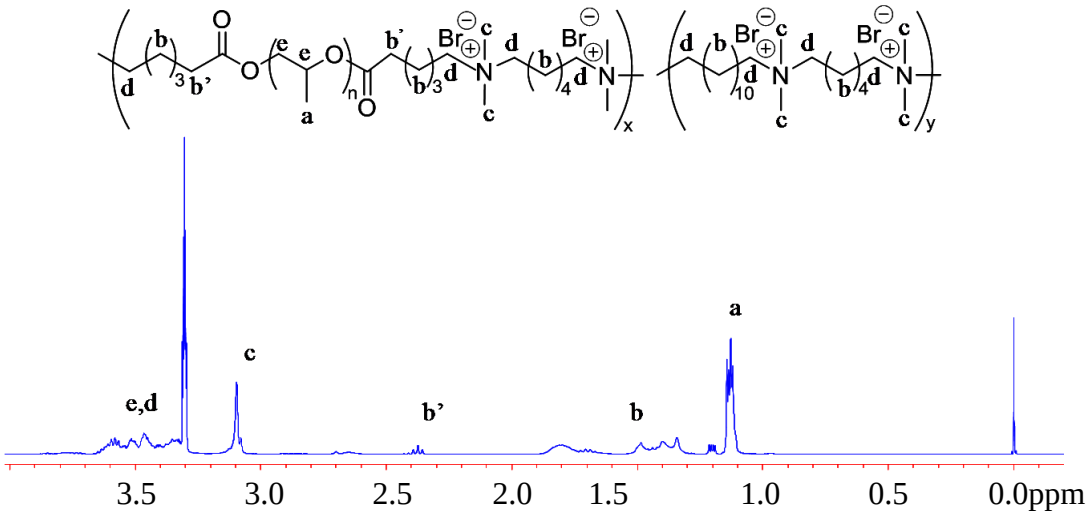

Figure 3.2. ^{1}H NMR (CD_3OD) of 1K PPG-ionene having 33 wt% HS

3.4 Characterization

^{1}H NMR spectroscopic analyses were performed on Varian INOVA 400 MHz spectrometer to confirm the monomer and polymer composition at ambient temperature. Matrix-Assisted Laser Desorption Ionization-Time of Flight/Mass Spectrometry (MALDI-TOF/MS) was performed on a Kompzact SEQ instrument using 100-180 power setting in positive ion linear mode. Laser wavelength was 337 nm, and the accelerating voltage was 20 kV in delayed extraction mode. The sample was prepared from a tetrahydrofuran (THF) solution with 2,5-hydroxybenzoic acid as the matrix and potassium iodide as the cationization reagent. Differential scanning calorimetery (DSC) was conducted on a TA Instruments Q100 under a nitrogen flow of 50 mL/min. Samples were first heated from room temperature to 150 °C at a heating rate of 10 ºC/min. The cooling rate was 10 ºC/min, and samples were cooled to -100 °C

and subsequently were heated to 150 ºC at the same rate. Thermogravimetric analysis (TGA) was conducted on a TA Instruments Hi-Res TGA 2950 under nitrogen at 10 ºC/min. Dynamic mechanical analysis (DMA) was conducted on a TA Instruments Q800 dynamic mechanical analyzer under dry air, tension mode at a frequency of 1 Hz, and temperature ramp of 3 ºC/min. Tensile tests were performed on 5500R Instron universal testing instrument with a cross-head speed of 10 mm/min at ambient conditions. Size exclusion chromatography (SEC) measurements were performed in THF at 40 ºC at flow rate of 1 mL/min using a Waters size exclusion chromatograph equipped with an autosampler, three in-line 5 µm PLgel Mixed-C columns, a Waters 410 refractive index (RI) detector operating at 880 nm, and a miniDAWN multiangle laser light scattering (MALLS) detector operating at 690 nm, which was calibrated with narrow polydispersity polystyrene standards. The DRI increment (d*n*/d*c*) was calculated online. All reported weight-average molecular weights were absolute molecular weights, which were obtained using a MALLS detector. Small angle X-ray scattering was performed on solvent-cast dried films. Small-angle x-ray scattering (SAXS) experiments were performed at the Station 4C1 of the Pohang Accelerator Laboratory (PAL) synchrotron radiation source (Pohang, Korea). The incident x-ray beam was tuned to a wavelength of 1.3009 Å and the sample-to-detector distances were 3046.71 mm and 1075.27 mm for low and medium q ranges, respectively. Two dimensional scattering images were recorded using a Mar CCD camera with exposure times of 60 sec at low q region and 30 sec at medium q region. The relationship between pixel and the momentum transfer vector q was determined by calibrating the scattering data with SEBS (low q) and silver behenate (medium q) standards. All scattering intensities were corrected for transmission, incident beam flux, and background scatter due to air and Kapton windows.

3.5 Results and Discussion

3.5.1 Synthesis and characterization of bromine end-capped PPG

Difunctional bromine end-capped PPG oligomers were synthesized from 1000, 2000, and 4000 g/mol PPGs using the synthetic strategy in Scheme 3.1.

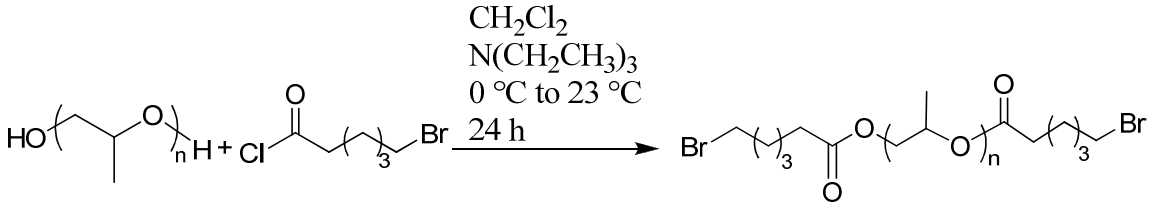

Scheme 3.1. Synthesis of bromine end-capped PPG using bromo-substituted acyl chlorides

Earlier, Leir et al.[12] demonstrated the synthesis of telechelic α,ω-bis(dimethylamino) poly(tetramethylene oxide) (BAPTMO). BAPTMO was synthesized using a living cationic polymerization strategy of THF. The synthesis involved multiple steps and the monomer to initiator ratio in living cationic polymerization dictated the final molecular weight. Dimethylamine was used to end-cap the oligomeric PTMO precursors. Careful control of the amount of dimethylamine was critical to the molecular weight and polydispersity of BAPTMO. However, this report describes a simple method to end-cap PPG using 6-bromohexanoyl chloride. This synthetic strategy is advantageous and the soft segment molecular weight is tunable with commercially available difunctional PPG diols. 6-bromohexanoyl chloride was used with purification and in excess (2.2 eq) amounts to end-cap the PPG hydroxyl ends. ^{1}H NMR spectroscopy confirmed the structures of 1000, 2000, and 4000 g/mol bromine end-capped PPGs (Figure 3.1). Molecular weights were determined using complementary techniques including SEC, ^{1}H NMR spectroscopy, and end group titration (Table 3.1).

Table 3.1. Number-average molecular weights from ^{1}H NMR, titration, and SEC

Sample	M_n NMR[a]	M_n Titration	M_n SEC[b]
4K PPG	3900	4007	4300
Br-4KPPG-Br	4400	ND	4400
2K PPG	1720	2077	1900
Br-2KPPG-Br	2800	ND	2300
1K PPG	1100	940	910
Br-1KPPG-Br	1400	ND	1300

ND: hydroxyl ends were not detected
[a] $CDCl_3$, 400 MHz, 23 °C
[b] THF, MALLS, 23 °C

Acid titration and MALDI-TOF/MS experiments ensured the absence of hydroxyl ends and difunctionality for bromine end-capped PPGs were confirmed with. The determination of hydroxyl content of PPG precursors and corresponding bromine functionalized PPGs was adapted from the *Acetic Anhydride Method* by Ogg et al.[34] In this method a 3:1 molar ratio of pyridine:acetic anhydride was added to the sample, and an acetyl-pyridine intermediate formed. Hydroxyl ends of PPG that remained unfunctionalized readily reacted with the acetyl-pyridine intermediate. Water subsequently hydrolyzed the salt and acetic acid was produced. The acetic acid was titrated with potassium hydroxide. After each titration the OH number was calculated using Equation 1. The OH number is equal to the milligrams of potassium hydroxide (KOH) per gram of sample. After calculating the OH value, the number average molecular weight was calculated for each sample using Equation 2.

$$\text{OH number} = \frac{(V_B - V_S) \times N \times M_w \text{ of KOH}}{\text{Weight of sample (g)}} \qquad \textbf{Equation 1}$$

V_B: volume of KOH used to titrate the blank
Vs: volume of KOH used to titrate the sample

$$M_n = \frac{2 \times M_w \text{ of KOH } (56.1) \times 1000}{\text{OH number}} \qquad \textbf{Equation 2}$$

Table 3.2 shows the OH value for each sample. The calculated OH values from the PPG precursors were comparable to commercial values,[35] which confirmed the high reliability of our data. The OH values for Br-PPG-Br oligomers were zero, which confirmed quantitative functionalization of PPGs.

Table 3.2. Hydroxyl number determination of PPG precursors and corresponding bromine end-capped PPG oligomers

Sample	OH Number	Bayer OH number	M_n (g/mol)
4K PPG	28	26.5–29.5	4000
Br-4KPPG-Br	0	N/A	N/A
2K PPG	54	56	2100
Br-2KPPG-Br	0	N/A	N/A
1K PPG	120	111	940
Br-1KPPG-Br	0	N/A	N/A

In addition, MALDI-TOF/MS confirmed the difunctionality of 1000 g/mol PPG dibromide. Earlier Bednarek et al.[36] terminated poly(ethylene oxide) with 2-bromopropionate through esterification reactions. In order to confirm the chain-end functionality, they used MALDI-TOF analysis and showed quantitative functionalization. Figure 3.3 shows the MALDI-TOF mass spectrum of 1000 g/mol PPG bromide with M_n= 1300 g/mol according to SEC. The spectrum shows that signals are separated by 58 molecular weight units, which corresponds to the poly(propylene glycol) repeating unit.

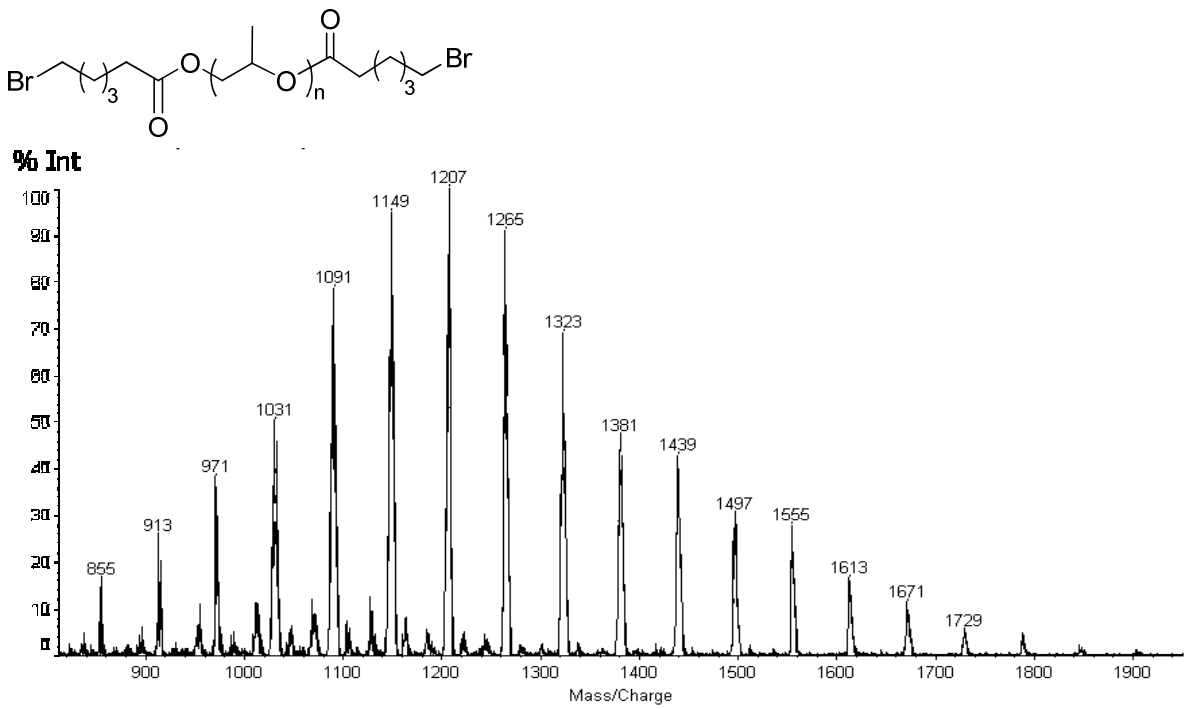

Figure 3.3. MALDI-TOF analysis of 1K bromine end-capped PPG, matrix: 2,5-hydroxybenzoic acid, charging agent: KI

In order to calculate the molecular weight of the end groups, the most probable, high intensity peak at *m/z* ratio of 1207 was chosen. The theoretical end group molecular weight equals 178 g/mol.

MALDI end group MW = [Single chain MW-(DP x Repeating unit MW)- K^+]/2

MALDI end group MW = [1207-(14 x 58)-39]/2 = 178 g/mol.

Thus, the theoretical and experimental molecular weights were equivalent and confirmed difunctionality.

3.5.2 Synthesis and characterization of PPG-based ammonium ionene

Ionenes containing 1000, 2000, and 4000 g/mol PPG soft segments were successfully synthesized (Scheme 3.2) using the Menshutkin reaction of a diamine with a various dihalide telechelic oligomers. It is well known that balanced (1:1) stoichiometry is required to obtain high

molecular weight polymers in step-growth polymerization,[37] and 1:1 stoichiometry was used in all polymerizations. Unlike previous ionene synthesis in the presence of solvent,[18] our polymerizations were performed in the absence of solvent for 24 h at 80 ºC under nitrogen. Upon completion of the reaction, the polymer was readily soluble in methanol for film casting. ^{1}H NMR spectroscopy confirmed the polymer structure. The resonance at 2.2 ppm due to the methyl protons of the 1,6-hexane diamine monomer shifted to 3.1 ppm after polymerization, which confirmed the quaternization of tertiary amino nitrogens.

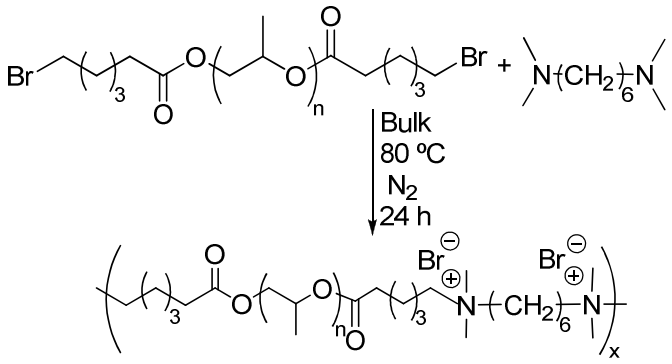

Scheme 3.2. Synthesis of PPG-based ammonium ionene

DSC analysis revealed a single T_g for all ionenes at approximately -66 ºC and corresponded to the T_g of the PPG phase (1000, 2000, and 4000 g/mol). This behavior was due to the microphase separation of PPG SS from the ionic HS. Thermal stability was measured using TGA, and all ionenes exhibited 5% weight loss at approximately 230 ºC. These thermal transitions are listed in Table 3. The segmented ionenes degraded in two distinct steps. The first weight loss corresponded to the weight percentage of the HS and the second weight loss corresponded to the weight percentage of the SS. The actual mechanism for thermal degradation is complex, however, Ruckenstein et al.[38] and Jerome et al.[39] proposed the dequaternization of nitrogens according to the Hoffman elimination path way. As expected, 1000 g/mol PPG ionene degraded faster than the 2000 g/mol PPG ionene and 4000 g/mol PPG ionene (Figure 3.4). The

faster degradation was attributed to the higher concentrations of HS with lower soft segment molecular weights.

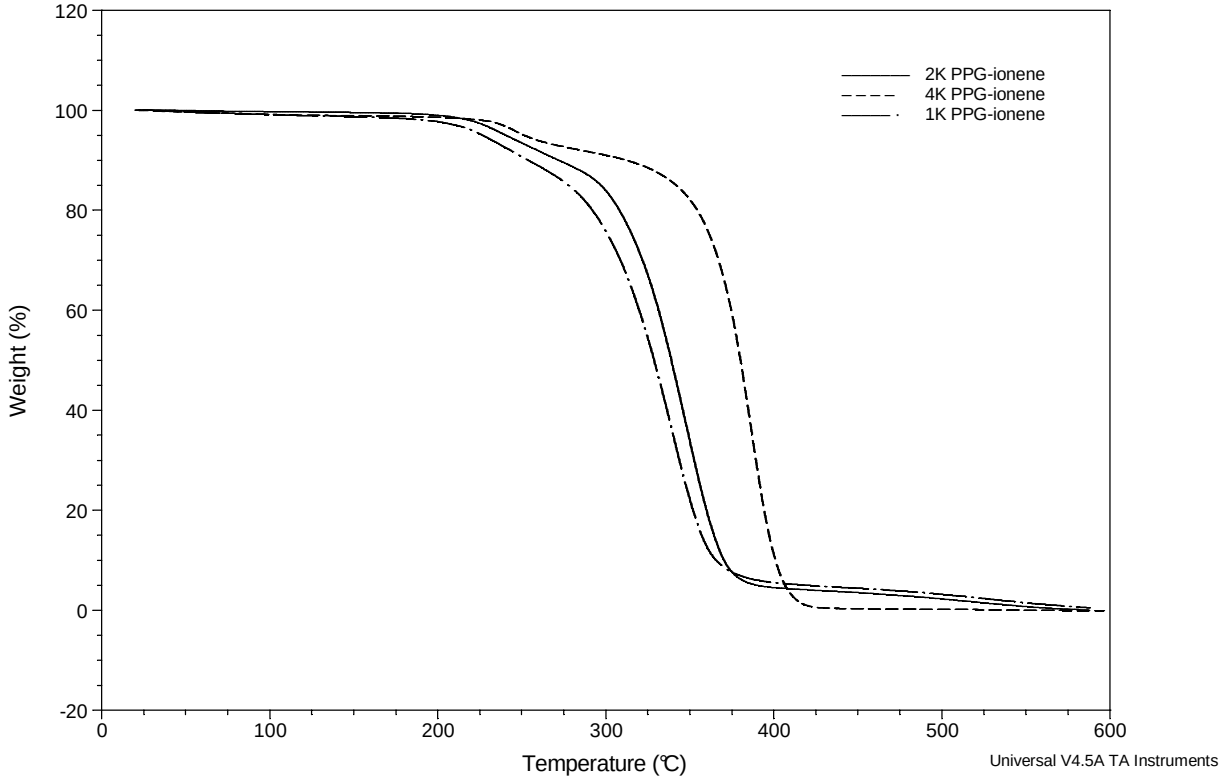

Figure 3.4. TGA curves for PPG-ionenes. Molecular weights in graph legend correspond to the PPG soft segment molecular weights

Table 3.3. Thermal transitions of PPG-based ionene series

Sample	T_g (°C) DSC	$T_{D(Onset)}$(°C) TGA
1000 g/mol PPG Ionene	-63	230
2000 g/mol PPG Ionene	-66	210
4000 g/mol PPG Ionene	-69	234

Previous work in our laboratory regarding structure-property relationships of 12,12-ammonium ionenes exhibited two transitions in DMA, and these transitions where attributed to the T_g and onset of flow with ionic dissociation.[18] In order to investigate the effect of the soft

segment molecular weight on the dynamic mechanical properties, DMA was performed on the 1000, 2000, and 4000 g/mol PPG ionenes. Figure 3.5 shows two transitions for PPG ionenes. The first transition was assigned to the T_g and the second transition attributed to the softening temperature which is believed to be the ionic aggregate dissociation followed by the flow.

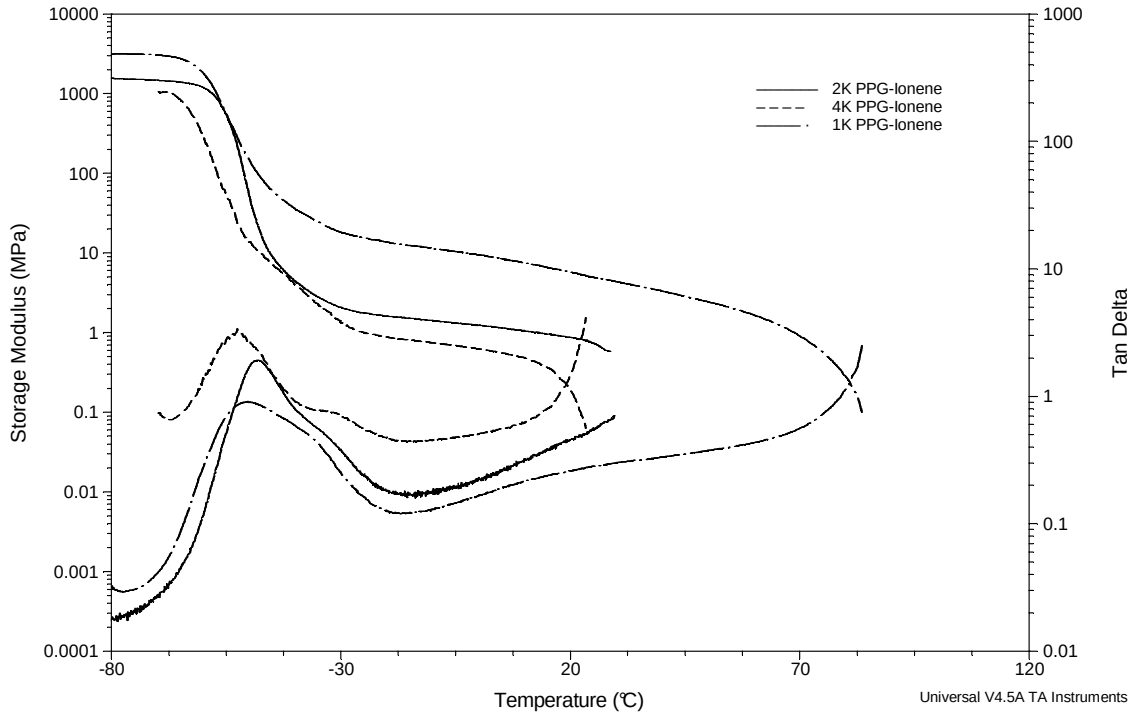

Figure 3.5. DMA curves of PPG-ionenes. Molecular weights in graph legend correspond to the PPG soft segment molecular weights

Table 3.4 shows that the T_g for various SS molecular weights was near the glass transition temperature of pure PPG, and the second transition shifted to higher temperatures with decreasing SS molecular weight. As expected, the ionic dissociation temperature was dependant on the ionene charge density. Higher charge density ionenes with shorter PPG soft segments have less mobility due to shorter distances between physical crosslinks and thus higher temperatures are required to dissociate the ionic aggregates, which lead to viscous flow. Lower molecular weight PPG segments led to shorter distances between physical crosslinks and at the

same time, low molecular weight PPG segments provided the corresponding ionene with higher HS content, which led to an increased rubbery plateau modulus.

Table 3.4. DMA Thermal Transitions of PPG-Based Ionenes

Sample	T_g (°C)	T_{flow}(°C)
1000 g/mol PPG Ionene	-60	80
2000 g/mol PPG Ionene	-60	23
4000 g/mol PPG Ionene	-63	20

X-ray scattering was performed and the data for the 2000 g/mol PPG ionene is depicted in Figure 3.6. Due to the difference in electron density of the hard segment relative to the soft segment, a single peak was observed in the SAXS profile. The distinct scattering peak with a Bragg spacing of 7.2 nm confirmed microphase separation, which was consistent with DSC and DMA results.

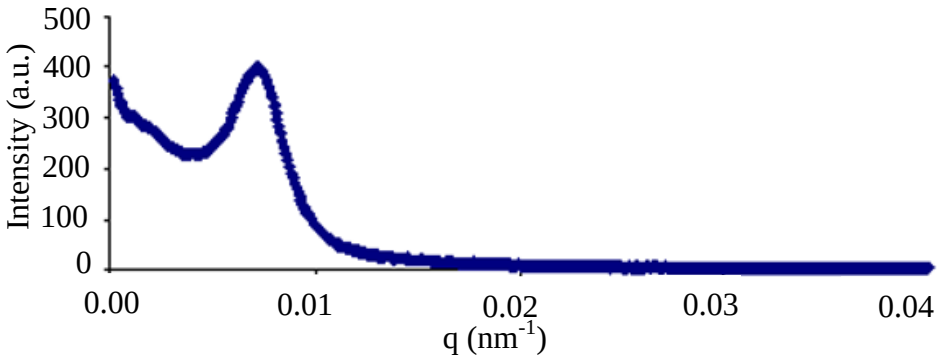

Figure 3.6. X-ray scattering profile for 2K PPG-ionene: Scattering intensity versus q

Charge density will influence the thermal and mechanical properties of ionenes.[40] In order to investigate the effect of charge density on the mechanical properties of PPG ionenes, an additional 1,12-dibromododecane monomer was added to the reaction mixture. In the following

section, we present the synthesis and characterization of ionenes having higher wt% HS due to the addition of a second low molar mass dibromide monomer.

3.5.3 Synthesis and characterization of PPG-based ammonium ionenes having higher HS contents

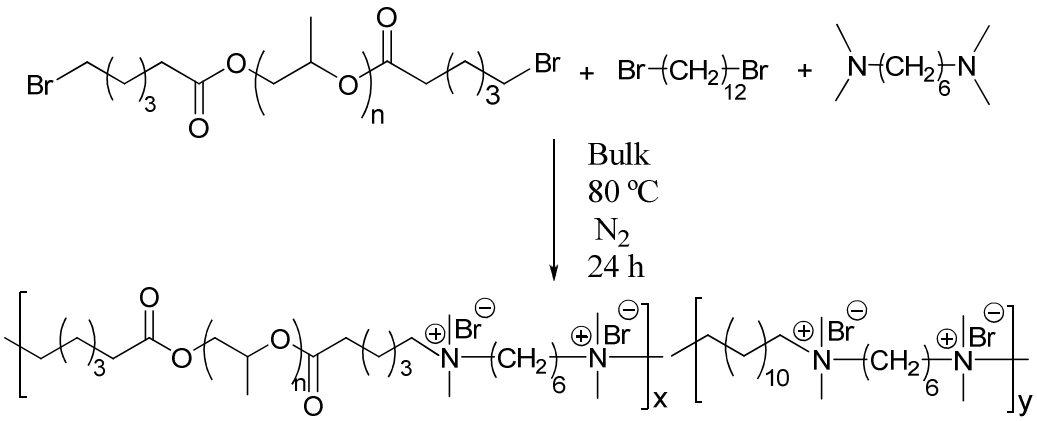

Scheme 3.3. Synthesis of PPG-ionenes having 33 wt% HS

Scheme 3.3 shows the synthesis of novel PPG ionenes introducing an aliphatic 1,12-dibromododecane monomer as a third monomer. Thermal properties of 1000, 2000, and 4000 g/mol PPG ionenes containing 33 wt% HS were analyzed using DSC and TGA. Table 5 shows the summary of thermal analysis results. These ionenes were quite comparable to the previous series in terms of T_g and thermal degradation temperature. All showed a single T_g, which was attributed to the T_g of pure PPG, and onset of thermal degradation temperatures near 240 ºC. Thermal stability was measured using TGA. 1000, 2000 and 4000 g/mol PPG ionenes containing 33 wt% HS exhibited 5% weight loss at approximately 240 ºC (Figure 3.7). In a similar fashion the degradation occurred in a two-step. The first degradation step was attributed to dequaternization, which corresponds to the weight percentage of the hard segment in the ionene backbone (33 wt%). As the SS molecular weight decreased, the quaternized nitrogen atoms were more frequently located throughout the backbone and thus degradation occurred faster.

Table 3.5. Thermal transitions of ionenes having 33 wt% HS

Sample	T_g (°C) DSC	$T_{D(Onset)}$(°C) TGA
1000 g/mol PPG Ionene-33 wt% HS	-60	241
2000 g/mol PPG Ionene-33 wt% HS	-65	238
4000 g/mol PPG Ionene-33 wt% HS	-66	242

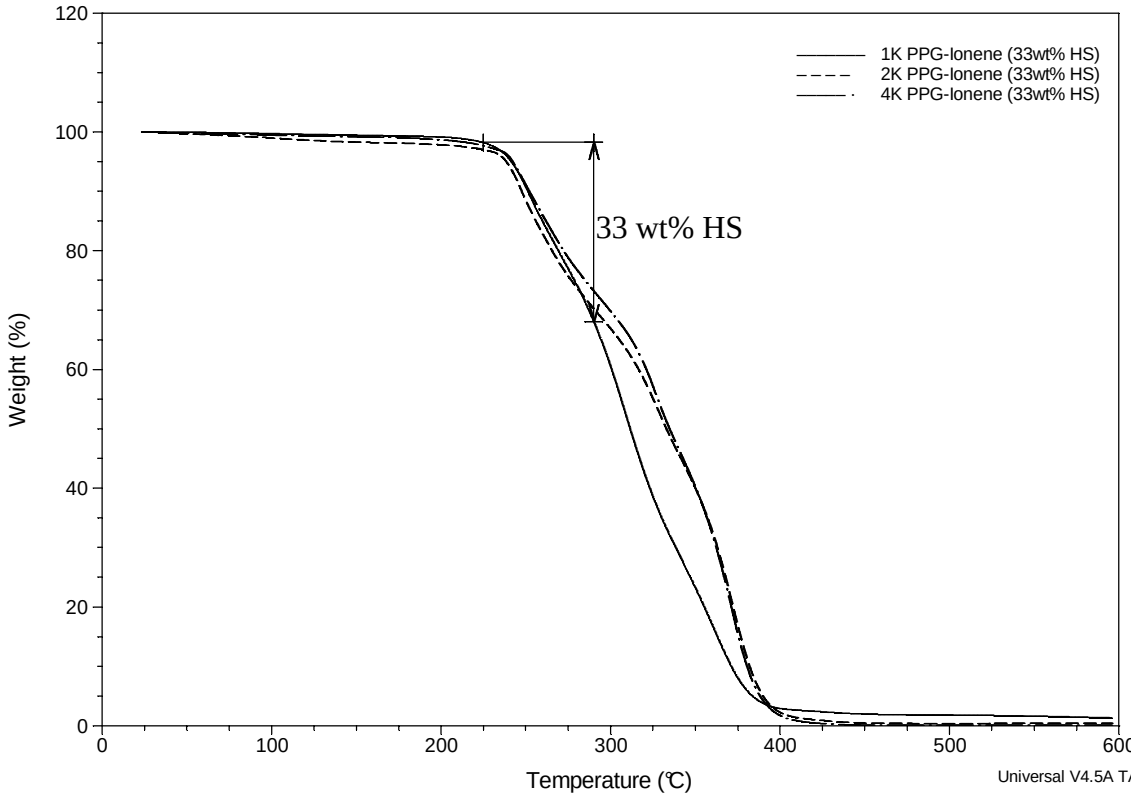

Figure 3.7. TGA overlays of PPG-ionenes having 33 wt% HS

Mechanical properties of 33 wt% HS ionenes were investigated using DMA and ambient tensile analysis. DMA confirmed the structural difference as a function of HS content and revealed the incorporation of 1,12-dibromododecane monomer throughout the ionene backbone.

Figure 3.8 shows three DMA transitions for 1000 and 2000 g/mol PPG-ionenes containing 33 wt% HS. Table 3.6 summarizes these transitions. The first transition was attributed to the glass transition temperature of the PPG soft segment, and the second transition was due to the glass transition temperature of the 6,12-ionene HS. The third transition suggested ionic dissociation and the onset of flow. DSC analysis of 6,12-ionene homopolymer shows a single T_g near 34 ºC. This T_g is similar to the second T_g of the 33 wt% HS ionene series (32-40 ºC). Therefore, DSC analysis for 6,12-ionene homopolymer and DMA of a PPG ionene having 33 wt% HS confirmed the microphase separation. In Figure 3.8 the 1000 g/mol PPG ionene having 33 wt% HS had a higher rubbery plateau modulus than the 2000 g/mol PPG ionene analogy. This shows the dependency of rubbery plateau modulus on charge density or SS molecular weight. Since the lower molecular weight PPG soft segment led to lower molecular weight between ionic sites, stronger physical crosslinking resulted. The 4000 g/mol PPG ionene film was too soft for DMA analysis.

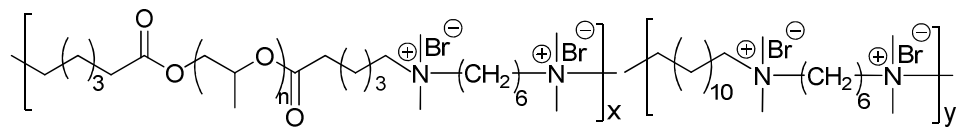

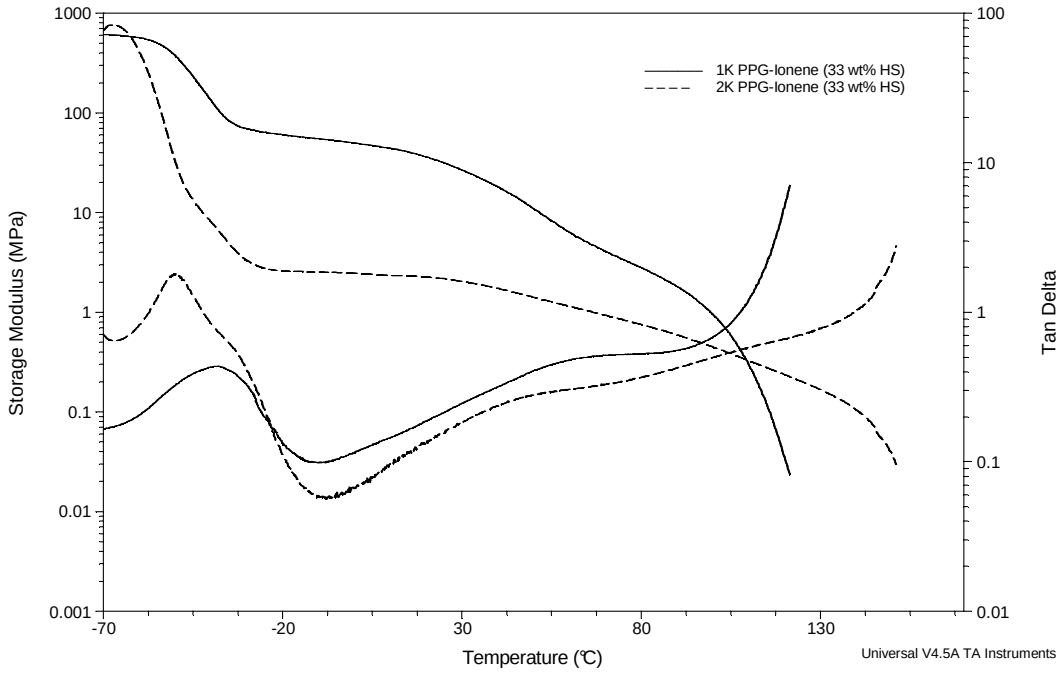

Figure 3.8. DMA analysis of 1K and 2K PPG-based ionenes having 33 wt% HS

Table 3.6. DMA thermal transitions of PPG-based ionenes having 33wt% HS

Sample	**T_g1 (°C)**	**T_g2 (°C)**	**T_{flow} (°C)**
1000 g/mol PPG Ionene	-53	40	100
2000 g/mol PPG Ionene	-65	32	143

Tensile analysis was performed on the PPG ionene series containing 33 wt% HS. The 33 wt% HS ionenes showed an ultimate tensile strength ranging from 0.4 to 2.5 MPa and elongations at break ranging from 20 to 80%. Figure 3.9 shows that the ionene having the shortest soft segment had the highest modulus. The 1000 g/mol PPG ionene had the highest tensile strength at a given elongation. As the spacer length increased, the concentration of the relatively harder ionic domains decreased, and therefore the modulus decreased.

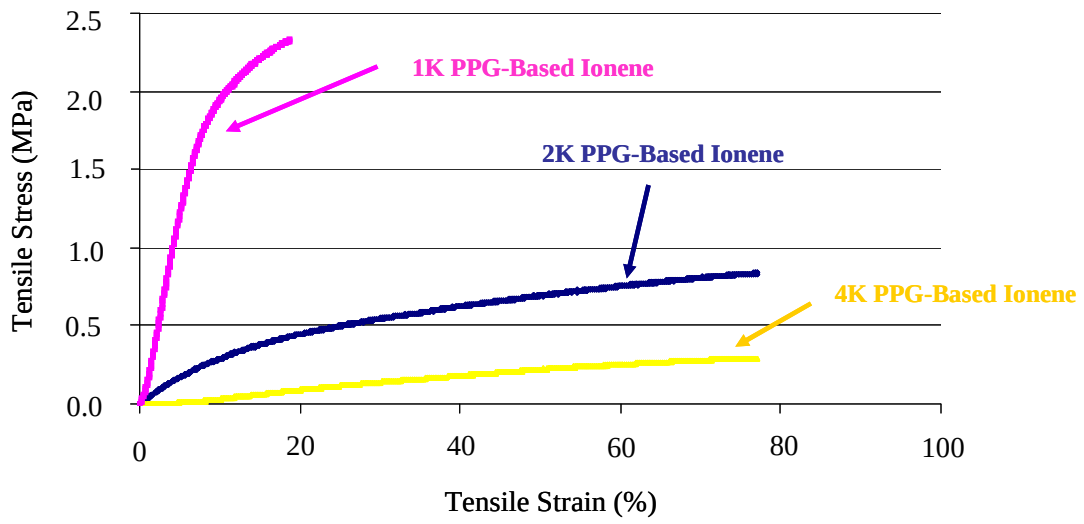

Figure 3.9. Tensile analysis of PPG ionenes containing 33 wt% HS

X-ray scattering was performed and Figure 3.10 shows that all ionenes containing 33 wt% HS exhibited a single scattering peak. The ionene containing 4000 g/mol PPG soft segment showed more distinct microphase separation and therefore had a sharper peak in lower q region. As the soft segment molecular weight decreased, the ionic scattering peak shifted to higher q values. According to $q = 2\pi/d$, the Bragg distance decreased as q_{max} shifted to higher values. Table 3.7 summarizes the Bragg distances.

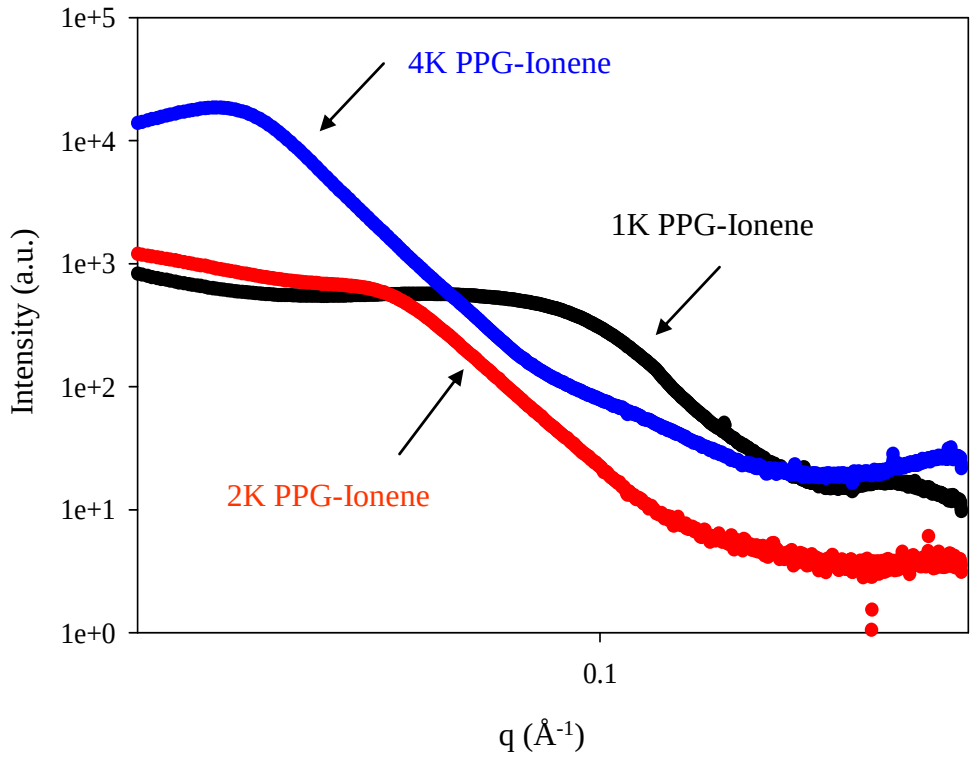

Figure 3.10. Scattering intensity vs *q* for ionenes having 33 wt% HS.

Table 3.7. Bragg distances of PPG-ionenes having 33 wt% HS

PPG MW	q(Å^{-1})	Bragg distance (Å)
1000 g/mol	0.027	66
2000 g/mol	0.050	126
4000 g/mol	0.095	234

3.5.4 Effect of hard segment content on the thermal and mechanical properties of segmented PPG-based ionenes

Upon the synthesis of segmented ionenes having various wt% of hard segments, it was important to examine the effect of HS content on the thermal and mechanical behavior of these ionenes. The ionenes containing 1000 g/mol PPG SS had 12 wt% HS, which derived from the 1,6-hexane diamine monomer, and 33 wt% HS was derived from the sum of 1,6-hexane diamine and 1,12-dibromododecane monomers. Table 3.8 shows the thermal analysis of the two ionenes

using DSC and TGA. Both revealed single T_g's, consistent with pure PPG, and a thermal degradation temperature near 240 ºC. A significant difference was revealed in DMA, and the ionene containing 33 wt% HS showed a higher rubbery plateau modulus than the ionene containing 12 wt% HS. The ionene containing 33 wt% HS showed a second T_g which was not seen for the ionene containing 12 wt% HS ionene. The onset of flow in the ionene containing 33 wt% HS ionene shifted from 80 ºC in the ionene containing 12 wt% HS ionene to 100 ºC in the ionene containing 33 wt% HS ionene (Figure 3.11).

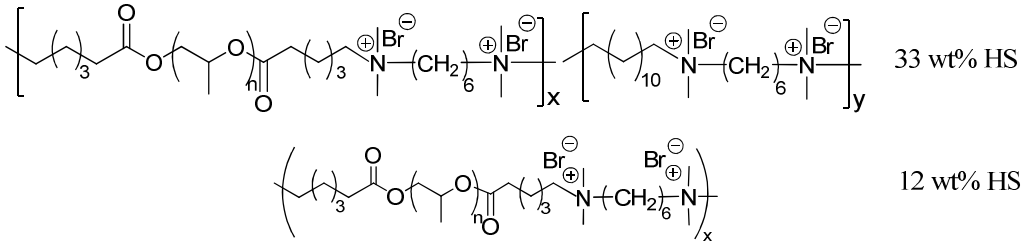

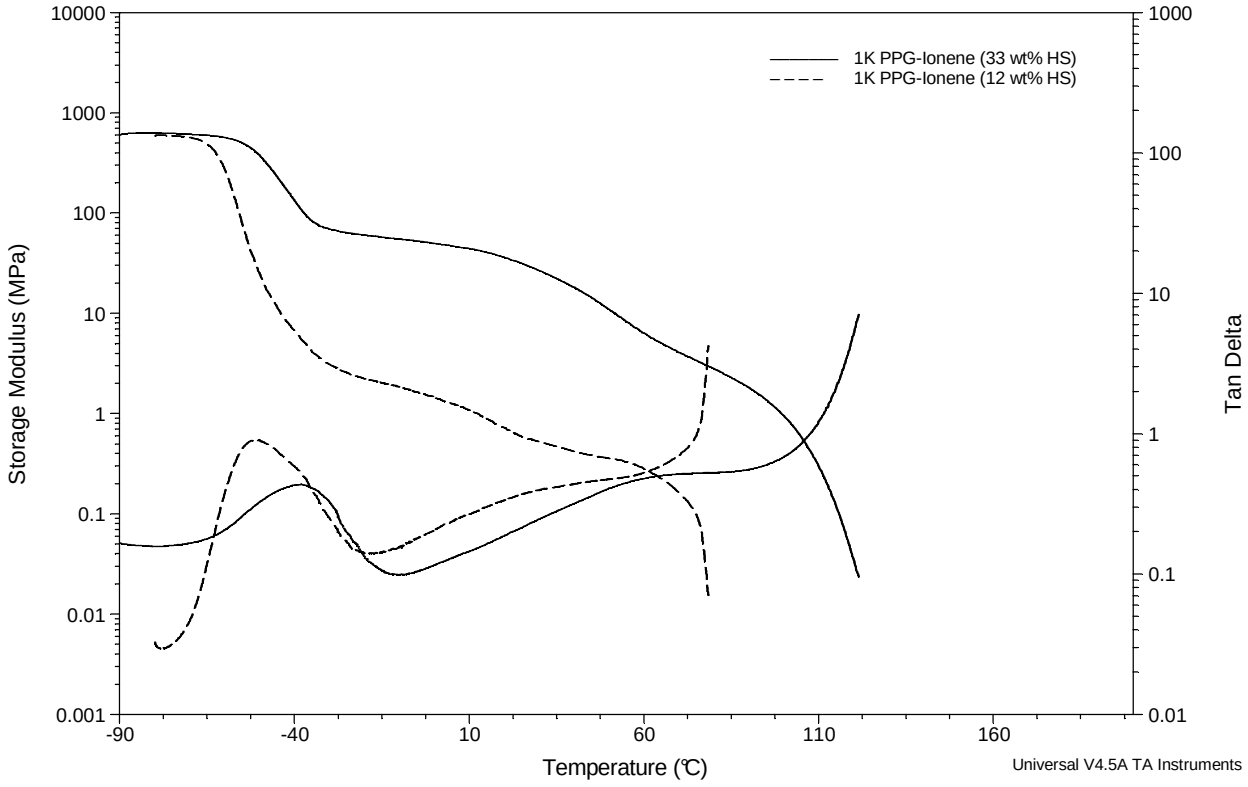

Figure 3.11. DMA curves of 1K PPG-ionenes having 12 and 33 wt% HS

Table 3.8. Thermal transitions of 1K PPG-based ionenes having 12wt% and 33 wt% HS

HS wt%	**SS wt%**	$T_{d(5\%)}$ **(°C)**	T_g **(°C)**
12	88	245	-63
33	67	241	-60

The ionenes containing 2000 g/mol PPG SS in both series had 6 wt% and 33 wt% HS. The thermal transitions are quite comparable to one another (Table 3.9). The DMA overlays are shown in Figure 3.12. The rubbery plateau modulus for the 33 wt% HS ionene is higher than for the ionene with 6 wt% HS.

Table 3.9. Thermal transitions of 2K PPG-ionenes having 6 wt% and 33 wt% HS

HS wt%	**SS wt%**	$T_{d(5\%)}$ **(°C)**	T_g **(°C)**
6	94	226	-66
33	67	238	-65

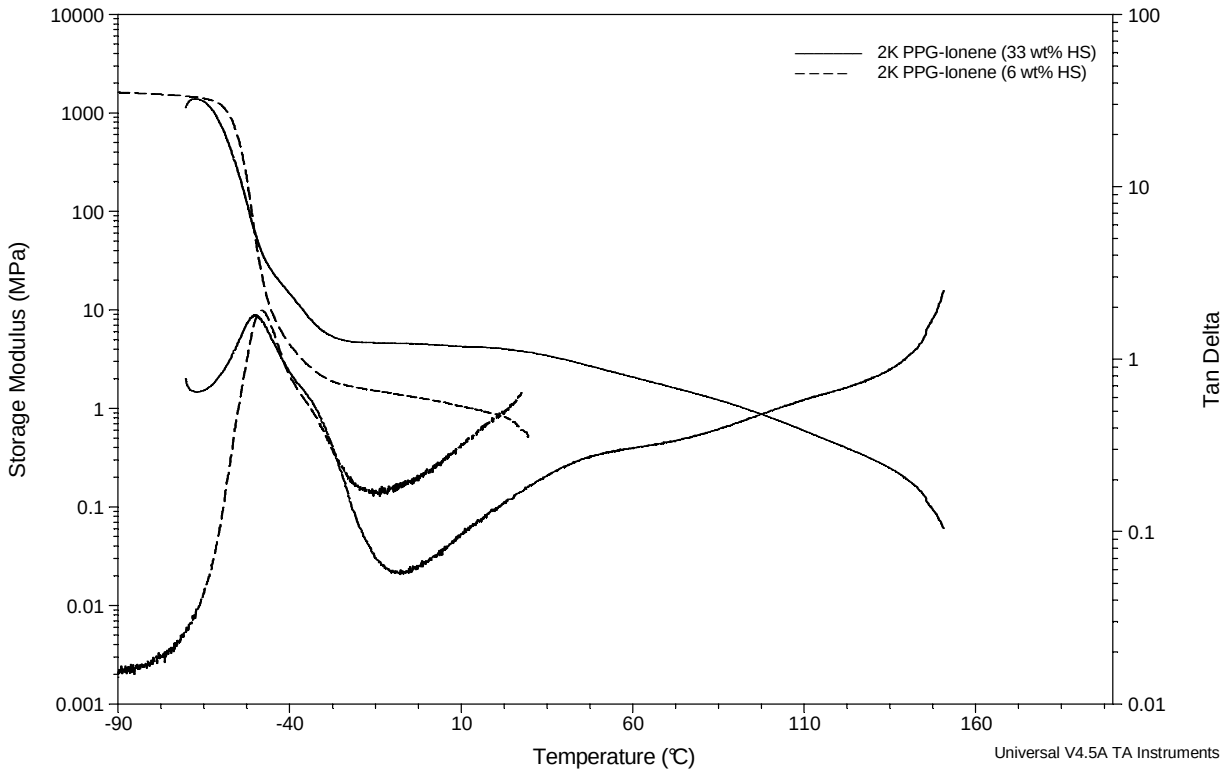

Figure 3.12. DMA of 2K PPG-ionenes having 6 and 33 wt% HS

3.6 Conclusions

Novel PPG dibromide of 1000, 2000, and 4000 g/mol molecular weights were successfully synthesized via the reaction of an acid-chloride with PPGs. The molecular weights from ^{1}H NMR, SEC and titration experiments of bromine-terminated oligomers were measured and were quite comparable to one another. MALDI-TOF and titration experiments confirmed the difunctionality of these oligomers. Upon synthesis and characterization of bromine-terminated PPG macromonomers, ammonium ionenes having amorphous PPG soft segment were synthesized for the first time. ^{1}H NMR spectroscopy confirmed the macromolecular structures of segmented ionenes. All ionenes possessed microphase separation. Thermal studies using DSC revealed a single T_g for PPG-based ionenes at approximately -66 ºC. The thermal degradation

temperature was approximately 230-240 ºC for all ionene polymers. SAXS profile of the 2000 g/mol PPG-ionene containing 6 wt% HS indicated a single peak at 7.2 nm that confirmed the microphase separation. DMA data from all ionenes showed that SS molecular weight or charge density influences the rubbery plateau modulus along with the softening temperature in each series. The PPG ionenes without an aliphatic 1,12-dibromododecane HS showed poor mechanical properties having low ionic dissociation temperature ranging from 20-80 ºC. Adding an aliphatic 1,12-dibromododecane enhanced the mechanical properties. The onset of flow increased to 100-140 ºC for 1000 and 2000 g/mol PPG ionenes containing 33 wt% HS. The studies on morphology of the segmented ionenes are being continued.

3.7 Acknowledgements

We acknowledge Jong Keun Park from Dr. Robert Moore's group at Virginia Tech for performing SAXS analysis. This material is based upon work supported in part by the Kimberly-Clark Corporation.

3.8 References

[1] Gibbs, C. F.; Marvel, C. S. *J. Am. Chem. Soc.* **1934,** 56, 725-7.
[2] Hadek, V., Noguchi, H., Rembaum, A. *Polymer Preprints* **1971,** 12, (90).
[3] Noguchi, H.; Rembaum, A. *Macromolecules* **1972,** 5, (3), 253-60.
[4] Rembaum, A.; Baumgartner, W.; Eisenberg, A. *J. Polym. Sci., Part C: Polym. Lett.* **1968,** 6, (3), 159-71.
[5] Williams, S. R.; Long, T. E. *Prog. Polym. Sci.* **2009**.
[6] Kohjiya, S.; Ohtsuki, T.; Yamashita, S. *Makromol. Chem., Rapid Commun.* **1981,** 2, (6-7), 417-20.
[7] Kohjiya, S.; Yamashita, S. *Kautsch. Gummi Kunstst.* **1991,** 44, (12), 1128-32.
[8] Dimitrov, I. V.; Berlinova, I. V. *Macromol. Rapid Commun.* **2003,** 24, (9), 551-555.
[9] Burmistr, M. V.; Sukhyy, K. M.; Shilov, V. V.; Pissis, P.; Polizos, G.; Spanoudaki, A.; Gomza, Y. P. *Solid State Ionics* **2005,** 176, (19-22), 1787-1792.
[10] Somoano, R.; Yen, S. P. S.; Rembaum, A. *J. Polym. Sci., Part C: Polym. Lett.* **1970,** 8, (7), 467-79.
[11] Williams, S. R.; Salas-de la Cruz, D.; Winey, K. I.; Long, T. E. *Polymer* **2009**.
[12] Leir, C. M.; Stark, J. E. *J. Appl. Polym. Sci.* **1989,** 38, (8), 1535-47.
[13] Feng, D.; Wilkes, G. L.; Crivello, J. V. *Polym. Prepr. (Am. Chem. Soc., Div. Polym. Chem.)* **1989,** 30, (2), 229-30.
[14] Feng, D.; Wilkes, G. L.; Leir, C. M.; Stark, J. E. *J. Macromol. Sci., Chem.* **1989,** A26, (8), 1151-81.
[15] Ikeda, Y.; Yamato, J.; Murakami, T.; Kajiwara, K. *Polymer* **2004,** 45, (25), 8367-8375.
[16] Casson, D.; Rembaum, A. *Macromolecules* **1972,** 5, (1), 75-81.
[17] Layman, J. M.; Borgerding, E. M.; Williams, S. R.; Heath, W. H.; Long, T. E. *Macromolecules* **2008,** 41, (13), 4635-4641.
[18] Williams, S. R.; Borgerding, E. M.; Layman, J. M.; Wang, W.; Winey, K. I.; Long, T. E. *Macromolecules* **2008,** 41, (14), 5216-5222.
[19] Li, S. D.; Huang, L. *Gene Ther.* **2006,** 13, (18), 1313-1319.
[20] Storrie, H.; Mooney, D. J. *Adv. Drug Del. Rev.* **2006,** 58, (4), 500-514.
[21] Elouahabi, A.; Ruysschaert, J.-M. *Mol. Ther.* **2005,** 11, (3), 336-347.
[22] Trukhanova, E. S.; Izumrudov, V. A.; Litmanovich, A. A.; Zelikin, A. N. *Biomacromolecules* **2005,** 6, (6), 3198-3201.
[23] Nguyen, T. T.; Grosberg, A. Y.; Shklovskii, B. I. *J. Chem. Phys.* **2000,** 113, (3), 1110-1125.
[24] Putnam, D.; Gentry, C. A.; Pack, D. W.; Langer, R. *Proc. Natl. Acad. Sci. U. S. A.* **2001,** 98, (3), 1200-1205.
[25] Zhao, X.; Pan, F.; Zhang, Z.; Grant, C.; Ma, Y.; Armes, S. P.; Tang, Y.; Lewis, A. L.; Waigh, T.; Lu, J. R. *Biomacromolecules* **2007,** 8, (11), 3493-3502.
[26] Heath, W. H.; Senyurt, A. F.; Layman, J.; Long, T. E. *Macromol. Chem. Phys.* **2007,** 208, (12), 1243-1249.
[27] Zelikin, A. N.; Putnam, D.; Shastri, P.; Langer, R.; Izumrudov, V. A. *Bioconjugate Chem.* **2002,** 13, (3), 548-553.
[28] Jacquet, B.; Lang, G. Quaternized polymer for use as a cosmetic agent in cosmetic compositions for the hair and skin. 77-8496574217914, 19771108., 1980.
[29] Factor, A.; Heinsohn, G. E. *J. Polym. Sci., Part C: Polym. Lett.* **1971,** 9, (4), 289-95.

[30] Cakmak, I.; Ulukanli, Z.; Tuzcu, M.; Karabuga, S.; Genctav, K. *Eur. Polym. J.* **2004,** 40, (10), 2373-2379.
[31] Klun, T. P.; Wendling, L. A.; Van Bogart, J. W. C.; Robbins, A. F. *J. Polym. Sci., Part A: Polym. Chem.* **1987,** 25, (1), 87-109.
[32] Narita, T.; Ohtakeyama, R.; Nishino, M.; Gong, J. P.; Osada, Y. *Colloid. Polym. Sci.* **2000,** 278, (9), 884-887.
[33] Tashiro, T. *Macromol. Mater. Eng.* **2001,** 286, (2), 63-87.
[34] Ogg, C. L.; Porter, W. L.; Willits, C. O. *Ind. Eng. Chem., Anal.* **1945,** 17, 394-7.
[35] MaterialScience., B. Arcol polyol ppg-1000, acclaim polyol ppg-2200, acclaim polyol ppg-4200. http://bayermaterialsciencenafta.com/index.html
[36] Bednarek, M.; Biedron, T.; Kubisa, P. *Macromol. Rapid Commun.* **1999,** 20, (2), 59-65.
[37] Rogers, M. E.; Long, T. E.; Turner, R. S., *Introduction to synthetic methods in step-growth polymers*. Wiley-Interscience: Hoboken, N.J, 2003.
[38] Ruckenstein, E.; Chen, X. *Macromolecules* **2000,** 33, (24), 8992-9001.
[39] Yano, S.; Tadano, K.; Jerome, R. *Macromolecules* **1991,** 24, (24), 6439-42.
[40] Feng, D.; Venkateshwaran, L. N.; Wilkes, G. L.; Leir, C. M.; Stark, J. E. *J. Appl. Polym. Sci.* **1989,** 38, (8), 1549-65.

Chapter 4. Synthesis and Characterization of Salt-responsive Segmented Poly(propylene glycol)-Based Ammonium Ionenes

4.1 Abstract

A series of poly(propylene glycol) (PPG)-based ammonium ionenes having various hydrophilic (HPL) to hydrophobic (HPB) molar ratios were synthesized. The salt-triggering property of PPG-ionenes having three different PPG number-average molecular weights was investigated. The 1K PPG-ionenes showed solubility (optical clarity) in both water and salt solution. The 2K PPG-ionenes up to HPL/HPB value of 27 showed cloudy dispersions in water and in 1 wt% NaCl solutions. 4K PPG-ionenes possessed the salt-responsive character compared to other PPG-ionenes having 1K and 2K PPG segments. The 4K PPG-ionenes showed a trend in 1 wt% NaCl solutions. All ionenes ranging from HPL/HPB values of 1 to 19 showed milky dispersions in water and suspended particles in 1 wt% NaCl and complete film precipitation was observed at a HPL/HPB molar ratio of 19. Further investigation of the solution properties of 1K PPG-ionenes using dynamic light scattering and solution rheology experiments were performed on soluble 1K PPG-ionene series.

Keywords: polyelectrolyte effect, salt-responsive ionene, poly(propylene glycol)

4.2 Introduction

Polyelectrolytes are polymers that are ionized in water. There is growing interest in the understanding and applications of polyelectrolytes. Ionic associations in polyelectrolytes influence their distinct behavior. Linear polyelectrolytes in dilute solutions, have rod-like chain conformations due to the repulsion of charges which is the so called polyelectrolyte effect.[1] When salt is added to polyelectrolytes, the charges are screened and chains will have coil-like conformations. Ionenes are one type of polyelectrolyte. They are polycations that have quaternized nitrogen atoms throughout their backbone. They are synthesized using a Menshutkin reaction, which results from reacting a ditertiary amine with an alkyl dihalide.[2] They are named *x*,*y*-ionenes, *x* represents the number of methylene units from the diamine monomer and *y* represents the number of methylene units in the dihalide monomer.

The solubility of polyelectrolytes in monovalent salt solutions depends on charge density, condensation of counterions and phase separation behavior.[3] Polyelectrolytes having lower charge densities will precipitate out at lower concentrations of salt. This is due to the fact that there are lower numbers of counterions that need to condense. The solubility of polyelectrolytes has four stages in water and multivalent salt solutions.[4] In stage one, pure water, the polyelectrolyte shows an extended rod-like conformation. In stage two, ion-bridging occurs between divalent counterions and two ionic sites on the polymer backbone and thus polyelectrolyte remains soluble. In stage three, due to the high level of charge screening, the polyelectrolyte precipitates out ("salting out"). In stage four, when the salt concentration is increased even higher, the polyelectrolyte will redissolve ("salting in") in the solution. Mueller et al.[5] reported the "salting out" and "salting in" effects for quaternized poly(*N*,*N*-dimethylaminoethyl methacrylate) (PDMAEMA) salts in the presence of NaI. Ballauf et al.[6]

showed similar effects for spherical polyelectrolyte brushes. Therefore, in order to measure the solution properties of polyelectrolytes including molecular weight, viscosity, solution rheology, and salt-triggering, salt solutions are used to screen polyelectrolyte charges.

Layman et al.[7] from our group, reported absolute weight-average molecular weights of 6,12- and 12,12-ammonium ionenes using aqueous size exclusion chromatography with solvent/salt solutions as mobile phase. A 54/23/23 water/methanol/glacial acetic acid (solvent portion) including 0.54 *M* NaOAc (salt portion) with pH of 4 showed monomodal peaks from multiangle laser light scattering (MALLS) detector. They investigated other solvent/salt mixtures in which the salt concentrations varied and led to bimodality in light scattering traces.

Rembaum et al.[8] extensively studied the solution properties of high charge density 3,4- and 6,6-ionenes. They measured the viscosities of ionene solutions in the presence and absence of added 0.4 *M* KBr salt. Ionene polyelectrolytes showed rigid rod-like conformations in the absence of salt. The viscosity was similar to that of uncharged polymers in the presence of salt.

McKee et al.[9] investigated the rheological behavior of PDMAEMA·HCl solutions in the presence of added NaCl in 80/20 water/methanol mixture. Scaling relationships between specific viscosity and polymer concentrations showed polyelectrolyte behavior in PDMAEMA·HCl solutions. Various amounts of NaCl ranging from 1 wt% to 50 wt% were added to PDMAEMA·HCl solutions. Scaling relationships of PDMAEMA·HCl solutions in high salt concentrations were similar to neutral polymers.[10] Specific viscosity decreased with increasing NaCl. The salt screened the charges on the polymer backbone and changed the chain conformation from rod-like to coil-like conformation. Coil-like conformations have smaller volume in solution and therefore the specific viscosity decreases compared to rod-like conformations.

Salt-triggering is a property in which a polymer is insoluble in monovalent salt solution (NaCl) having certain ionic strength and soluble in hard water with up to 200 ppm (parts per million) calcium and magnesium ions. Bunyard et al.[11] patented triggerable cationic polymers applicable in binder compositions. Binder materials are used for flushable personal care products, wet wipes for personal use, make-up removals, nail polish removals, etc. A number of other approaches in obtaining salt-responsive polymers have been patented in recent years.[12-17]

Investigating the properties of the polymer when it is a dry film and when it is exposed to 1 wt% NaCl solution is of high importance for the applications mentioned above. In order to measure the modulus and elastic damping of the material, dynamic mechanical analysis (DMA) is used. The wet strength property is more challenging due to the softness of the films. Misawa et al.[18] synthesized ionene-based hydrogels. They characterized the mechanical properties (storage modulus and loss modulus vs percent strain) of these hydrogels using cone and plate rheometer. The effect of spacer length on gelation properties was investigated.

Studies on ionenes have shown that charge density is critical for achieving a salt-responsive solubility in the targeted ionic strength range. High charge density ionenes do not trigger in the targeted ionic range. Therefore dilution of charge with use of hydrophobic segments such as poly(propylene glycol) is essential in obtaining salt-triggering. In this chapter the synthesis of ion-sensitive PPG-based ammonium ionenes along with their salt-triggering behavior is discussed. Besides their salt-responsiveness, ionenes have potential applications as antimicrobial agents,[19, 20] this behavior is significantly advantageous for personal care product applications that are suggested for salt-triggering cationic polymers.

4.3 Experimental

4.3.1 Materials

Poly(propylene glycol) 2200, 4200 (Acclaim) and 1000 (Arcol) were purchased from Bayer Material Science. 6-bromohexanoyl chloride (97%) was purchased from Alfa Aesar. Triethyl amine was purchased from Aldrich and distilled from calcium hydride. 1,12-dibromododecane (98%) was purchased from Sigma-Aldrich and recrystallized from ethanol. *N*,*N*,*N*′,*N*′-tetramethyl-1,6-hexanediamine (99%) was purchased from Acros Organics. Dichloromethane (DCM, HPLC grade was passed through an alumina column and a molecular sieves column before use. Sodium chloride (ACS certified crystalline) was used as recieved.

4.3.2 Synthesis of PPG-based ammonium ionenes

In chapter three, the synthesis and characterization of bromine end-capped PPG oligomers (Br-PPG-Br) were widely discussed. Bromine end-capped PPG (2 g, 1 eq) and *N*,*N*,*N*′,*N*′-tetramethyl-1,6-hexanediamine (1 eq) were added to a two-neck, round-bottomed flask equipped with an overhead mechanical stirrer and nitrogen inlet. The reaction was allowed to proceed for 24 h at 80 ºC in bulk. The polymer produced in bulk was used directly to perform solution property experiments.

4.3.3 Synthesis of PPG-based ammonium ionenes having an aliphatic 1,12-dibromododecane as part of hard segment (HS)

A flame-dried, 50 mL, two-neck, round-bottomed flask was charged with 1:1 equivalent ratios of dibromides (bromine end-capped PPG and 1,12-dibromododecane) to diamine (*N*,*N*,*N*′,*N*′-tetramethyl-1,6-hexanediamine). The flask was purged with dry N_2. Polymerization was performed in bulk for 24 h at 80 ºC. Table 4.1 lists the equivalents of dibromides and

diamines used to synthesize a series of PPG-ionenes having various hydrophilic to hydrophobic molar ratios.

4.3.4 Salt-trigger solubility test

Salt-triggering is an ability in which a polymer sample dissolves in DI water and precipitates or "triggers" in the targeted ionic strength which is 1-5 wt%, in our case preferably 1 wt% NaCl solution. In order to investigate this property in the PPG-ionene series, 80 mg of the bulk polymer is added to 10 mL of DI water and 80 mg is added to 10 mL of 1 wt% NaCl solution. The solutions stand at room temperature for 24 h. The optical clarity determines whether a sample is soluble or insoluble. In order to ensure the insolubility of a sample after 24 h, the solution was heated to 50 ºC for 1 to 2 minutes, if the solution remained optically cloudy, the sample was confirmed to be insoluble.

4.4 Characterization

^{1}H NMR spectroscopic analyses were performed on Varian INOVA 400 MHz spectrometer to confirm the monomer and polymer composition in $CDCl_3$ and CD_3OD respectively. Solution rheology was performed on VOR Bohlin strain-controlled solution rheometer at 25 ºC using concentric cylinder geometry. The bob and cup diameters were 14 and 15.4 mm respectively. The rheometer was calibrated with newtonian standard solutions. Dynamic light scattering measurements were performed on Malvern Zeta Sizer Nano Series Nano-ZS instrument using dispersion technology software (DTS) version 4.20 at a wavelength of 633 nm using a 4.0 mW, solid state He-Ne laser at a scattering angle 173º. The experiments were performed at room temperature. Polymer samples were prepared at 8 mg/mL and allowed to dissolve or stand in

both DI water and NaCl solutions overnight. Samples were then poured into the clean cuvettes. The aggregate diameter size vs the salt concentration was investigated.

4.5 Results and Discussion

A number of ionenes having 1K, 2K, and 4K PPG segments were synthesized with the Menshutkin reaction. These ionenes were used to investigate the salt-triggering behavior, which is the solubility in DI water and insolubility in 1 wt% NaCl solution. Scheme 4.1 illustrates the synthesis of ionenes having HPL/HPB molar ratio of 1.0 HPL/HPB ratio represents the mole equivalents of hydrophilic segment (HPL) over the mole equivalents of hydrophobic segment (HPB). In this ionene the *N*,*N*,*N*′,*N*′-tetramethyl-1,6-hexanediamine corresponds to the hydrophilic segment (HPL) and Br-PPG-Br corresponds to the hydrophobic segment (HPB).

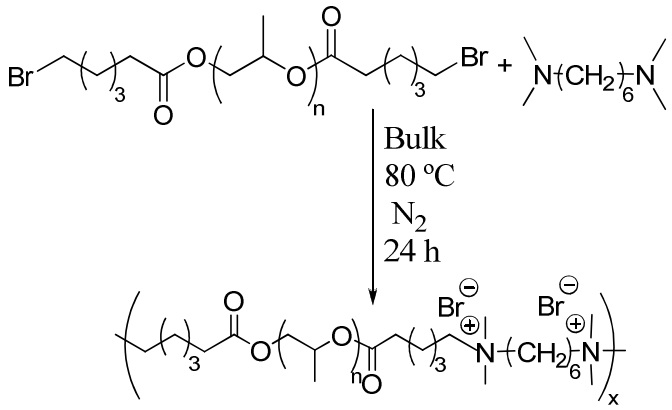

Scheme 4.1. Synthesis of PPG-ionene having HPL/HPB value of 1.0

Scheme 4.2 illustrates the synthesis of PPG-ionenes having higher weight percentage of hydrophilic segment. This ionene has 1,12-dibromododecane as part of its hard segment. The higher molar ratios of hard segment increase the charge density and enhance the solubility of ionenes in water. In this ionene the *N*,*N*,*N*′,*N*′-tetramethyl-1,6-hexanediamine and 1,12-dibromododecane correspond to the hydrophilic segment (HPL) and Br-PPG-Br corresponds to the hydrophobic segment (HPB). A series of ionenes were synthesized to investigate their salt-

triggering behavior starting from three different number-average molecular weights of PPG. The equivalent moles of monomers and HPL/HPB ratios used to synthesize these ionene series are listed in Table 1. The stoichiometric balance of (1:1) equivalents of dibromides to diamine was used.

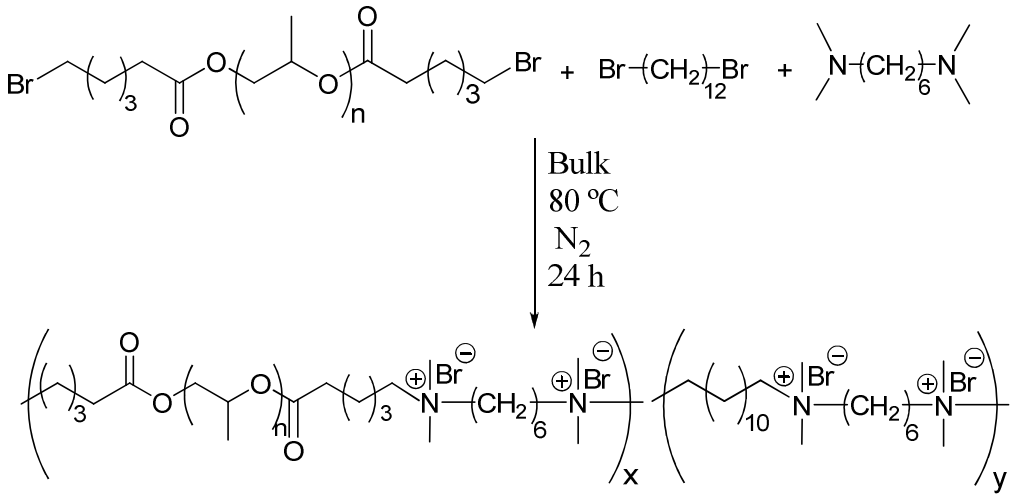

Scheme 4.2. Synthesis of PPG-ionenes having higher HPL content

Table 4.1. Molar ratios of HPL and HPB segments

PPG M_n (g/mol)	**Br-PPG-Br (Eq)**	**1,12-dibromodecane (Eq)**	***N,N,N′,N′*-tetramethyl-1,6-hexanediamine (Eq)**	**HPL/HPB**
1K,2K,4K	1	0	1	1
1K	0.80	0.20	1	1.5
1K	0.66	0.34	1	2
1K	0.50	0.50	1	3
2K	0.34	0.66	1	5
2K	0.29	0.71	1	6
2K	0.22	0.78	1	8
4K	0.20	0.80	1	9
2K	0.18	0.82	1	10
4K	0.15	0.85	1	12
2K	0.12	0.88	1	15
4K	0.1	0.9	1	19
2K	0.07	0.93	1	27
4K	0.04	0.96	1	49

Upon synthesizing the ionene series with various HPL/HPB, a graph of HPL/HPB molar ratios versus PPG number-average molecular weights was plotted to investigate the salt-triggerable polymer (Figure 4.1). 1K PPG-ionenes having HPL/HPB values of 1.0, 1.5, 2.0, and 3.0 were synthesized. 1K PPG-ionenes are the highest charge density samples compared to 2K and 4K PPG-ionenes due to shorter segments between the quaternized sites along the backbone. 1K PPG-ionenes were soluble or optically clear in DI water and 1 wt% NaCl solutions. 2K PPG-ionenes having HPL/HPB values of 1.0, 5.0, 6.0, 8.0, 10, 15, and 27 were synthesized. These ionenes showed cloudy dispersions in DI water and 1wt% NaCl solutions. There was no significant trend observed between the lower HPL/HPB ratios and higher HPL/HPB ratios of 2K PPG-ionenes. Increasing the molecular weight of hydrophobic PPG, enhanced the salt-triggering ability. 4K PPG-ionenes having HPL/HPB values of 1.0, 9.0, 12, 19, and 49 were synthesized (Figure 4.2). Samples having HPL/HPB values of 1.0, 9.0, 12, and 19 showed milky dispersions in DI water (Figure 4.3). Interestingly these ionenes showed a solubility trend in 1 wt% NaCl solution, in that they showed suspended particles at lower HPL/HPB values of 1.0, 9.0, 12 and complete film precipitation in 1 wt% NaCl solution for HPL/HPB value of 19. The 4K PPG-ionene sample having a HPL/HPB value of 49 showed cloudy dispersions in both water and 1 wt% NaCl solution, similar to the 2K PPG-ionenes. This is due to the high hydrophilicity of the ionene backbone that did not allow the precipitation to occur at 1 wt% NaCl solution. Therefore it is possible to find the desired salt-triggerable sample (solubility in water and insolubility in salt) in the HPL/HPB window greater than 19 and smaller than 49.

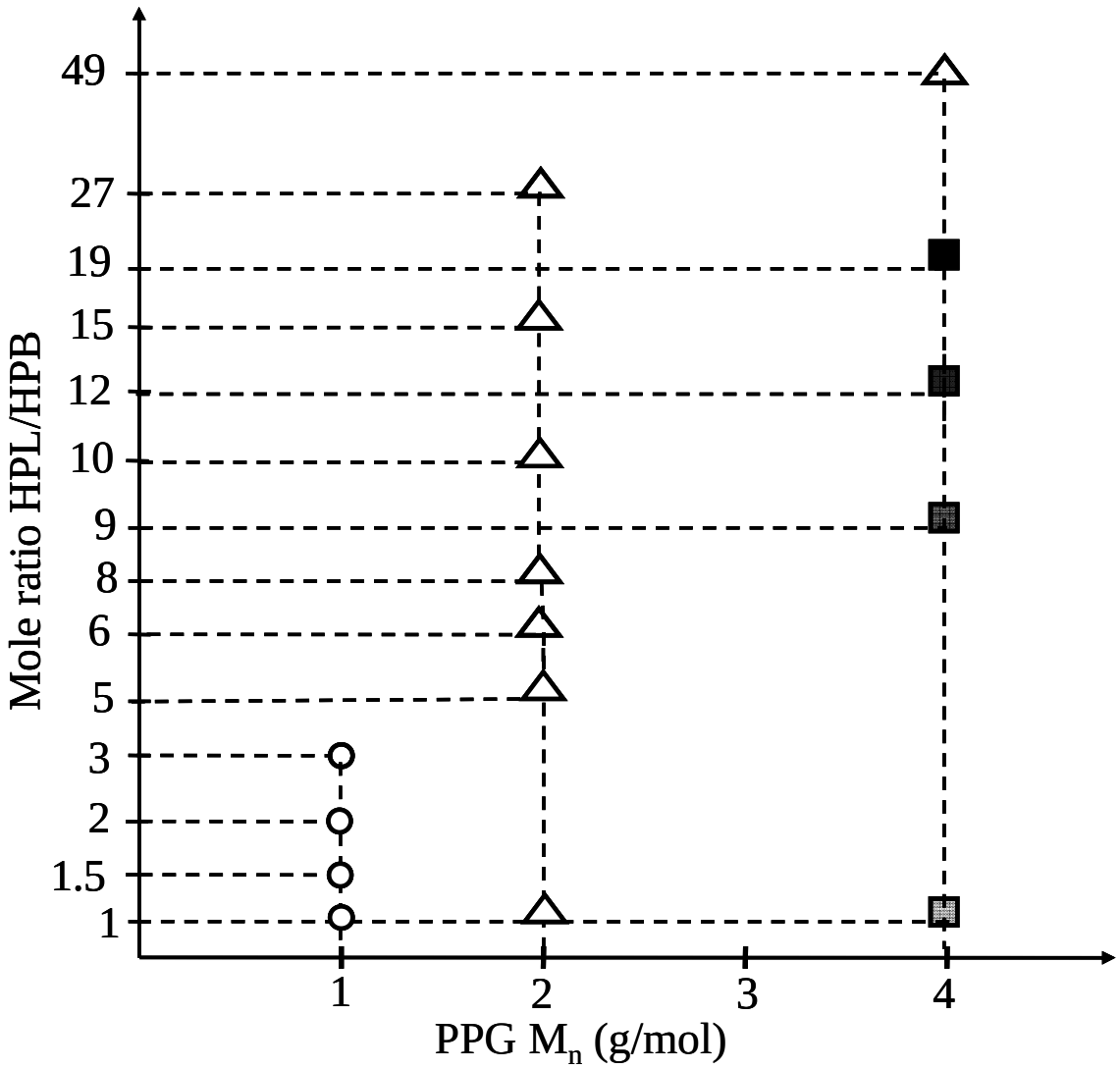

Figure 4.1. Salt-responsive plot for PPG-ionenes. Circle: water-soluble and salt-soluble ionene Triangle: cloudy dispersion in water and 1 wt% NaCl. Square: gray to black shows suspension to precipitation

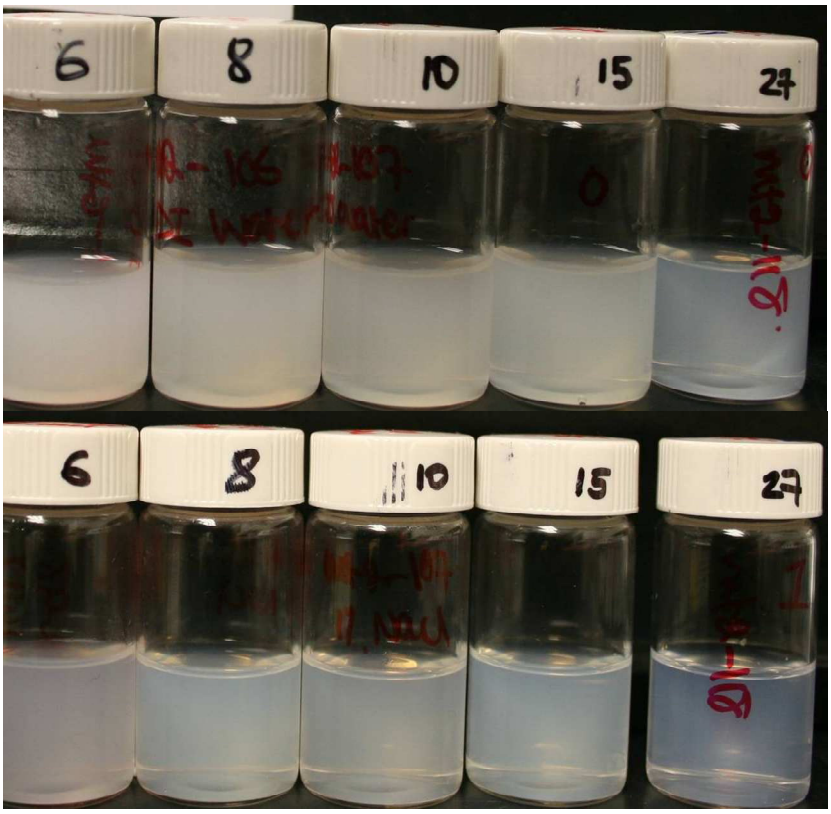

Figure 4.2. 2K PPG-ionenes with HPL/HPB values of 6 to 27 in DI water (top) and in 1 wt% NaCl (bottom)

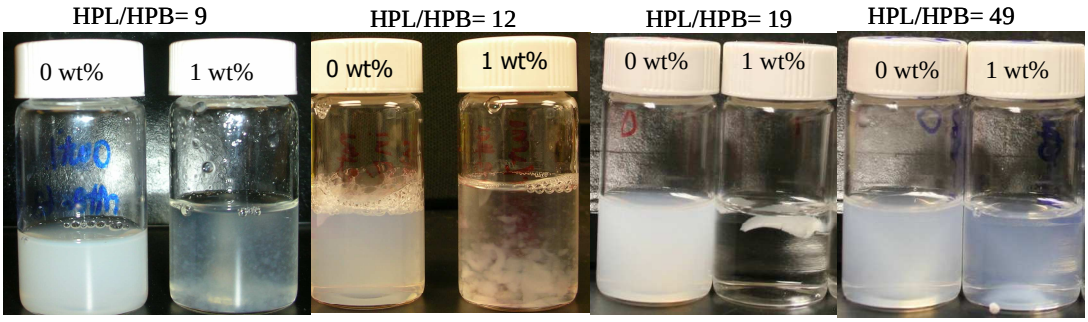

Figure 4.3. 4K PPG-ionenes having HPL/HPB values of 9 to 49 in DI water and 1 wt% NaCl

As shown in Figure 4.3 the ionene sample, which shows the salt-triggering effect in 1 wt% NaCl, is the 4K PPG-ionene having a HPL/HPB value of 19. Substituting 1,12-dibromododecane with 1,4-dibromobutane enhanced the solubility of this ionene in water due to the increase in charge density (Scheme 4.3). The charge displacement using 1,4-dibromobutane is more frequent

in the corresponding ionene. This ionene showed a milky dispersion in water and milky suspension in 1 wt% NaCl. Increasing the NaCl concentration to 5 wt% caused the ionene to precipitate, although the ionene film precipitate did not have mechanical stability and the film precipitate disintegrated in 5 wt% NaCl solution (Figure 4.4).

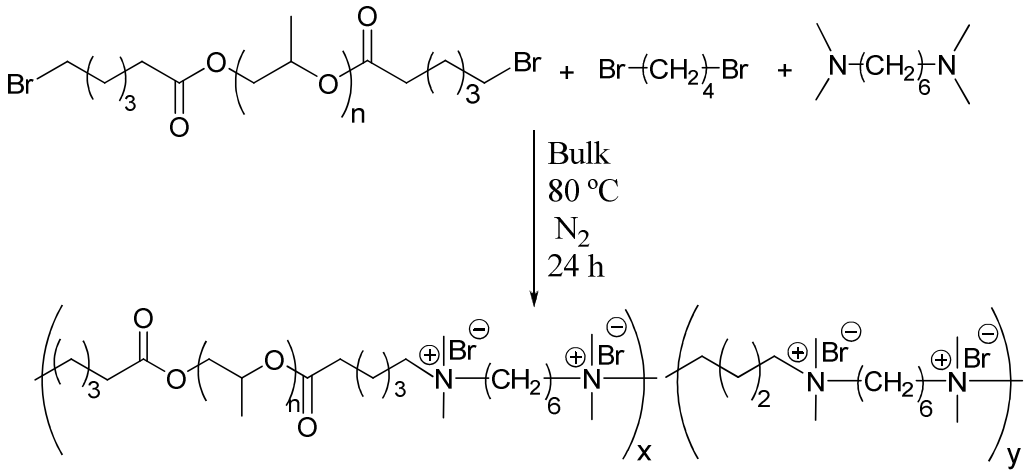

Scheme 4.3. Synthesis of 4K PPG-ionene having HPL/HPB value of 19

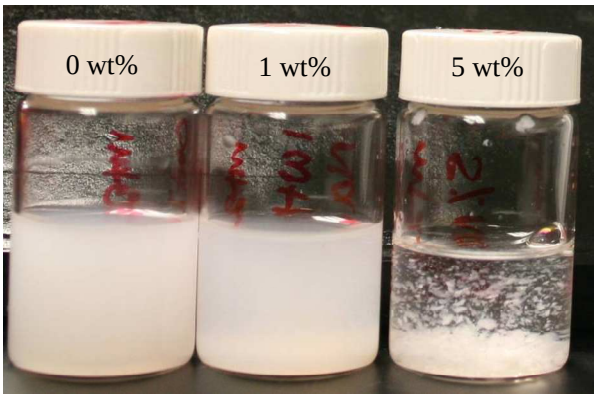

Figure 4.4. 4K PPG-ionene having HPL/HPB value of 19 in DI water, 1 wt% NaCl, and 5 wt% NaCl

While investigating the salt-triggering sample, the solution properties of 1K PPG-ionene having a HPL/HPB value of 3 were studied. This ionene sample was soluble in DI water and 1 wt% NaCl solution. In order to investigate the effect of salt on the size of aggregates, dynamic

light scattering (DLS) was performed on various concentrations of ionene ranging from 0.5 to 7 wt%. 1K PPG-ionene sample showed optical clarity in water and NaCl solutions. The 0.5 and 7 wt% solutions of 1K PPG-ionene in DI water and 1 wt% NaCl showed bimodal DLS curves. A peak in the range of 10 to 100 nm in size and another in the range of 100 to 1000 nm were observed. The aggregate sizes were smaller in NaCl solutions compared to DI water (Figure 4.5). This was due to salt screening behavior of the ionene with NaCl. The size of larger aggregates was plotted against the polymer concentrations in Figure 4.6. It is shown that the size of aggregates decrease in NaCl solution compared to DI water.

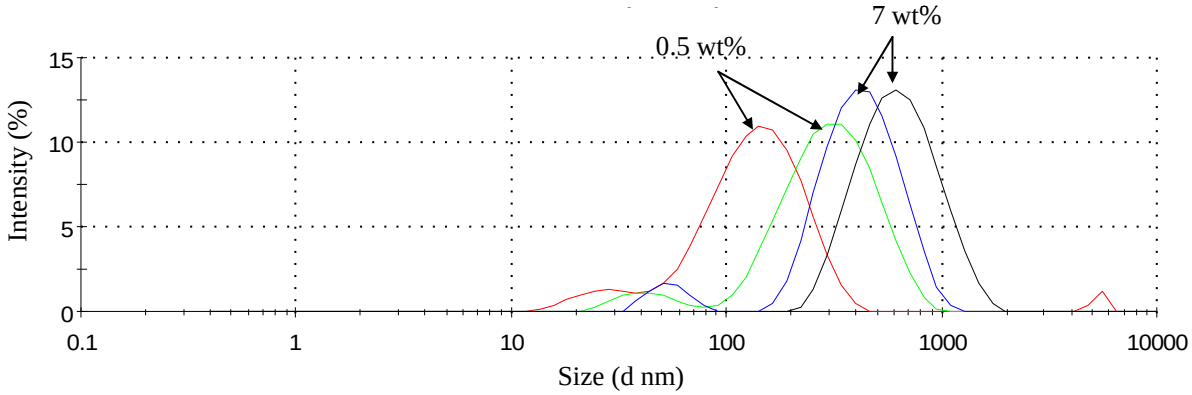

Figure 4.5. DLS analysis of 0.5 wt% and 7 wt% 1K PPG-ionene having HPL/HPB value of 3 in DI water and 1 wt% NaCl

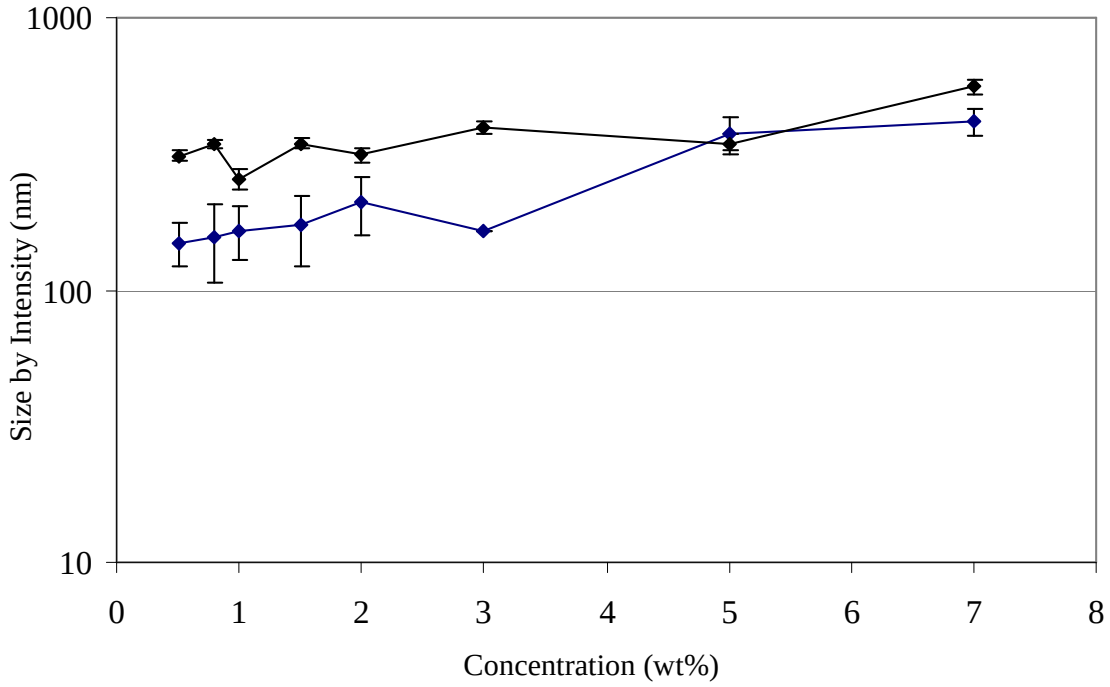

Figure 4.6. Effect of salt on aggregate size of 1K PPG-ionene having HPL/HPB value of 3.0

Limited solution rheology studies on 1K PPG-ionenes having a HPL/HPB value of 3.0 were performed to investigate the scaling relationship between specific viscosity and concentration. Figure 4.7 illustrates a plot of specific viscosity versus polymer concentration. Specific viscosity is calculated using: $\eta_{sp} = (\eta_0 - \eta_s)/\eta_s$, η_0: corresponds to zero shear viscosity of the solution, and η_s: corresponds to the solvent viscosity. Concentrations ranging from 0.5 to 10 wt% ionene solutions were tested. In order to make a conclusion that 0.5 wt% to 7 wt% is the semidilute unentangled regime and above the 7 wt% is the semidilute entangled regime, it is necessary to make higher concentrated ionene solutions up to 35 wt% or higher.

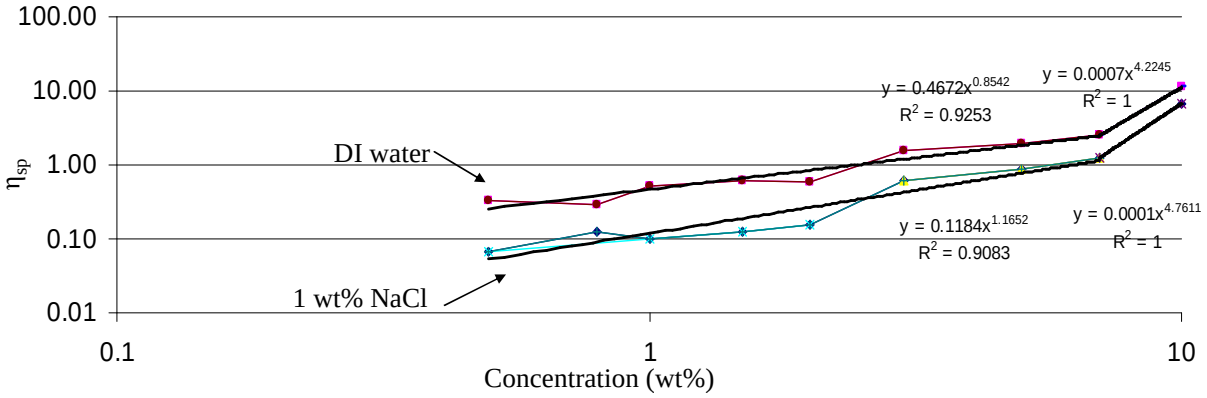

Figure 4.7. Specific viscosity versus concentration for 1K PPG-ionene solutions at 25 ºC

4.6 Conclusions

1K, 2K, and 4K PPG-ionenes having various HPL/HPB molar ratios were successfully synthesized. Salt-triggering of this series of ammonium-based ionenes was studied. The 1K PPG-ionenes having HPL/HPB of 1 to 3 were soluble in DI water and 1 wt% NaCl solutions and did not show salt-triggering behavior. The 2K PPG-ionenes ranging from HPL/HPB values of 1 to 27 showed cloudy dispersions in water and 1 wt% NaCl solutions. The 4K PPG-ionenes with HPL/HPB values of 1 to 49 showed milky suspensions in DI water and precipitations at HPL/HPB value of 19. So far, this ionene was the most suitable sample for showing salt-triggering behavior in 1 wt% NaCl. Limited solution studies using dynamic light scattering and solution rheology were performed on 1K PPG-ionene having HPL/HPB value of 3.0.

4.7 Acknowledgements

This material is based upon work supported in part by the Kimberly Clark Corporation. We acknowledge helpful discussions with Dr. Clay Bunyard, Prof. Michael Rubinstein, and Prof. Robert Moore.

4.8 References

[1] Leyte, J. C. *J. Polym. Sci., Part A: Gen. Pap.* **1964,** 2, (12), 5287-90.
[2] Abboud, J. L. M.; Notario, R.; Bertran, J.; Sola, M. *Progress in Physical Organic Chemistry* **1993,** 19, 1-182.
[3] Ikegami, A.; Iami, N. *J. Polym. Sci.* **1962,** 56, 133-52.
[4] Solis, F. J.; Olvera de la Cruz, M. *J. Chem. Phys.* **2000,** 112, (4), 2030-2035.
[5] Plamper, F. A.; Schmalz, A.; Penott-Chang, E.; Drechsler, M.; Jusufi, A.; Ballauff, M.; Mueller, A. H. E. *Macromolecules (Washington, DC, U. S.)* **2007,** 40, (16), 5689-5697.
[6] Mei, Y.; Ballauff, M. *Eur. Phys. J. E* **2005,** 16, (3), 341-349.
[7] Layman, J. M.; Borgerding, E. M.; Williams, S. R.; Heath, W. H.; Long, T. E. *Macromolecules* **2008,** 41, (13), 4635-4641.
[8] Casson, D.; Rembaum, A. *Macromolecules* **1972,** 5, (1), 75-81.
[9] McKee, M. G.; Hunley, M. T.; Layman, J. M.; Long, T. E. *Macromolecules* **2006,** 39, (2), 575-583.
[10] Lauten, R. A.; Nystrom, B. *Macromol. Chem. Phys.* **2000,** 201, (6), 677-684.
[11] Branham, K. D.; Chang, Y.; Lang, F. J.; McBride, E.; Bunyard, C. Water-dispersible and ion-sensitive compositions as binders for disposable products. 2002-US49052002077040, 20020219., 2002.
[12] Lang, F. J.; Branham, K. D.; Chang, Y.; Chen, F. M.; Johnson, E. D.; Lindsay, J. D.; Mumick, P. S.; Pomplun, W. S.; Schick, K. G.; Schultz, W. T.; Soerens, D. A.; Sun, T.; Wang, K. Y. Ion-sensitive, water-dispersible polymers useful as binder compositions for disposable products and production method thereof. 2000-564213 6429261, 20000504., 2002.
[13] Farwaha, R.; Pauls, S. P., Jr.; Mumick, P. Salt-sensitive binder compositions for strengthening nonwoven fabrics used in wet wipes, diapers and personal care products. 2006-US129282006118745, 20060406., 2006.
[14] Jones, R. B.; Hobar, B. R.; Goldstein, J. E.; Robeson, L. M. Improvement in the wet tensile strength of nonwoven webs. 2005-84271589138, 20050418., 2005.
[15] Kakiuchi, S.; Ishii, M.; Nakae, A.; Ikoma, S. Water-disintegrable cleaning sheet containing an aqueous cleaning agent including an organic solvent. 89-122081372388, 19891130., 1990.
[16] Komatsu, M.; Toki, I. Polymers with salt-sensitive water solubility for binders of nonwoven fabrics. 91-29170405125123, 19911107., 1993.

[17] Bunyard, W. C.; Branham, K. D.; Lostocco, M. R.; Calhoun, G.; Weston, R.; Lang, F. J.; Possell, K. Ion triggerable, cationic polymers, their manufacture and use in wipe items. 2002-2516562004063888, 20020920., 2004.
[18] Misawa, Y.; Koumura, N.; Matsumoto, H.; Tamaoki, N.; Yoshida, M. *Macromolecules (Washington, DC, U. S.)* **2008,** 41, (22), 8841-8846.
[19] Narita, T.; Ohtakeyama, R.; Nishino, M.; Gong, J. P.; Osada, Y. *Colloid. Polym. Sci.* **2000,** 278, (9), 884-887.
[20] Rembaum, A. *Applied Polymer Symposia* **1973,** No. 22, 299-317.

Chapter 5. Future directions

5.1 Synthesis and characterization of Poly(propylene glycol) (PPG)/Poly(ethylene glycol) (PEG) random and alternating copolymer ionenes

Poly(ethylene glycol) (PEG) is a well known commercially available water-soluble polymer. Many PEG-containing polymers have been synthesized and used in different types of applications. The hydrophilicity and hydrophobicity of segmented copolymers can be tuned using PPG as the hydrophobic (HPB) segment and PEG as the hydrophilic (HPL) segment. Various number-average molecular weights of PPG and PEG will influence the salt-triggering behavior as well as the mechanical and morphological performance of these ionenes. The salt-triggering behavior can be observed in segmented ionenes having high number-average molecular weight PPG and low number-average molecular weight PEG. Due to the crystalline PEG segment, the mechanical properties of PPG/PEG copolymers will improve compared to PPG-ionene homopolymers. The phase separation behavior is expected in these systems. The properties of random copolymer ionene will be compared to alternating copolymer ionenes. Figure 5.1 and Figure 5.2 are the proposed synthetic routes for random and alternating PPG/PEG copolymers respectively.

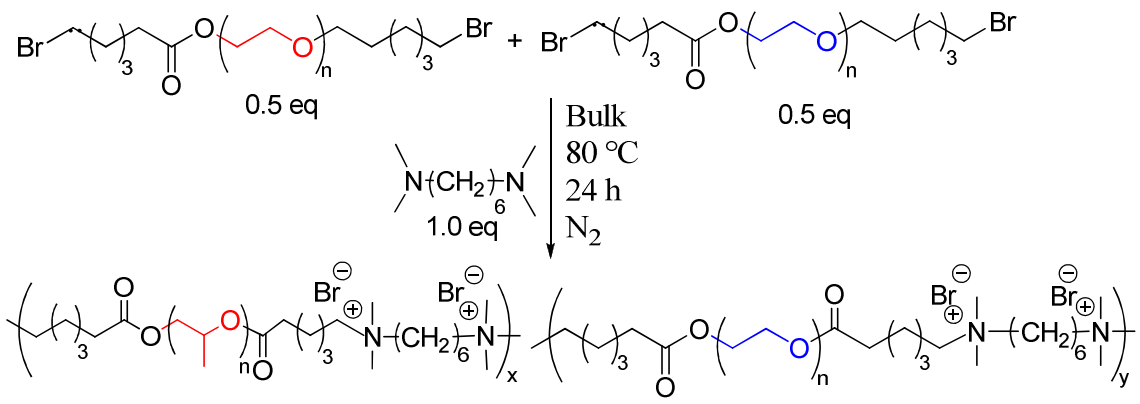

Figure 5.1. Synthesis of PPG/PEG random copolymer ammonium ionene

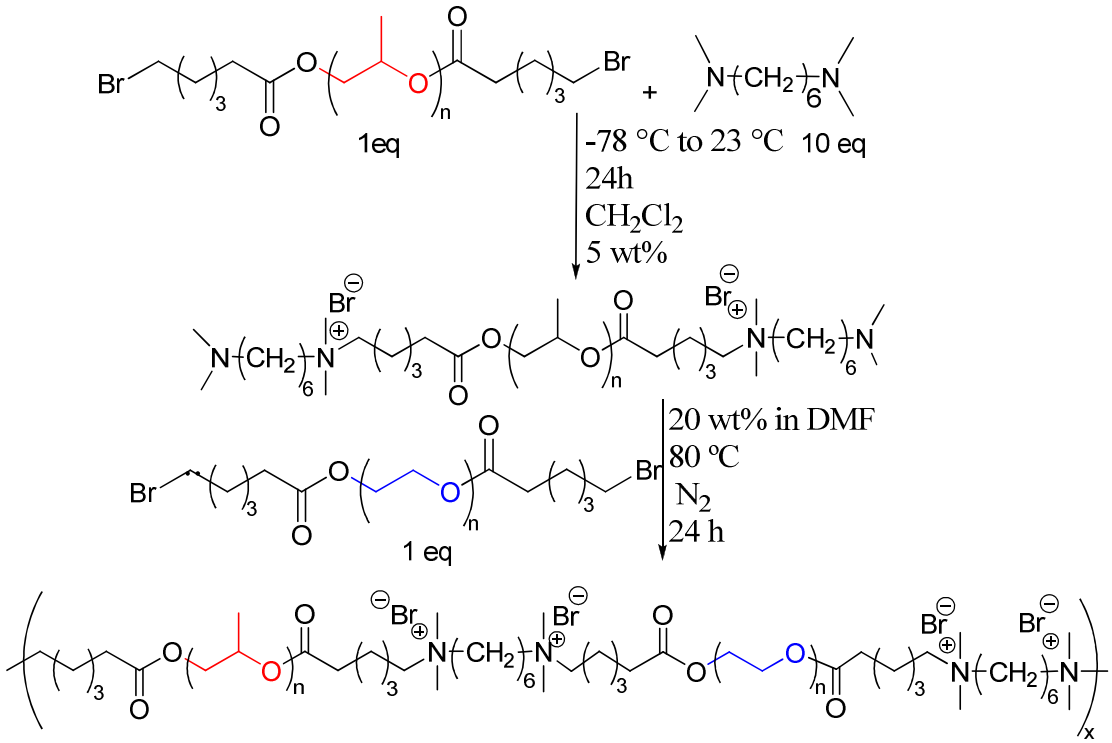

Figure 5.2. Synthesis of PPG/PEG alternating copolymer ammonium ionene

5.2 Synthesis and characterization of novel ammonium-based ionenes containing diverse counterions

Counterions influence the properties of ionenes due to the changes in ionic aggregate formations. It is necessary to study the effect of various counterions on thermal, mechanical and morphological behavior of ammonium ionenes. The size of counterion influences the thermal transitions of the polymer. It is expected that if we increase the size of counterion, the glass transition temperature would decrease. Small counterions allow better packing for polymer chains compared to bulky counterions. One of the proposed syntheses is the anion exchange in segmented PPG-based ammonium ionenes (Figure 5.3).

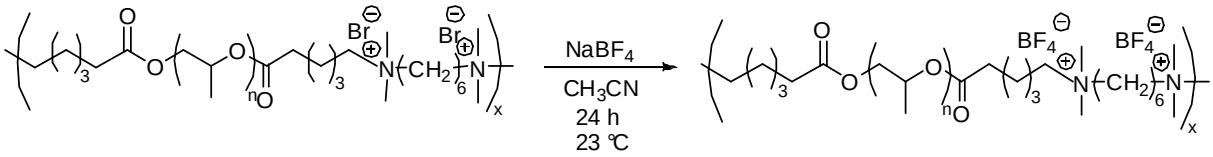

Figure 5.3. Anion exchange of PPG-based ionenes

5.3 Synthesis and characterization of imidazolium-ionenes

The synthesis and characterization of imidazolium-based ionenes are not well-documented in the literature. Imidazolium containing polymers exhibit high conductivities and are used in electroactive devices. Recently, in our research group, the synthesis and characterization of poly(tetramethylene oxide) (PTMO)-based imidazolium ionenes and the effect of hard segment content on ionene properties were studied. It is interesting to investigate the effects of various polyether spacers such as atactic poly(propylene glycol) on the properties of imidazolium-based ionenes. It is expected to observe microphase separation behavior in these ionenes. It is beneficial to compare the mechanical properties of ionenes containing imidazole ring to ionenes having six methylene units as part of their hard segments. Since imidazole ring imparts rigidity

to the backbone compared to six aliphatic methylene units, therefore higher thermal transitions might be observed and the rubbery plateau modulus can increase for imidazolium-based ionene. Figure 5.4 represents the synthesis of PPG-based imidazolium ionene.

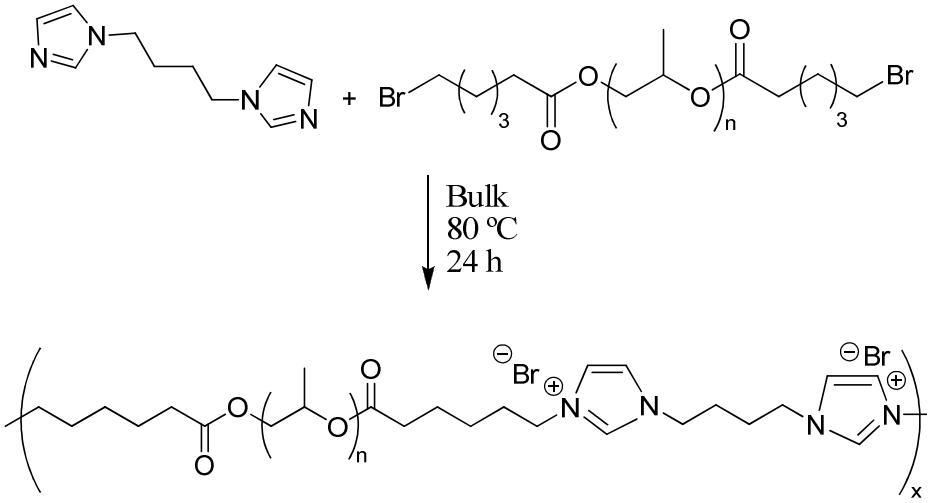

Figure 5.4. Synthesis of PPG-based imidazolium ionene

5.4 Synthesis and characterization of highly branched segmented ionenes

Branching can significantly influence the physical properties, rheology, and processing behavior of macromolecules. High degrees of branching prevents chain entanglement, decreases the melt viscosity which leads to enhancements in melt processibility. Most work on ionenes has focused on the synthesis and characterization of ionenes with linear topology. However, a few studies have focused on the synthesis and characterization of star-shaped, hyperbranched, and comb ionenes with aliphatic soft segments. Our laboratory, previously studied the synthesis and characterization of hyperbranched PTMO-based ionene using an *oligomeric* A_2 plus B_3 methodology.

The synthesis of segmented branched ionenes is with introducing a branching agent (Figure 5.5). The pentaerythritol tetrabromide acts as a branching agent, and the effects of branching on

mechanical properties, rheological behavior, and solubility characteristics of segmented ionenes can be investigated.

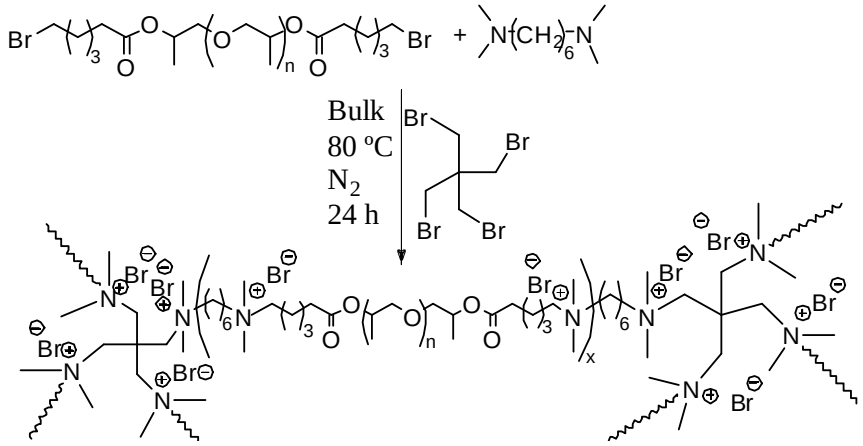

Figure 5.5. Synthesis of highly branched segmented PPG-based ionene

5.5 Synthesis and characterization of self-healing ammonium ionenes

Many polymers that show self-healing behavior were synthesized in recent years. Self-healing is a behavior in which a material can detect when it is damaged and heal itself either spontaneously (autonomic) or with the aid of a stimulus (non-autonomic). Ionomers are a type of non-autonomic materials which their self-healing was explored recently. Ionic associations or physical crosslinks in ionomers is the reason to their healing behavior. When the fractured ionomer is heated above its T_g, the polymer softens and the ionic aggregates will disorder. When the heating is continued above the ionic dissociation temperature, the ionic aggregates dissociate and chains cross the crack interface. Upon cooling the ionic aggregates reorient and reform strong electrostatic interactions and this is where polymer heals. One of the quantitative techniques to measure healing is tensile testing before damage and after healing. However,

quantitative analysis on self-healing behavior of high charge density ionenes as well as segmented ionenes as types of ion-containing polymer needs to be explored.